Characterizing the role of the endocannabinoid system's catabolic enzymes FAAH and MAGL in the development of functional sensorimotor activities in zebrafish

by

Lakhan Singh Khara

A thesis submitted in partial fulfillment of the requirements for the degree of

Master of Science

in

Physiology, Cell, and Developmental Biology

Department of Biological Sciences
University of Alberta

Abstract:

The endocannabinoid system (eCS) plays a critical role in a variety of homeostatic and developmental processes. Generally, the eCS relies on the naturally produced compounds known as endocannabinoids (eCBs), which are lipophilic signaling molecules that interact with cannabinoid receptors to regulate biological activities of the central and peripheral systems. In terms of its developmental roles, the eCS is becoming more well known for its involvement in neural development and motor function; however, the role of eCB signaling in functional sensorimotor development remains to be examined. One way to study the roles of eCB signaling is to perturb the system by targeting the enzymes responsible for degrading the eCBs. Thus, the two eCB catabolic enzymes known as fatty acid amide hydrolase (FAAH) and monoacylglycerol lipase (MAGL) are of interest in many studies that investigate the roles of eCB signaling. The two main eCBs are known as anandamide (AEA) and 2-arachidonoylglycerol (2-AG). FAAH is responsible for degrading AEA, while MAGL breaks down 2-AG. In this thesis, the catabolic enzymes FAAH and MAGL were inhibited either simultaneously, or individually, during the first ~24 hours of zebrafish embryogenesis, and the properties of contractile events and sensorimotor escape responses were studied in animals ranging in age from 1 day post-fertilization (dpf) to 10 weeks. This perturbation of the eCS resulted in alterations to contractile activity, which was observed at 1 dpf. Inhibition of MAGL using JZL 184, and dual inhibition of FAAH and MAGL using JZL 195 decreased escape swimming activity at 2 dpf. Treatment with JZL 195 also produced alterations in the properties of the 2 dpf short latency C-start escape response. Furthermore, animals treated with JZL 195 exhibited deficits in escape responses elicited by auditory/vibrational (A/V) stimuli at 5 and 6 dpf. A/V response deficits were also present during the juvenile developmental stage (8–10-week-old fish), thus demonstrating a

prolonged impact to sensorimotor activities. Overall, from performing different sensorimotor assessments, the results indicate that MAGL has a more significant role than FAAH does in zebrafish sensorimotor development. These findings demonstrate that eCS perturbation affects sensorimotor function and underscores the importance of eCB signaling in the development of motor and sensory processes.

Since eCBs are known to interact with a variety of different receptor systems, the involvement of canonical and non-canonical cannabinoid receptors was also studied in this thesis. In particular, the CB1R and CB2R cannabinoid receptors, along with transient receptor potential (TRP) channels, and the Sonic Hedgehog (SHH) signaling pathway were examined for their potential roles in eCS-related sensorimotor development. To investigate the potential involvement of these receptor systems, developing animals were co-treated with pharmacological inhibitors of the CB1R, CB2R, TRPA1/TRPV1/TRPM8 channels, and a Smoothened (SMO) agonist, alongside the eCS enzyme inhibitors during the first ~24 hours of development. Escape swimming was then assessed at 2 dpf. The CB1R antagonist AM 251 prevented locomotor deficits caused by eCS perturbation, while the CB2R antagonist AM 630 was not effective in restoring locomotor activity. Inhibition of TRPA1/TRPV1/TRPM8 using AMG 9090 rescued the locomotor reductions caused by JZL 195, but not the reductions caused by JZL 184. The SMO agonist purmorphamine attenuated the effects of JZL 184 and JZL 195 on swimming distance, but not mean swimming velocity. After observing the involvement of these receptor systems on the eCS-related deficits in 2 dpf escape swimming, their roles in mediating the alterations to A/V-induced escape responses at 6 dpf were also assessed. Here, none of the co-treatments produced a detectable recovery to the reductions in A/V responsiveness caused by JZL 195. Overall, these

findings provide one of the first investigations examining the interactions between the eCS and its non-canonical receptor systems in vertebrate sensorimotor development.

Taken together, this work provides an overview which demonstrates that the activity of the eCS enzymes FAAH and MAGL are essential for different aspects of sensorimotor development in zebrafish, and provides insight towards the canonical and non-canonical cannabinoid receptor mechanisms that mediate eCS-related motor development.

Preface:

This thesis is an original work by Lakhan S. Khara. Approval for this study was obtained from the Animal Care and Use Committee: Biosciences, under the protocol AUP #00000816, and adhered to the Canadian Council on Animal Care guidelines of the humane use of animals for research purposes.

The results presented in chapter 3 and parts of the discussion in chapter 5 have been published as Khara, L.S., Amin, M.R. & Ali, D. W. "Inhibiting the endocannabinoid degrading enzymes FAAH and MAGL during zebrafish embryogenesis alters sensorimotor function" by the *Journal of Experimental Biology*. Published: May 2022.

The work in this accepted manuscript was conceptualized by L.S.K, and M.R.A. The data collection and analysis were performed by L.S.K. Methodology was developed by L.S.K in collaboration with M.R.A. Manuscript composition and writing was done by L.S.K. with review and editing support from D.W.A. Supervision and funding acquisition was done by D.W.A.

Acknowledgements:

To my supervisor Dr. Declan Ali, I would like to express my sincerest gratitude. Your compassion, guidance, patience, and support has helped shape me into the learner and mentor that I have become. I'm grateful for the opportunities that you've afforded to me during my time in your lab which has helped me grow immensely in terms of my academic abilities, my work ethic, and my capabilities as a leader. I'm thankful to have been able to work with you these past two and a half years, and aside from our shared scientific interests in neurobiology, it's great to know that we both also share a similar passion for running and cycling as well!

To the members of my supervisory committee: Thank you Dr. Ted Allison for helping me along the way in offering your research insights, writing guidance, and presentation advice through my time in grad school. Thank you Dr. John Chang for all your support going all the way back to when I was still an undergrad student taking all of your Zoology classes, to now when I have even been a TA to help teach your old lab course. I truly appreciate the mentorship that I've received from both of you over the past few years!

I'm very grateful for the many friends and colleagues here at the UofA, thank you to all the members of the Ali Lab: Ruhul, Hae-Won, Kazi, Sufian, Andrew, Parastoo, and Beibei, and to the members of other labs: Enezi, Arash, Aaron, Connor, and everyone else who I may not have mentioned here by name – it's been quite the ride, sharing the grad school journey with all of you. All the laughs, advice, insights, support, venting, and enjoyable moments have all been a pleasure. I'm thankful to have had the opportunities to work with and get to know all of you over the course of this degree. I think it would be a mild understatement to say that the past two and a half years have been crazy, but here we are. Though, it's a shame that COVID ruined our plans to make a tradition out of having our lab potlucks because I had some great dishes lined up that I never got to share!

There's no question as to whether I could be where I am without my loved ones. Thank you to my family at home for all your support through my journey so far. You have helped me and taught me a lot, and through everything, I have learned to keep an open mind towards what life gives and takes, and that strength, courage, and compassion will carry me forward.

To my dearest friends who have been part of my support system over the years: those that I've grown up with, the "Boons," the "Fellas," the "FoTC," and all the others who have been around me. Although our *fond* memories consist of a near endless list of things: the walks, the therapy sessions, sports, the MBM ice cream, overnight studying, hiking, the "Sunrise Classics," torturous running and cycling sessions, late-night McDonalds, and more, it's all been a blast. Thanks for always having each other's backs, thanks for all the memories we've shared, and here's to many more!

Table of Contents

List of Tables:

List of Figures:

List of Abbreviations:

μM – micromolar

2-AG – 2-arachidonoylglycerol

A/V – auditory/vibrational

AEA – anandamide

cAMP – cyclic adenosine monophosphate

CB1R – cannabinoid receptor 1

CB2R – cannabinoid receptor 2

CBD – cannabidiol

cm – centimeter

CNS – central nervous system

DAGL – diacylglycerol lipase

DMSO – dimethyl sulfoxide

dpf – days post-fertilization

eCB – endocannabinoid

eCS – endocannabinoid system

FAAH – fatty acid amide hydrolase

hpf – hours post-fertilization

Hz – hertz

LCMS – liquid chromatography and mass spectrometry

LMPA – low-melting point agarose

LTD – long-term depression

MAGL – monoacylglycerol lipase

mRNA – messenger ribonucleic acid

M-Cell – Mauthner cell

mg – milligram

min – minute

mL – milliliter

mm – millimeter

ms – millisecond

NAPE-PLD – N-acyl phosphatidylethanolamine-specific phospholipase D

nM – nanomolar

OEA – oleoylethanolamide

PEA – palmitoylethanolamide

PKA – protein kinase A

PTCH – Patched

qPCR - quantitative polymerase chain reaction

s – second

SEM – standard error of the mean

SHH – Sonic Hedgehog

SMO – Smoothened

SREBP – sterol regulatory-element binding protein

THC – Δ-9-tetrahydrocannabinol

TL – Tubingen Longfin

TRP – transient receptor potential

Chapter 1. Introduction

1.1 The endogenous cannabinoid system – introduction and history

Despite its evolutionary conservation and historical implications, the endocannabinoid system (eCS) remains a fascinatingly complex and elusive system. For most, hearing of the eCS quickly sparks a connection to cannabis and the cannabis plant: *Cannabis sativa*. This is especially apparent today with the growing interest and prevalence for cannabis, as societal, political and medical advancements continue; however, the use of cannabis actually dates back thousands of years. Cannabis has been documented in ancient texts indicating its uses in African, Asian and Middle Eastern regions in the pursuit of its therapeutic and euphoric capabilities, highlighting its historical influence throughout human history (Friedman and Sirven, 2017; Mathre, 2010; Russo, 2014). To illustrate this, some of the earliest cannabis preparations were used as herbal remedies to combat pain, rheumatism, seizures, and anxieties as far back as ~2700 BCE during the time of the Chinese Emperor Shen Nung, with similar uses being reported in India around ~1500 BCE as well. (Friedman and Sirven, 2017). From the history of these early periods, we see how humans had taken advantage of the neurobiological effects of cannabis without truly realizing how it is that our bodies are capable of responding to its influences (Russo, 2014). Thus, even without having a modern biological understanding of the eCS, the effects of cannabis were still partially understood by societies who utilized the plant's drug compounds (hereafter referred to as phytocannabinoids).

For a long time, the understanding of cannabinoids and their actions mostly lay within a familiarization for how cannabis can be used, with only a limited recognition as to why cannabis

exerts its effects on our bodies. It wasn't until the 1990s that the fundamental biology of the endocannabinoid system had really begun to take off, as Matsuda and colleagues cloned the first cannabinoid receptor in 1990 (Matsuda and Young, 1990). Following this discovery, a second cannabinoid receptor was cloned shortly thereafter (Munro et al., 1993). Due to their interactions with phytocannabinoids, the two receptors were aptly named cannabinoid receptor 1 and 2 (CB1R and CB2R), and these early findings quelled some of the mystery regarding how cannabis exerts many of its effects. These discoveries encouraged further investigations of cannabis; however, they also set the foundation towards building our understanding of the basic biology surrounding the eCS. As this foundation developed, many more discoveries were made along the way, and consequently, many intriguing questions towards the roles of the eCS have been pondered. As a result of this, the eCS is now implicated in a wide variety of physiological and developmental processes ranging from neurobiological development, metabolic activities, and immune function, but it's exact roles in these processes remains largely unknown, and is still a subject of rigorous study (Berghuis et al., 2007; Liu et al., 2016; Lu and Mackie, 2016; Martella et al., 2016; Pandey et al., 2009). With the goal of further unraveling the intricacies of the eCS, the work explored in this thesis aims to provide foundational information towards understanding the roles of the eCS, with a particular emphasis towards its involvement in early sensorimotor development.

1.2 The endocannabinoid system – overview

1.2.1 Endogenous cannabinoids (endocannabinoids)

Although phytocannabinoids represent the drug compounds of *C. sativa*, another class of cannabinoids known as endocannabinoids (eCBs) also exists. As the name suggests, eCBs are lipophilic cannabinoid compounds that are produced endogenously in biological systems. There are two main eCBs that act as eCS ligands: they are known as anandamide (AEA) and 2-arachidonoylglycerol (2-AG). AEA was first identified as an endocannabinoid in work studying the pig brain (Devane et al., 1992). The name "anandamide" is derived from the Sanskrit word "*Ananda,"* meaning "bliss," which calls back to the origins of cannabis and its relation to the eCS. After AEA was first identified, the identification of 2-AG followed shortly after, where it was first isolated from canine intestines, and from the brain of rats (Mechoulam et al., 1995; Sugiura et al., 1995). The early work studying these endocannabinoids found that they act similarly to phytocannabinoids in terms of receptor activity and behavioral effects.

With regard to the regulation of eCBs, they are produced and degraded based upon physiological demand; therefore, the levels of eCBs must be tightly modulated by a set of enzymes that control their synthesis and degradation. Synthesis of the eCBs is mediated by the enzymes N-acyl phosphatidylethanolamine-specific phospholipase D (NAPE-PLD) and diacylglycerol lipase (DAGL) for AEA and 2-AG respectively (Lu and Mackie, 2016). Furthermore, AEA is primarily broken down by the enzyme fatty acid amide hydrolase (FAAH), while 2-AG is degraded by monoacylglycerol lipase (MAGL) (Blankman et al., 2007; Cravatt et al., 1996). The enzymatic regulation of eCBs and the related signaling is outlined in Fig. 1.1.

With respect to the cannabinoid receptors of the eCS, AEA is known to preferentially bind to CB1R, while 2-AG has affinity towards both CB1R and CB2R (Zou and Kumar, 2018). A consequence of FAAH/MAGL inhibition is increased levels of AEA or 2-AG within the central nervous system (CNS), and it has been suggested that this represents an effective way to elevate eCB signaling, thereby upregulating cannabinoid receptor activation within the eCS (Gobbi et al., 2005; Griebel et al., 2015; Long et al., 2009a). Furthermore, indirect upregulation of eCB signaling by targeting FAAH and MAGL has been a method used by the Ali Lab to further study the developmental role of the eCS in zebrafish (Sufian, 2020).

1.2.2 Canonical cannabinoid receptors

Both the CB1R and CB2R cannabinoid receptors are inhibitory G-protein-coupled-receptors with 7 transmembrane domains (Galiègue et al., 1995). The CB1Rs are abundantly localized to regions of the CNS, with high messenger ribonucleic acid (mRNA) expression in the hippocampus, hypothalamus and telencephalon, and abundant receptor density within the forebrain, basal ganglia, brainstem, and spinal cord (Herkenham et al., 1991; Julian et al., 2003; Lam et al., 2006). CB2Rs on the other hand, are more extensively found in non-CNS regions such as the spleen, skeletal system, and liver, indicating their prevalence in immune and metabolic activities (Howlett, 2002; Munro et al., 1993). However, this differential distribution is not always the case, as CB1Rs are also located in non-CNS regions such as the gastrointestinal tract and liver, and CB2Rs are also present in the CNS in areas such as the hippocampus and in

glial cells, albeit at relatively low abundances when compared with CB1Rs. (Maccarrone et al., 2015; Onaivi et al., 2012; Stempel et al., 2016; Zou and Kumar, 2018).

In the CNS, cannabinoid receptors are typically located on presynaptic terminals, where the activation of these receptors initiates an inhibitory signaling mechanism which functions to modulate synaptic activity (Fig. 1.1). This localization of cannabinoid receptors to presynaptic sites is important because eCB signaling works in a retrograde fashion, where eCBs will first be released from postsynaptic cells, to which they will then bind to and activate the presynaptic cannabinoid receptors (Ohno-Shosaku et al., 2001; Tanimura et al., 2010). By activating cannabinoid receptors, cannabinoids modulate synaptic activity with downstream mechanisms that typically involve a suppression of neuronal activity (Mackie, 2008; Zou and Kumar, 2018). This can occur through the blockage of voltage-gated Ca^{2+} channels, which decreases the inflow of Ca^{2+} into the presynaptic terminal, resulting in decreased neurotransmitter release into the synaptic cleft. Cannabinoid receptor activation can also lead to the inhibition of adenylyl cyclase, which results in decreased production of cyclic adenosine monophosphate (cAMP), leading to decreased activity of protein kinase A (PKA), which would be associated with the downregulation of a number of biological processes (Fig. 1.2).

As already mentioned, eCBs are produced and broken down based on the physiological and homeostatic demands of the overall system (Lu and Mackie, 2016). Thus, during periods of high excitatory synaptic activity, eCBs will be synthesized and released across the synaptic cleft to bind to cannabinoid receptors, initiating inhibitory signaling cascades to suppress neuronal

activity, with the ultimate result being decreased neurotransmitter release (Di Marzo et al., 1994; Ohno-Shosaku et al., 2001; Stella and Piomelli, 2001). Although the interactions of eCBs with the CB1R and CB2R represents the canonical and most well characterized mechanisms of eCS activities, phytocannabinoids and eCBs are also known to interact with additional receptor systems which include a G-protein coupled receptor known as GPR55, as well as a variety of different ion channels such as TRPA1, TRPV1, and receptors found in developmental signaling pathways (Fig. 1.2) (Amin and Ali, 2019; Khaliullina et al., 2015; Zygmunt et al., 1999). These alternative receptor systems are broadly referred to as non-canonical cannabinoid receptors.

1.2.3 Transient receptor potential ion channels as cannabinoid receptors

The transient receptor potential (TRP) family of ion channels are well known for being involved in sensory systems and are often located on the neurons of sensory-related structures. In sensory systems, TRP channels typically play a role in the detection and transduction of different stimuli, as activation of these ion channels involves the influx of positively charged ions (Germanà et al., 2018). TRP channels are also known to be partially involved in neurobiological processes associated with the eCS (Muller et al., 2019). For instance, in the CNS of mice, AEA activates TRPV1 channels within the brain to induce long-term depression (LTD) in hippocampal synapses (Chávez et al., 2010). In zebrafish, a variety of TRP channels are found in different sensory structures including the retina, taste organs, olfactory epithelium, and the hair cells of both the inner ear and lateral line system (Germanà et al., 2018). The presence of TRP channels in sensory organs is significant because cannabinoids (both endogenous and phytocannabinoids) have an affinity for, and bind to and activate TRP channels (Morales et al., 2017; Muller et al., 2017). Both AEA and 2-AG are capable of activating TRP channels, leading to increased Ca^{2+}

currents (Watanabe et al., 2003). Consequently, this suggests that the development and function of neurobiological processes and sensory systems may be susceptible to altered eCS activity, as critical sensory structures are abundant in TRP channels which are capable of interacting with endocannabinoids. Because TRP channels are so intimately related to sensory function, there is a need to further understand the connection between the eCS and sensorimotor processes.

1.2.4 Sonic Hedgehog signaling and its interactions with cannabinoid signaling

The Sonic Hedgehog (SHH) signaling pathway is a critical pathway for early developmental processes such as cell differentiation, organogenesis, and neural tube formation (Choudhry et al., 2014; Ryan and Chiang, 2012). Vertebrate SHH signaling mainly occurs in the primary cilium of cells and typically involves binding of the SHH ligand to the Patched (PTCH) receptor, leading to its internalization and consequent activation of the transmembrane protein called Smoothened (SMO). SMO is normally suppressed in the absence of SHH-PTCH binding. Activation of SMO initiates a downstream signaling cascade that involves activation of Gli transcription factors to influence the transcription of SHH-related genes (Fig. 1.3). This represents the most typical form of SHH signaling known as canonical SHH signaling, whereas non-canonical SHH signaling involves the activation of Gli transcription factors in the absence of the SHH ligand, and is thought to function independently from the activation of SMO (Pietrobono et al., 2019).

Recent studies have found that eCBs and phytocannabinoids can act as potent inhibitors of SMO, causing a disruption in SHH signaling. An *in vitro* analysis has found that eCBs inhibit SHH signaling through suppressing the activity of SMO (Khaliullina et al., 2015). This study also used

a FAAH inhibitor to demonstrate that upregulation of eCB signaling results in a decrease in SHH activity. Similar findings were shown by Fish and colleagues, who used zebrafish to show that cannabinoid-induced microphthalmia could be rescued with *Shh* mRNA injections, or by treatment with CB1R antagonists (Fish et al., 2019). Likewise, another study also found that *Shh* mRNA injection prevents behavioral alterations caused by inhibiting the eCS enzymes FAAH and MAGL (Boa-Amponsem et al., 2019). An overview of the proposed signaling of the SHH pathway and its interactions with cannabinoids is depicted in Fig. 1.3. Previous investigations within the Ali Lab have also exemplified the developmental interactions of cannabinoids with the SHH pathway in how the SHH pathway may mediate some of the teratogenic effects of cannabidiol (CBD) (Son, 2021). These findings provide evidence to support that there is interplay between the eCS and SHH signaling, where activity of the eCS influences components of the SHH pathway, highlighting that both the eCS and SHH signaling together play significant roles in neurobiological development.

1.3 Zebrafish as a model organism for studying vertebrate development

1.3.1 Overview of the zebrafish model

Zebrafish (*Danio rerio*) are a freshwater species of teleost fish that have been used in different fields of biology for a variety of different purposes, serving as an extremely useful model organism. For studying aspects of vertebrate development, the zebrafish model has several advantages. First, zebrafish can be housed in large numbers and are inexpensive. They can also breed frequently, where large quantities of fertilized eggs are easily obtainable, making high-throughput studies far less cumbersome than in animal models which produce fewer offspring

during each brood (Kimmel et al., 1995; Lessman, 2011). Zebrafish chorions are transparent, and the embryos themselves are semi-transparent, meaning that their development is very easily observable, which would normally be problematic in mammalian models where the embryonic development of animals such as rats or mice can only be directly observed through invasive methods. Additionally, because zebrafish are externally fertilized and because they do not develop within the mother, researchers can access the developing animals with ease. This simplifies studies that are interested in observing the effects of different compounds or agents, as they can be directly applied to the water containing the animals (Achenbach et al., 2020; Zhang et al., 2015). Furthermore, this also makes certain imaging and molecular techniques easier to perform, as whole-animal and whole-mount options may be much more efficient than being required to isolate or section different cells or tissues (Thisse and Thisse, 2008).

Despite the many advantages, using zebrafish as a model organism also has drawbacks which must be acknowledged. Although external fertilization and the lack of a maternal connection can be an advantage, it is also a limitation if the embryonic-placental interactions are a crucial factor that must be considered, illustrating a drawback when comparing embryonic findings in zebrafish to mammalian models or humans. Thus, great care must be taken when translating or extrapolating findings to mammalian organisms. Additionally, while exposure to toxicants or pharmacological compounds is simplified in zebrafish embryos, the chorion membrane acts as a physical barrier, and thus presents a clear limitation, as it may be challenging to ascertain exactly how much of a compound crosses the chorion membrane to reach the tissues. This has been studied to an extent, but the exact permeability of the chorion to different compounds may be

unclear in some cases, as this may vary depending on the composition and solubility of different compounds (Wilson et al., 2020; Zhang et al., 2015).

1.3.2 Zebrafish embryonic development

Embryonic development in zebrafish occurs very rapidly and is classified into 7 stages: zygote, cleavage, blastula, gastrulation, segmentation, pharyngula, and hatching (Fig. 1.4) (Kimmel et al., 1995). Gastrulation is a very critical and sensitive period of embryonic development where the controlled rearrangement and movement of cells produces three embryonic germ layers: the ectoderm, endoderm, and mesoderm (Rohde and Heisenberg, 2007). In zebrafish, gastrulation takes place approximately between 5.25 hours post-fertilization (hpf) and 10.75 hpf (Kimmel et al., 1995). During gastrulation, the development of the notochord and muscle precursors begins. During segmentation, which takes place between 10-24 hpf, the overall body structure becomes more established as the notochord further develops and the somites give rise to muscle cells, leading to a morphological appearance that now more closely resembles an aquatic vertebrate (Ingham and Kim, 2005). Importantly, these early periods depend on a variety of developmental signaling mechanisms to ensure that normal development occurs properly. Between 2 and 3 days post-fertilization (dpf), hatching occurs, and after 3 dpf, the animals are typically referred to as larvae. Larval development continues until the fish reach adolescence at ~4 weeks post-fertilization, at which point they are then referred to as juveniles (Parichy et al., 2009). After ~11 weeks post-fertilization, the animals will be considered adults once they gain the ability to reproduce and possess viable male/female gametes. At that point, they will also have developed secondary sex characteristics (Parichy et al., 2009). Overall, many facets of zebrafish development have been well characterized, and they are often relied on for studies that

investigate questions regarding the mechanisms of physiological and developmental processes due to their numerous advantages in usage, and from the wide array of different techniques that can be utilized.

1.3.3 Zebrafish locomotor and sensorimotor development

Zebrafish possess a wide variety of locomotor and sensorimotor behaviors which are present at different periods of their early life stages, and because of this, zebrafish are a useful model for studying neuromuscular development, and for assessing the development of sensorimotor function (McArthur et al., 2020; Sztal et al., 2016). Starting at ~18 hpf, zebrafish embryos exhibit spontaneous bursts of contractile tail movements while still encased within their chorion (Colwill and Creton, 2011a; de Oliveira et al., 2021). This motor activity provides one of the first indicators of functional locomotor development, representing the early synaptic connections within the neuromuscular system (Grunwald et al., 1988; Saint-Amant, 2006).

At 2 dpf, zebrafish embryos exhibit incredibly rapid escape behaviors in response to mechanical stimuli (Saint-Amant and Drapeau, 1998). This response is a swift tail flip that is typically referred to as a short latency C-start escape response, which is a hardwired reflex response that is crucial for survival (Colwill and Creton, 2011b). This response is dependent on the reticulospinal neuron circuits of the hindbrain with a significant excitatory input from the pair of Mauthner cells (M-cells) and their homologues, MiD2cm/MiD3cm, whose activation is essential in triggering an escape response (Burgess and Granato, 2007; Kimmel et al., 1990). Escape responses begin with a C-shaped bend of the tail in the direction away from the stimulus,

followed by bursts of swimming to propel the animal away from the perceived threat. This escape response can be elicited by mechanical stimuli such as a light touch to their head. At this early time point (2 dpf), embryos are not yet capable of performing continuous beat-and-glide swimming, as this develops between 3 and 4 dpf, meaning that the swimming elicited by mechanical stimuli can be observed from its onset, and tracked until it comes to a stop (Drapeau et al., 2002).

In addition to mechanical stimuli, zebrafish also display short latency C-start escapes in response to auditory/vibrational (A/V) stimuli (Kohashi et al., 2012). Unlike the locomotor behaviors at 2 dpf, this A/V response is not present until ~3 dpf, but it matures and becomes highly functional as early as 6 dpf, as it is thought that auditory function and receptiveness becomes much more robust during this short period of time due to a large increase in the number and density of inner ear hair cells (Lu and DeSmidt, 2013). Similar to touch-evoked escape however, the M-cells are required for the proper function of this sensorimotor response, as they communicate the efferent response, and are needed for the recruitment of motor systems (Bang et al., 2002; Burgess and Granato, 2007; Kohashi et al., 2012). Thus, zebrafish embryos and larvae are quite useful for studying functional sensorimotor development.

1.3.4 Zebrafish as a model for studying the developmental role of the endocannabinoid system

When it comes to studying eCS, zebrafish have been an attractive animal model due to the high evolutionary conservation of the eCS (Elphick, 2012; Krug and Clark, 2015). In terms of the

cannabinoid receptors, zebrafish and humans possess a degree of sequence identity, where zebrafish and humans share a sequencing identity of 69% for nucleotides and 73.6% for the amino acid sequence identity in the *CB1* gene. (Lam et al., 2006). The amino acid sequencing of the *CB2* gene between zebrafish and humans however is less similar, as they only share 39% of their amino acid sequence identity (Rodriguez-Martin et al., 2007). These patterns in sequence identities for both of the cannabinoid receptors are also very similar when compared with rats and mice (Lam et al., 2006; Rodriguez-Martin et al., 2007). Overall, zebrafish possess a functional eCS, complete with nearly all the major endogenous receptors, enzymes, and ligands found within the eCS of other vertebrates (Bailone, 2022).

Due to the utility of zebrafish as a model for studying drug toxicology, zebrafish have been used in a variety of studies to assess the effects of phytocannabinoids and their potential impacts through the eCS (Ellis, 2019). Previous studies in the Ali Lab have observed the effects of phytocannabinoids and the role of the eCS by exposing embryonic zebrafish to different phytocannabinoids to overstimulate the eCS during early development. In brief, exposure to Δ-9-tetrahydrocannabinol (THC) and CBD alters synaptic activity of the neuromuscular junction and leads to aberrant development of motor neurons and reticulospinal neurons (Ahmed et al., 2018; Amin et al., 2020). Another group found that exposure to CBD in zebrafish caused morphological defects and resulted in behavioral alterations (Pandelides et al., 2020). Furthermore, hypolocomotion is also observed in zebrafish that have been exposed to phytocannabinoids such as THC, (-)THC, and CBD during embryonic and larval development (Akhtar et al., 2013; Amin et al., 2020; Carty et al., 2018; Kanyo et al., 2021).

As the effects of phytocannabinoids have been studied in zebrafish, so too has the developmental role of the eCS. Studies that perturb aspects of the endogenous system demonstrate a variety of developmental alterations which are similar to those found in zebrafish phytocannabinoid studies. There have been notable studies that employ the use of morpholino injections to knock down the expression of specific eCS genes to study the role of the eCS in neuronal and motor development. First, the study by Watson and colleagues demonstrated that a *CB1* morpholino results in defective axonal growth of reticulospinal neurons, along with dysfunctional pathfinding of axons across the midline (Watson et al., 2008). Another study which used a *dagla* morpholino also found that axonal growth across the midline was defective, where fewer axons established proper contacts in the midbrain-hindbrain regions (Martella et al., 2016). Zebrafish have also been used to study the role of the eCS in growth and metabolism. Exposure to AEA led to an upregulation of eCS activity in which the genetic expression of the sterol regulatory-element binding protein (SREBP), and the genetic expression of the insulin-like growth factors IGF-1 and IGF-2 were increased, indicating that eCB signaling during early periods may somehow interact with the regulation of factors involved in larval growth (Migliarini and Carnevali, 2008).

Studies have also found that motor and behavioral alterations arise from perturbations of the eCS, as embryonic inhibition of FAAH and MAGL causes behavioral alterations that are observed in animals that have developed into their juvenile stage (Boa-Amponsem et al., 2019). Additionally, research conducted in the Ali Lab has also used zebrafish to demonstrate that the eCS is involved in neuronal and motor development, as blocking the CB1R and CB2R during embryogenesis alters the morphology of primary motor neurons and leads to hypolocomotion

(Sufian et al., 2019). Similar findings have also been reported through inhibiting the catabolic enzymes FAAH and MAGL (Sufian et al., 2021). In their 2021 study in particular, Sufian and colleagues observed defective branching in primary and secondary motor neurons in embryonic zebrafish, and decreased free swimming in zebrafish larvae. These findings helped lay the initial groundwork for understanding the roles of FAAH and MAGL as it pertains to zebrafish motor development. However, these findings primarily focus on basic neuronal characteristics and basal locomotive capabilities. Thus, our current understanding of how eCB signaling is involved in the overall development and function of more complex motor and sensorimotor programs is still limited. Although more expansive assessments will be required to further examine functional development, the previous findings discussed above have utilized the zebrafish model to greatly advance our foundational knowledge of the eCS, and given the current state of the literature, it is clear that this system plays a significant role in different aspects of homeostatic and neurobiological development.

1.4 Research objectives

Despite the previous findings, there is still much to explore regarding how eCB signaling contributes to aspects of motor development and function during early life. Although the previous investigations have shown that perturbations of the eCS influences motor development, these studies have primarily examined neuronal and locomotor characteristics, thus it remains unclear how some of these alterations truly influence the functionality of motor or sensorimotor activities. Therefore, to address this gap in the current literature, the purpose of my thesis is to explore how an early perturbation of the eCS - by inhibiting the enzymes FAAH and MAGL - impacts functional sensorimotor development in young zebrafish. Furthermore, to extend this

aim, this work also seeks to identify the potential receptor systems that are involved in interacting with the eCS in sensorimotor development.

To investigate this overall purpose, my thesis is composed of two research objectives:

1. **Overstimulate the endocannabinoid system during zebrafish embryogenesis by inhibiting the enzymes that degrade endocannabinoids, then assess how locomotor and sensorimotor function has been affected during embryonic, larval, and juvenile stages.**

Rationale: Previous studies make use of the pharmacological compounds URB 597, JZL 184, and JZL 195 as selective inhibitors of FAAH and MAGL. Given the findings of these studies, it is clear that these are tools which can be used to upregulate or overstimulate eCB signaling. Furthermore, since the previous literature that investigated developmental exposures to phytocannabinoids demonstrated a range of alterations to neurobiological development, including neuronal and synaptic defects, motor deficits, and changes to sensory activities, targeting the endogenous components of the eCS is critical to further understand the role of the eCS in the development of functional sensorimotor activities. Thus, I hypothesize that perturbing the eCS during embryogenesis by using inhibitors of the eCS catabolic enzymes FAAH and MAGL will upregulate eCB signaling. I also hypothesize that an upregulation of eCB signaling during embryogenesis will reduce locomotor activity and alter sensory responsiveness in which the zebrafish C-start escape response will be negatively impacted.

2. **Identify which receptor systems are involved in mediating the sensorimotor alterations caused by the inhibition of endocannabinoid degradation enzymes**

Rationale: Although prior studies have identified that phytocannabinoids and eCBs interact with multiple different receptor systems and signaling pathways, how these receptor systems and pathways interact with the eCS to facilitate normal neurobiological development is largely unknown. More specifically, it is unclear whether there is interplay between the eCS and non-canonical cannabinoid receptor systems when it comes to the motor and sensorimotor aspects of early development. Thus, I first hypothesize that FAAH and MAGL inhibition will broadly result in an increased activation of the receptors which bind to the endocannabinoids AEA and 2-AG. From the known binding affinities of AEA and 2-AG, I also hypothesize that deficits in C-start escape behaviors induced by FAAH/MAGL inhibition will be mediated through preferential interactions with the CB1R, as well as TRP channels, and the SHH signaling pathway.

In pursuit of these research objectives, this thesis investigates the important role that the eCS plays in sensorimotor development. To do this, sensorimotor assessments were studied at a range of time points during early periods of zebrafish development, and the effects of eCS perturbation on these sensorimotor activities was examined. Importantly, this work supports and further expands upon the foundational information pertaining to the neurobiological role of the eCS by first examining an array of specific behavioral activities, and by investigating the role of canonical and non-canonical cannabinoid receptors in mediating functional sensorimotor development.

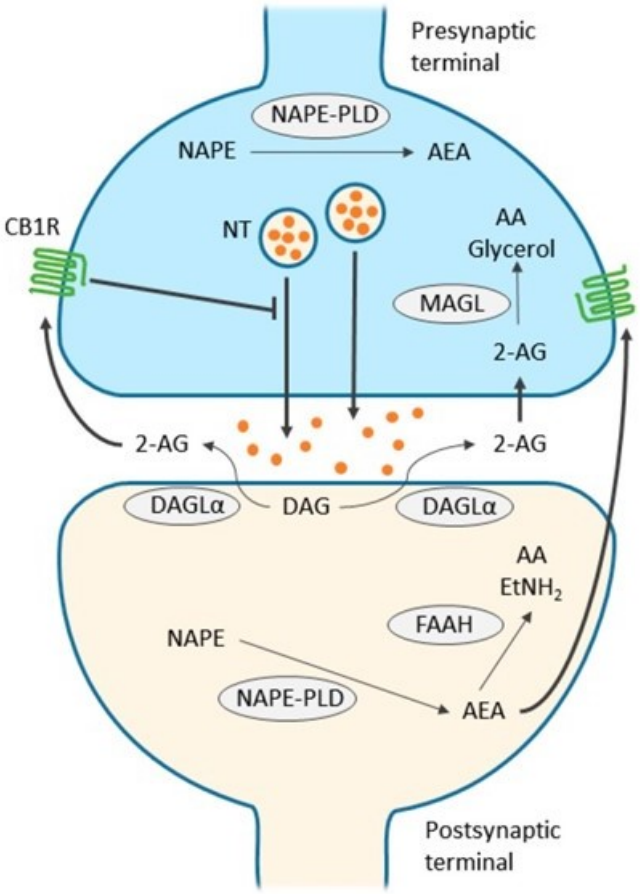
Presynaptic terminal
NAPE-PLD
NAPE
AEA
CB1R
NT
AA
Glycerol
MAGL
2-AG
2-AG
2-AG
DAGLα
DAG
DAGLα
AA
EtNH2
FAAH
NAPE
NAPE-PLD
AEA
Postsynaptic terminal

Figure 1.1: Schematic of endocannabinoid synthesis, degradation, and signaling at a synapse. The synthesis and degradation of the endocannabinoids (eCBs) anandamide (AEA) and 2-arachidonoylglycerol (2-AG) are tightly regulated by the anabolic enzymes known as N-acyl phosphatidylethanolamine-specific phospholipase D (NAPE-PLD) and diacylglycerol lipase (DAGL) that are involved in synthesizing AEA and 2-AG respectively. The catabolic enzymes fatty acid amide hydrolase (FAAH) degrades AEA, while monoacylglycerol lipase (MAGL) degrades 2-AG. These enzymes regulate the retrograde signaling of eCBs, where the eCBs are synthesized and released from a postsynaptic cell into the synaptic cleft. The eCBs then bind to and activate cannabinoid receptors located on presynaptic terminals to modulate neurotransmitter (NT) release and synaptic activity. This figure was adapted from Zou and Kumar, (2018).

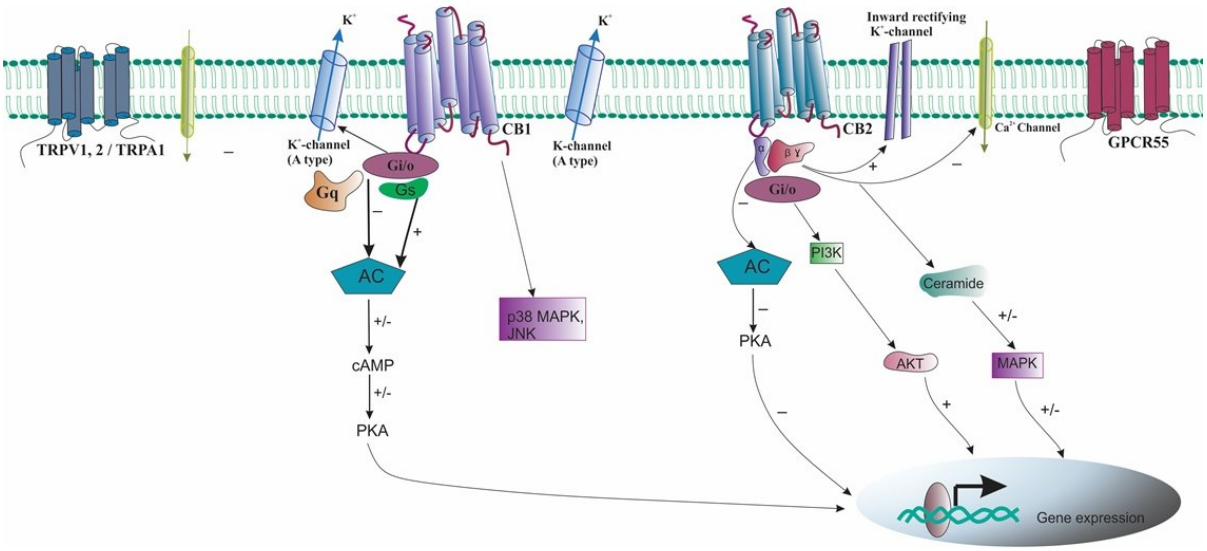
TRPV1, 2 / TRPA1
K+
K+-channel (A type)
Gi/o
Gq
Gs
CB1
K+
K-channel (A type)
Inward rectifying K+-channel
CB2
Ca2+ Channel
GPCR55
AC
cAMP
PKA
p38 MAPK, JNK
PI3K
Ceramide
AKT
MAPK
Gene expression

Figure 1.2: Endocannabinoids interact with a variety of receptor mechanisms that include but are not limited to the CB1R and CB2R cannabinoid receptors. Cannabinoids are known to be capable of interacting with different receptor systems with notable examples being the CB1R/CB2R canonical cannabinoid receptors, TRPV and TRPA families of cation channels, and GPR55. Not all intracellular mechanisms that result from cannabinoid binding are known, but the most well characterized effects of cannabinoid activity involve inhibitory signaling cascades that begin with the downregulation of adenylyl cyclase (AC) leading to decreased production of cyclic adenosine monophosphate (cAMP). Typically, this results in reduced activity of protein kinase A (PKA), which normally is involved in modulating the activity of downstream factors in different biological processes. This figure was adapted from Amin and Ali, (2020).

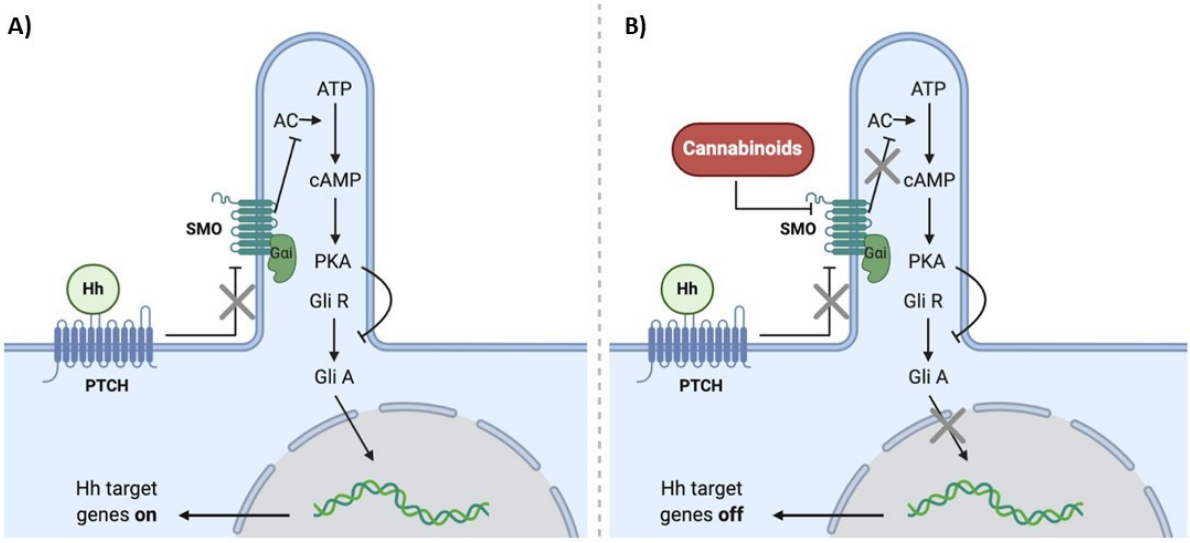
A)
ATP
AC
cAMP
SMO
Gαi
PKA
Hh
Gli R
PTCH
Gli A
Hh target
genes on
B)
ATP
AC
Cannabinoids
cAMP
SMO
Gαi
PKA
Hh
Gli R
PTCH
Gli A
Hh target
genes off

Figure 1.3: Overview of mechanisms of canonical Sonic hedgehog (SHH) signaling and its proposed interactions with cannabinoids. (A) Under normal conditions within the primary cilium of vertebrates, the pathway becomes stimulated by the SHH ligand. The Patched (PTCH) receptor normally suppresses the activity of Smoothened (SMO), however when SHH binds to the PTCH receptor, the suppression of SMO is relieved, and SMO now becomes active. Once SMO is active, an intracellular signaling cascade is initiated, where the activity of adenylyl cyclase (AC) is inhibited, leading to the decreased production of cyclic adenosine monophosphate (cAMP). Decreased cAMP results in reduced activity of protein kinase A (PKA). When PKA activity is reduced, this leads to Gli transcription factors being predominantly in their active (Gli A) state, where they will translocate into the nucleus leading to an upregulated transcription of SHH target genes. **(B)** Proposed mechanisms of SHH signaling in the presence of cannabinoids. Cannabinoids are believed to inhibit SMO by directly binding to it causing the opposite effect of canonical SHH activation. When cannabinoids bind, PKA becomes more active through an increase in AC activity, which leads to a reduction in Gli A translocation, ultimately resulting in a downregulation of SHH target genes. This image was created using BioRender.com by Son, (2021), and is originally adapted from Fish et al., (2019).

From: Kimmel et al. Stages of embryonic development of the zebrafish Dev. Dyn. 203:253-310, 1995

Figure 1.4: Early developmental stages of zebrafish embryonic development. The rapid development of zebrafish (*Danio rerio*) is depicted by Kimmel et al., (1995), where the morphological changes are outlined over the first 48 hours of embryogenesis. During this period of 48 hours, the developmental stages of zygote, cleavage, blastula, gastrulation, segmentation, and pharyngula occurs, where hatching typically occurs soon after 48 hours post-fertilization (hpf). This image was adapted from Kimmel et al., (1995).

Chapter 2. Materials and methods

2.1 Animal care

The animals used in this study were wild type zebrafish (*Danio rerio*) of the Tubingen Longfin (TL) strain. All animal housing and experimental procedures in this study were approved by the Animal Care and Use Committee of the University of Alberta (AUP #00000816) and was in compliance with the Canadian Council on Animal Care guidelines of the humane use of animals for research purposes. For breeding and egg collection, adult male and female zebrafish were placed in breeding tanks on the evening before eggs were required. The following morning, eggs were collected immediately after fertilization. Embryos and larvae were housed in a 28.5°C incubator set on a 12-hour light/dark cycle. Embryos and larvae were provided with embryo media (60 mg/ml Instant Ocean, pH 7.0).

2.2 Pharmacological drug exposure paradigm

The main pharmacological compounds used in this study (all obtained from Adooq Bioscience, CA, USA) are the selective FAAH inhibitor URB 597 (Catalog Number: A11049) at the concentrations of 1, 2, 5, 10, and 20 μM, the selective MAGL inhibitor JZL 184 (Catalog Number: A12747) at the concentrations of 1, 2, 5, 10, and 20 μM, and the dual FAAH/MAGL inhibitor JZL 195 (Catalog Number: A12390) at the concentrations of 1, 2, and 5 μM. A schematic outlining the enzyme targets of these compounds is depicted in Fig. 2.1. Fewer concentrations of JZL 195 were used due to it having similar effects as the combined treatment with both URB 597 and JZL 184 (Figs. 3.7 & 3.8). In chapter 4 of this thesis, animals were co-treated with the CB1R antagonist AM 251 (Selleck Chemicals, TX, USA, Catalog Number:

S2819), the CB2R antagonist AM630 (Adooq Bioscience, CA, USA, Catalog Number: A14993), the TRPA1/TRPV1/TRPM8 inhibitor AMG 9090 (Alomone Labs, Jerusalem, Israel, Catalog Number: A-300), or the SMO agonist purmorphamine (Sigma-Aldrich, MO, USA, Catalog Number: SML0868). The concentrations used for these four drugs were 10 nM for AM 251, 1 μM for AM 630, 0.01 μM for AMG 9090, and 5 μM for purmorphamine. All compounds listed here were dissolved in dimethyl sulfoxide (DMSO), and 0.1% DMSO was used as the vehicle control. Drug exposures took place immediately after egg fertilization until 24 hpf, effectively spanning from ~0-24 hpf (Sufian et al., 2021). This exposure paradigm is outlined in Fig. 2.2. Embryos were exposed to compounds via the embryo media. At 24 hpf, all exposure media was washed-out and replaced with fresh embryo media. Following the exposure period, animals were allowed to develop until needed for further experiments at the ages of 1-6 dpf for embryos and larvae, and 8-10 weeks for juvenile animals.

2.3 Spontaneous coiling activity at 1-day post-fertilization

At 1 dpf, the assessments of spontaneous coiling activity were performed using DanioScope 1.1 (Noldus, Wageningen, The Netherlands) to analyze video recordings of embryos still encased within their chorion membrane (de Oliveira et al., 2021; Zindler et al., 2019). Video recordings of the 1 dpf embryos were taken under a dissecting microscope connected to a high-speed camera (AOS S-PRI 1995, AOS Technologies, Dättwil, Switzerland). This motor activity was assessed immediately after the wash-out of exposure compounds. Spontaneous coiling activity (%) was measured to indicate the proportion of time that embryos were actively contracting, while the burst count/min represents the mean number of contractions performed by embryos averaged per minute. This experiment was performed in chapter 3 of this thesis.

2.4 Escape swimming performance at 2 days post-fertilization

To assess escape swimming following a C-start escape response, individual 2 dpf embryos were positioned in the center of a 140 mm Petri dish containing embryo media. The Petri dish was set on top of an infrared backlight source to be viewed by a Basler GenICam scanning camera (Basler acA1300-60gm) with a 75 mm f2.8 C-mount lens, provided by Noldus. Escape swimming in zebrafish embryos was triggered by delivering an acute mechanical stimulus to the head of the embryo by using a thin fishing line (Berkley Fishing, Spirit Lake, IA, USA; model # BGQS60C-15). Each embryo was tested alone in this open field to minimize the potential interactions with other fish, and to avoid any obstacles in the swimming paths. Swimming performance was analyzed using the movement tracking software EthoVision XT-11.5 (Noldus, Wageningen, The Netherlands). Mean swimming distance (cm) and mean swimming velocity (cm/s) were analyzed as metrics of locomotion when assessing escape swimming performance. This experiment was performed in chapter 3 and in chapter 4 of this thesis.

2.5 Embedded escape response assessments at 2 days post-fertilization

To assess parameters that represent the characteristics of the initial C-start escape response, embryos at 2 dpf were partially immobilized using 2% low-melting point agarose (LMPA) at 26-30°C. The LMPA gel was cut away from the tails of the embryos allowing for the tail's full range of motion, while leaving the head embedded in place – similar to methods used previously (Shan et al., 2015). The embryos were immersed in embryo media and were allowed to acclimate for 20 minutes. Mechanical stimuli were applied by ejecting a 15 ms pulse of 2% phenol red

(Sigma-Aldrich) from a Picospritzer II (General Valve Corporation). The pulse was delivered through borosilicate glass micropipettes (Stutter Instrument; O.D.: 1.2 mm, I.D.: 094 mm, length: 10 cm), which were pulled using a Flaming/Brown Stutter Instrument micropipette puller (Stutter Instrument model P-97). The pipettes were positioned above the embryo's otolith, and delivered a single acute stimulus to the head, which evoked a C-start tail flip. This behavior was video recorded using the AOS S-PRI 1995 high-speed camera noted in section 2.3.

Video recordings were analyzed using the motion analysis software ProAnalyst (Xcitex Inc., Woburn, MA, USA). Focusing on the C-shaped bend of the embryo's tail, the following parameters were assessed: latency to initiate C-start escape response (ms), maximum speed of tail contraction (mm/ms), maximum acceleration of tail contraction (mm/ms^2), angle of C-bend (degrees), time to achieve maximum C-bend angle (ms), and angular velocity (degrees/ms). This experiment was performed in chapter 3 of this thesis.

2.6 Assessing the responsiveness to auditory/vibrational stimuli at 3-6 days-post fertilization

Embryos and larvae aged 3, 4, 5, and 6 dpf were assessed for their responsiveness to auditory/vibrational (A/V) stimuli in a manner similar to previous methods (Ahmed et al., 2018; Kohashi et al., 2012). Six fish were placed into a 35 mm x 10 mm Petri dish containing embryo media and were allowed to acclimate for 20 minutes prior to the application of the stimulus. The A/V stimulus was created using Audacity (version 2.2.1) to generate a sawtooth waveform audio tone of 500Hz at 95-100 decibels – measured at its source – and was played through a set of

computer speakers (Logitech Z150, Logitech, Newark, CA, USA). Escape responses triggered by the A/V stimulus were video recorded using an AOS S-PRI 1995 high-speed camera. Following the delivery of the A/V stimulus, the proportion of animals that performed a short latency C-start escape in response to the stimulus was recorded, and the auditory response rate (%) was then determined from the proportion of responding animals. This experiment was performed in chapter 3 and in chapter 4 of this thesis.

2.7 Assessment of the responsiveness to auditory/vibrational stimuli in 8–10-week-old juveniles

Juvenile zebrafish between the ages of 8 and 10 weeks were used for A/V response assessments. This experiment used an identical set-up in terms of 20-minute acclimation period, stimulus delivery, and video recording as the larval assessments, however, the juvenile fish were tested individually and were placed in a modified 120 mL glass specimen jar (Fisher Scientific) filled with 50 mL of 28.5°C dechlorinated water. This set-up was used as opposed to a Petri dish to appropriately accommodate for the increased size of the juvenile animals. This experiment was performed in chapter 3 of this thesis.

2.8 Statistics

All experimental replicates represent separate cohorts of fish which were obtained from independent breeding sets. All data and statistical analyses were performed using GraphPad Prism (version 9.2.0., GraphPad Software, San Diego, CA, USA). Normality of data was examined using the Shapiro-Wilk test. In chapter 3 of this thesis, all data values are reported as

mean values ± standard error of the mean (SEM). For statistical testing, One-Way ANOVA followed by Dunnett's multiple comparisons test against the 0.1% DMSO vehicle control was performed to determine statistical differences ($p<0.05$). For the notation of statistical significance, * indicates the treatment groups which are significantly different from the vehicle control group where: * $p<0.05$, ** $p<0.01$, *** $p<0.001$.

In chapter 4 of this thesis, the data for the 2 dpf escape response experiments (Figs. 4.1-4.4) did not pass the Shapiro-Wilk normality test, and therefore was treated as non-parametric. Thus, the results in Figs 4.1-4.4 are presented as box-and-whisker plots where the median value is represented by the horizontal line within each box, while the box around the median indicates the interquartile range. Error bars (whiskers) indicate the maximum and minimum values for each group. To determine whether swimming distance (cm) or mean swimming velocity (cm/s) was altered by individual drug treatments and co-treatments, nonparametric analysis was performed using either the Mann-Whitney test only if a single comparison was to be made, or in most cases by using the Kruskal-Wallis test followed by Dunn's multiple comparisons test to determine statistical differences between treatment groups ($p<0.05$). The 6 dpf A/V response data in chapter 4 (Figs. 4.5-4.7) passed the Shapiro-Wilk test and are presented as bar graphs representing the mean values ± SEM, where statistical analysis was performed using One-Way ANOVA followed by Tukey's post-hoc test to determine whether A/V escape response rate (%) was significantly altered by individual drug treatments and co-treatments ($p<0.05$). For the notation of statistical significance, columns which share the same letter(s) of the alphabet are not statistically different from one another.

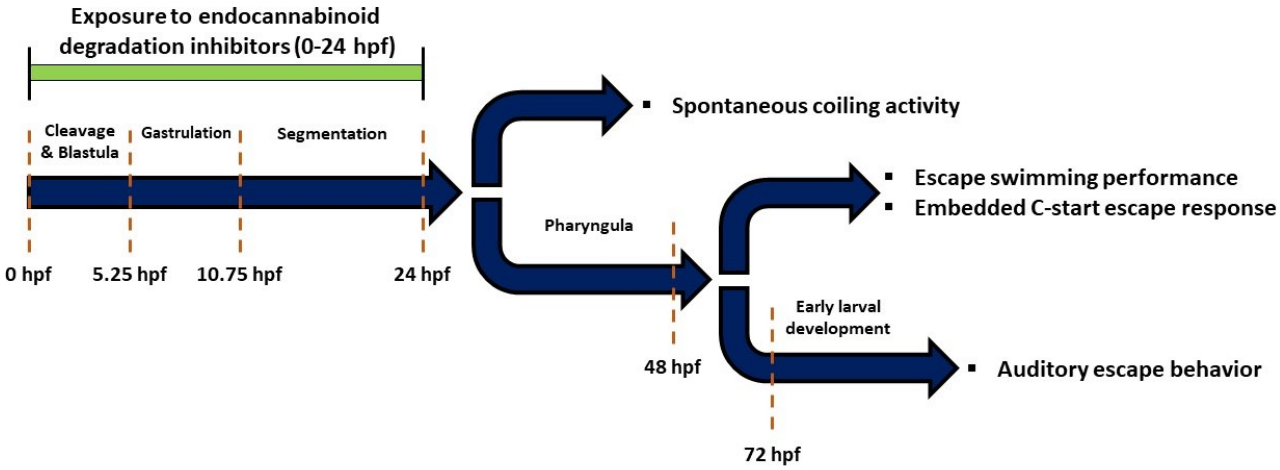
Exposure to endocannabinoid degradation inhibitors (0-24 hpf)
Cleavage & Blastula
Gastrulation
Segmentation
0 hpf
5.25 hpf
10.75 hpf
24 hpf
Spontaneous coiling activity
Pharyngula
Escape swimming performance
Embedded C-start escape response
48 hpf
Early larval development
Auditory escape behavior
72 hpf

Figure 2.1: Exposure paradigm and experiment outline. Wildtype zebrafish (*Danio rerio*) of the TL strain were used in all experiments. Adult males and females were arranged in breeding tanks and eggs were collected the following morning. Drug exposure began immediately after egg collection within the first hour of fertilization, effectively spanning the duration of ~0 to 24 hours post-fertilization (hpf). At 24 hpf, drug solutions were washed-out thoroughly with embryo media and the embryos were provided with fresh embryo media and incubated at 28.5°C until reaching the respective age for each experiment. Experiments assessing the spontaneous coiling activity were performed at 1-day post-fertilization (dpf). Escape swimming and embedded C-start escape experiments were performed at 2 dpf. Auditory escape experiments were performed between 3-6 dpf and were also performed in animals that reached the age of 8-10-weeks.

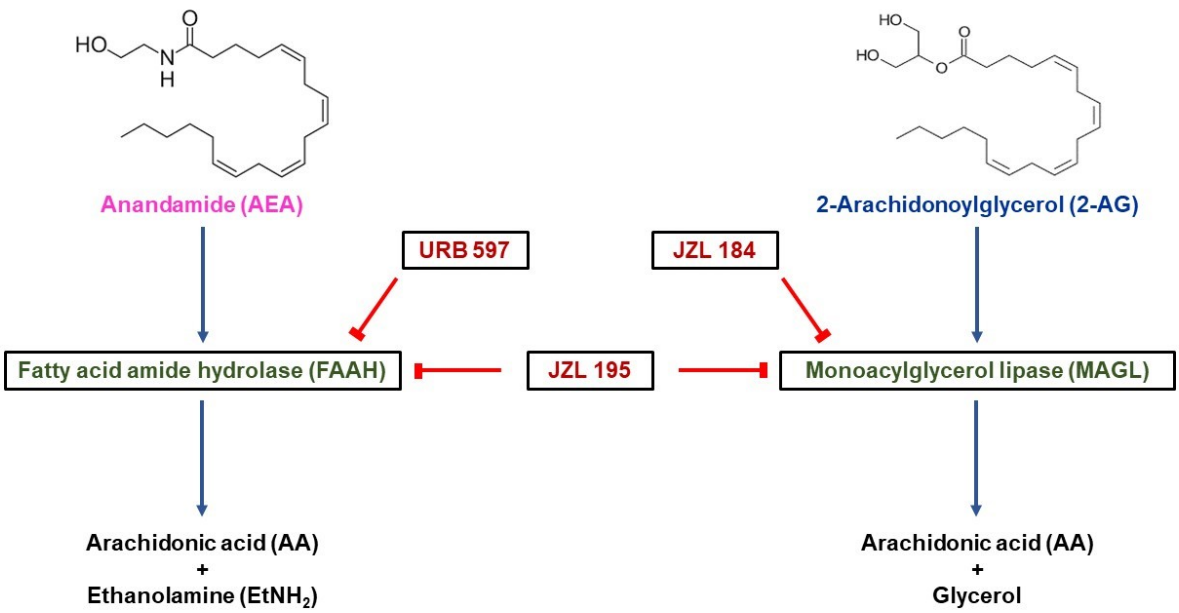
Anandamide (AEA)
2-Arachidonoylglycerol (2-AG)
URB 597
JZL 184
Fatty acid amide hydrolase (FAAH)
JZL 195
Monoacylglycerol lipase (MAGL)
Arachidonic acid (AA)
+
Ethanolamine (EtNH2)
Arachidonic acid (AA)
+
Glycerol

Figure 2.2: Schematic of pharmacological inhibitors of endocannabinoid catabolic enzymes. The enzymes fatty acid amide hydrolase (FAAH) and monoacylglycerol lipase (MAGL) are the primary enzymes mediating the breakdown of anandamide (AEA) and 2-arachidonoylglycerol (2-AG). FAAH hydrolyzes AEA into arachidonic acid (AA) and ethanolamine ($EtNH_2$), while MAGL hydrolyzes 2-AG into AA and glycerol. URB 597 is a selective inhibitor of FAAH, and when used, it is expected to reduce the degradation of AEA. JZL 184 is a selective inhibitor of MAGL, and when used, it is expected to reduce the degradation of 2-AG. JZL 195 is a dual inhibitor of both FAAH and MAGL, and when used, it is expected to simultaneously reduce the degradation of both AEA and 2-AG. Overall, these pharmacological compounds are expected to upregulate endocannabinoid (eCB) signaling by inhibiting the enzymes that degrade the eCBs.

Chapter 3. Results: Inhibiting the endocannabinoid degrading enzymes FAAH and MAGL during zebrafish embryogenesis alters sensorimotor function

3.1 Inhibition of eCB degradation enzymes reduces contractile activity in embryos

Because zebrafish motor development is known to be affected by eCS perturbation, my first assessments revolved around examining one of the earliest observable locomotor processes known as burst activity (Colwill and Creton, 2011a; de Oliveira et al., 2021). This spontaneous coiling activity provides the earliest indication of locomotor development, representing the initial formation of immature synaptic contacts between the CNS and muscle fibers at the neuromuscular junction (Grunwald et al., 1988; Saint-Amant, 2006). The experiments in the following section were replicated 4 times (N=4).

Vehicle-treated embryos exhibited a mean burst activity of 4.1 ± 0.4% (n=93) (Fig. 3.1A, C, E). Treatment with 1, 2, and 5 μM URB 597 did not significantly affect burst activity (Fig. 3.1A). However, embryos treated with 10 and 20 μM URB 597 exhibited a significant reduction in burst activity at (1.7 ± 0.3%) ($p<0.001$, n=41) and (2.0 ± 0.4, $p<0.01$, n=60) respectively. Animals treated with 1, 2, 5, 10, and 20 μM JZL 184 experienced a significant decrease in burst activity relative to the vehicle-treated animals ($p<0.05$), with the largest reductions occurring in the 20 μM JZL 184 group (2.1 ± 0.3%, $p<0.001$, n=80) (Fig. 3.1C). These reductions appear to display a dose-dependent trend. With regards to the dual FAAH/MAGL inhibitor JZL 195, treatment with 1 μM JZL 195 did not cause significant impacts to burst activity. However,

treatment with 2 and 5 μM JZL 195 resulted in decreased burst activity with mean activity percentages of 1.8 ± 0.2% and 2.2 ± 0.3% ($p<0.001$, n=63 and n=75), respectively (Fig. 3.1E).

The burst count showed a similar trend to the burst activity. Vehicle treated embryos displayed a mean count of 4.1 ± 0.4 bursts per minute (n=93) (Fig. 3.1B, D, F). 10 and 20 μM URB 597 treated animals experienced a significant reduction in mean burst count/min (2.1 ± 0.4, $p<0.01$, n=41 and 2.9 ± 0.4, $p<0.01$, n=60, respectively) (Fig. 3.1B). JZL 184 treatment resulted in a reduction in mean burst count/min in all tested concentrations ($p<0.05$) (Fig. 3.1D). Lastly, treatment with 2 and 5 μM JZL 195 resulted in a significantly decreased burst count/min of 2.1 ± 0.2 ($p<0.001$, n=63) and 2.9 ± 0.4 ($p<0.05$, n=75), respectively (Fig. 3.1F).

3.2 Escape swimming is negatively impacted by MAGL inhibition and by dual FAAH/MAGL inhibition

Developing as a more advanced contractile movement, the C-shaped tail flip elicited at the onset of C-start escapes is a hardwired reflex response that is crucial for survival (Colwill and Creton, 2011b). Escape swimming begins with a C-start, followed by bursts of swimming to quickly propel the animal away from the aversive stimulus. In this next series of experiments, I analyzed the escape swimming that takes place after a C-start has been performed by 2 dpf embryos. The experiments in this section were replicated a total of 4 times (N=4). The traces in Fig. 3.2A outline the swimming paths taken by individual animals following a C-start escape response.

Vehicle-treated embryos displayed a mean swimming distance of 6.4 ± 0.6 cm (n=49) (Fig. 3.2B, D, F). Animals exposed to URB 597 (any concentration) did not experience significant alterations to escape swimming relative to the vehicle control ($p>0.05$) (Fig. 3.2B). However, treatment with JZL 184 at concentrations equal to or greater than 5 μM resulted in significantly shorter swimming distances compared with controls (Fig. 3.2D) ($p<0.01$). 24-hour treatment with JZL 195 resulted in severe reductions with mean swimming distances of 3.8 ± 0.5 cm ($p<0.001$, n=38) in the 1 μM JZL 195 group, to values as low as 0.7 ± 0.1 cm ($p<0.001$, n=38) in the 5 μM treated group (Fig. 3.2F).

The mean velocity of escape swimming in vehicle-treated embryos was 0.30 ± 0.03 cm/s (n=49) (Fig. 3.2C, E, G). URB 597 and JZL 184 treatments did not affect mean swimming velocity in a statistically significant manner ($p>0.05$, n=37-49) (Fig. 3.2C, E), however animals treated with JZL 195 experienced significant reductions in escape swimming escape velocity (Fig. 3.2G). For instance, embryos treated with 1 μM JZL 195 had a mean velocity of 0.19 ± 0.02 cm/s ($p<0.01$, n=38), while 2 μM and 5 μM JZL 195 treated animals demonstrated mean velocities of 0.14 ± 0.02 cm/s ($p<0.001$, n=37), and 0.04 ± 0.01 cm/s ($p<0.001$, n=38), respectively. These results indicate that singular inhibition of FAAH does not have an effect on escape swimming at 2 dpf, whereas inhibition of MAGL alters swimming distance, and dual inhibition of FAAH/MAGL together has a profound impact on escape swimming.

3.3 C-start escape properties are adversely affected primarily by dual FAAH/MAGL inhibition

Next, I investigated parameters associated with the C-start escape response evoked by mechanical stimuli. To do this, I embedded 2 dpf embryos in 2% LMPA gel to isolate the initial C-shaped contraction. Representative time-lapse photos of a C-bend response is shown in Fig. 3.3A. Here, I used concentrations of enzyme inhibitors that had intermediate and maximal effects on escape swimming as determined in the previous set of experiments. I then assessed parameters such as the latency of the response, peak velocity, peak acceleration, rotational angle, and time to maximum bend (Figs. 3.3 & 3.4). The experiments described within this section were replicated 5 times (N=5).

Vehicle treated embryos demonstrated a mean C-start response latency of 10.2 ± 0.7 ms (n=20) (Fig. 3.3B). A significant increase in response latency relative to the vehicle control was seen in embryos treated with 20 μM JZL 184 (13.0 ± 1.2 ms, $p<0.05$, n=16) and 5 μM JZL 195 (17.8 ± 1.3 ms, $p<0.001$, n=15). In terms of the maximum speed of the tail during the C-bend, vehicle treated animals achieved a maximum speed of 0.23 ± 0.01 mm/ms (n=20) (Fig. 3.3C) and only animals treated with 5 μM JZL 195 had a reduced max speed of 0.19 ± 0.02 mm/ms ($p<0.05$, n=15). No other treatment resulted in changes to this metric. With respect to peak acceleration of the C-bend, vehicle control embryos displayed a maximum acceleration of 0.11 ± 0.01 mm/ms^2 (n=20) (Fig. 3.3D), and the only treatment that resulted in a change to this parameter was 5 μM JZL 195, where the peak acceleration was 0.08 ± 0.01 mm/ms^2 ($p<0.01$, n=15).

The mean rotational angle achieved by the tail was 158 ± 9.9 degrees in vehicle treated embryos (n=20) (Fig. 3.4A). Treatment with 5 μM JZL 195 resulted in a small but significant reduction in the C-bend angle (129 ± 6.6 degrees, $p<0.05$, n=15). Despite this significant reduction in the angle of the C-bend caused by 5 μM JZL 195, there was no significant impact on the time to complete a full C-bend (Fig. 3.4B). Finally, vehicle control embryos exhibited an angular velocity of 5.4 ± 0.4 degrees/ms (n=20), which was significantly reduced by 5 μM JZL 195 (4.3 ± 0.3 degrees/ms, $p<0.05$, n=15) (Fig. 3.4C). These findings show that inhibition of MAGL, and the inhibition of both FAAH and MAGL together leads to altered properties in the C-start escape response of embryonic zebrafish.

3.4 Dual inhibition of FAAH/MAGL produces deficits to auditory/vibrational responsiveness

Short latency C-start escapes also occur in response to auditory stimuli which can be evoked by delivering an auditory/vibrational (A/V) stimulus (Burgess and Granato, 2007; Kohashi et al., 2012). A/V stimuli-induced responses develop after 3 dpf and are functionally mature by 6 dpf (Kohashi et al., 2012). The experiments described here on 3 and 4 dpf animals were replicated 4 times (N=4), while experiments on 5 and 6 dpf fish were replicated 5 times (N=5).

Examining the A/V responsiveness in embryos and larvae from 3-6 dpf revealed that vehicle treated animals demonstrate a mean A/V escape response rate of 12.5 ± 4.2% at 3 dpf (n=24) (Fig. 3.5A), and a response rate of 37.5 ± 4.2% at 4 dpf (n=24) (Fig. 3.5B). There were no statistically significant differences amongst any of the treatments at 3 and 4 dpf, indicating that at

these stages, the functional development of this response proceeds normally. At 5 dpf, vehicle control larvae exhibited a mean A/V escape response rate of 80 ± 6.2% (n=30) (Fig. 3.5C). Treatment with URB 597 or JZL 184 had no effect on the response rate while treatment with 2 μM JZL 195 caused A/V response deficits with a mean response rate of 46.7 ± 9.7%, ($p<0.05$, n=30). The treatment of 5 μM JZL 195 also caused a reduction, as the mean response rate was 43.3 ± 4.0% ($p<0.01$, n=30). At 6 dpf, the responsiveness to A/V stimuli in control animals became more robust with a mean response rate of 93.3 ± 4.0% (n=30) (Fig. 3.5D). Treatment with 5 or 20 μM of either URB 597 or JZL 184 once again did not produce any significant alterations to A/V responsiveness, whereas treatment with 2 and 5 μM JZL 195 both caused a significant decline in the responsiveness to A/V stimulus with response rates of 60.0 ± 11.3% ($p<0.05$, n=30), and 53.3 ± 8.2% ($p<0.05$, n=30) for 2 and 5 μM JZL 195 respectively.

3.5 Juvenile zebrafish experience response deficits to auditory/vibrational stimuli following FAAH/MAGL inhibition

To determine whether the impairments to A/V responsiveness displayed by JZL 195 treated larvae were also experienced in older animals, I raised fish into their late juvenile stages (8-10 weeks) and tested them for A/V responsiveness across 3 cohorts (N=3) (Fig. 3.6A). Animals treated with 2 μM JZL 195 were tested here, as this was the minimal concentration that altered A/V responsiveness at 5 and 6 dpf. Vehicle control animals demonstrated an A/V escape response rate of 85 ± 2.6% (n=26) (Fig. 3.6B), while juvenile zebrafish that had previously been exposed to 2 μM JZL 195 during embryogenesis displayed a significantly reduced response rate of 55.1 ± 6.2% ($p<0.05$, n=25), which was similar to larval fish. This finding shows that the

sensorimotor deficits caused by eCS perturbation persists into the late juvenile period of development.

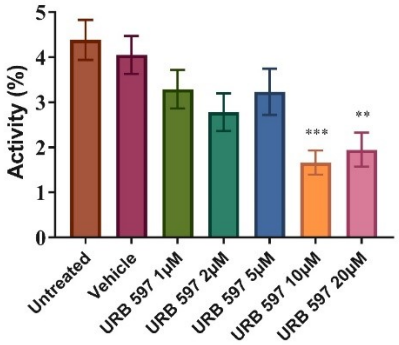
Activity (%)
0
1
2
3
4
5
***
**
Untreated
Vehicle
URB 597 1μM
URB 597 2μM
URB 597 5μM
URB 597 10μM
URB 597 20μM

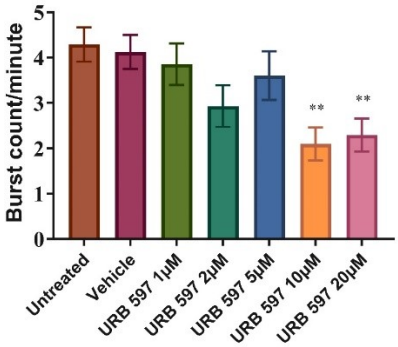
Burst count/minute
0
1
2
3
4
5
**
**
Untreated
Vehicle
URB 597 1μM
URB 597 2μM
URB 597 5μM
URB 597 10μM
URB 597 20μM

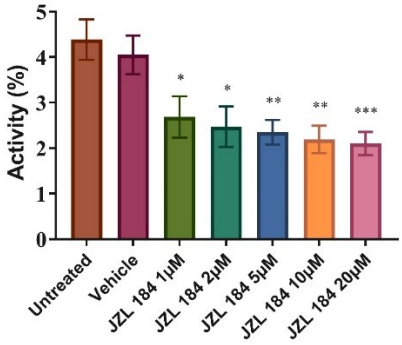
Activity (%)
0
1
2
3
4
5
*
*
**
**
***
Untreated
Vehicle
JZL 184 1μM
JZL 184 2μM
JZL 184 5μM
JZL 184 10μM
JZL 184 20μM

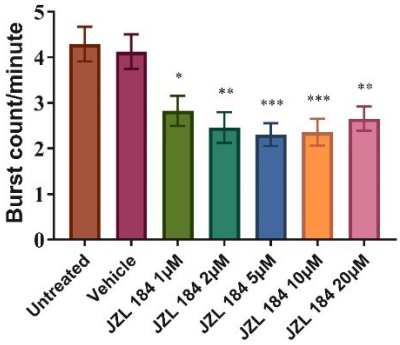
Burst count/minute
0
1
2
3
4
5
*
**
***
***
**
Untreated
Vehicle
JZL 184 1μM
JZL 184 2μM
JZL 184 5μM
JZL 184 10μM
JZL 184 20μM

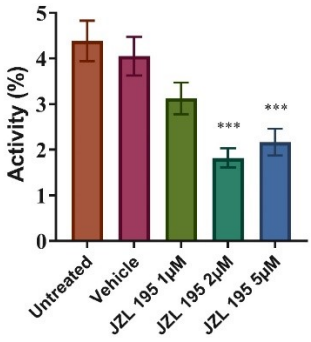
Activity (%)
0
1
2
3
4
5
***
***
Untreated
Vehicle
JZL 195 1μM
JZL 195 2μM
JZL 195 5μM

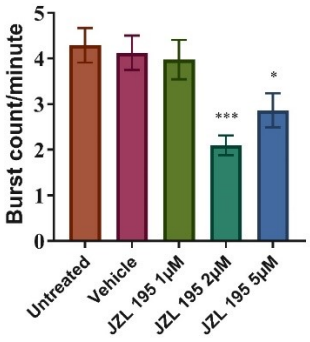
Burst count/minute
0
1
2
3
4
5
***
*
Untreated
Vehicle
JZL 195 1μM
JZL 195 2μM
JZL 195 5μM

Figure 3.1: Contractile activity of embryos is reduced from inhibiting endocannabinoid degrading enzymes. Spontaneous coiling activity of embryos at the age of 1-day post-fertilization (dpf) was video-recorded and analyzed using DanioScope 1.1. (**A and B**) Effects on activity (%) and burst count/min for untreated animals (n=92), the vehicle (n=93) and treatment concentrations of 1, 2, 5, 10, and 20 μM for URB 597 (n=62, 44, 58, 41, and 60, respectively). (**C and D**) Effects on activity (%) and burst count/min for the vehicle (n=93) and treatment concentrations of 1, 2, 5, 10, and 20 μM for and 1, 2, 5, 10, and 20 μM for JZL 184 (n=49, 53, 68, 54, and 80, respectively). (**E and F**) Effects on activity (%) and burst count/min for the vehicle (n=93) and treatment concentrations of 1, 2, and 5 μM JZL 195 (n=45, 63, and 75, respectively). All treatments were run together, but for ease of viewing, the graphs are separated according to the compound being tested. Thus, the controls in **A**, **C,** and **E** are similar, and the controls in **B**, **D,** and **F** are similar. Activity (%) represents the proportion of time spent performing coiling movements over the recording period, while burst count/min represents the average number of individual contractions per minute. N=4 experiments with 11-23 animals per experiment for each treatment. * Indicates treatment groups which are significantly different from the vehicle control group where: * $p<0.05$, ** $p<0.01$, *** $p<0.001$ (One-Way ANOVA, followed by Dunnett's multiple comparisons test). Columns indicate mean values, while error bars represent standard error of the mean (SEM).

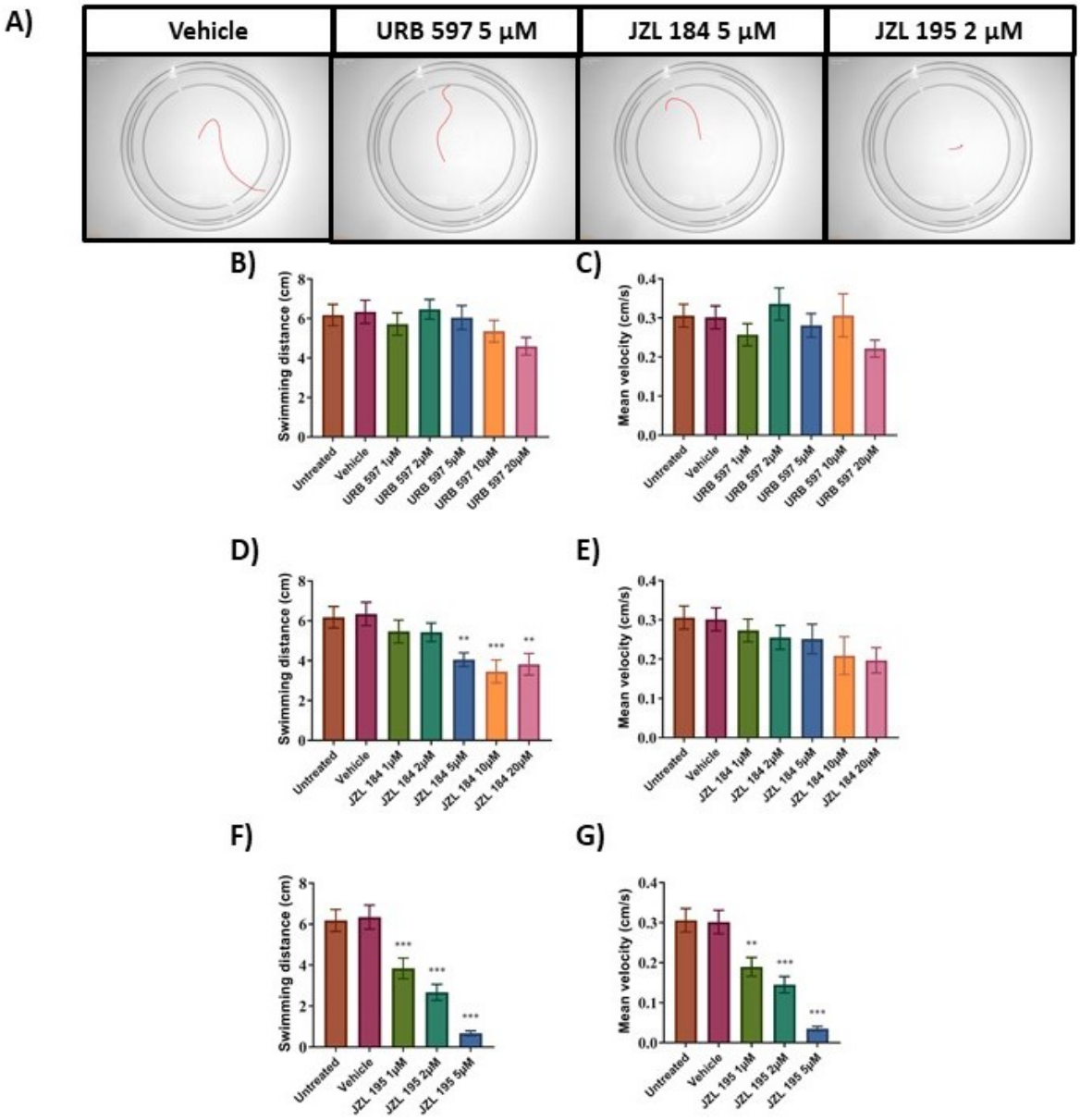
A)
Vehicle
URB 597 5 µM
JZL 184 5 µM
JZL 195 2 µM
B)
Swimming distance (cm)
Untreated
Vehicle
URB 597 1µM
URB 597 2µM
URB 597 5µM
URB 597 10µM
URB 597 20µM
C)
Mean velocity (cm/s)
D)
E)
JZL 184 1µM
JZL 184 2µM
JZL 184 5µM
JZL 184 10µM
JZL 184 20µM
F)
G)
JZL 195 1µM
JZL 195 2µM
JZL 195 5µM

Figure 3.2: Escape swimming is severely reduced by MAGL and dual FAAH/MAGL inhibition. Escape swimming at 2 days post-fertilization (dpf) was assessed following an acute touch stimulus. (**A)** Representative tracings of the swimming path are shown for: untreated animals, vehicle, 5 μM URB 597, 5 μM JZL 184, and 2 μM JZL 195. (**B and C**) The effects of untreated animals (n=44), the vehicle (n=49), 1, 2, 5, 10, and 20 μM URB 597 (n=39, 45, 49, 42, and 43, respectively) on swimming distance and velocity. (**D and E**) The effects of vehicle (n=49), 1, 2, 5, 10, and 1, 2, 5, 10, and 20 μM JZL 184 (n=37, 41, 46, 40, and 40, respectively) on swimming distance and velocity. (**F and G**) The effects of vehicle (n=49), 1, 2, 5, 10, and 1, 2, and 5 μM JZL 195 (n=38, 37, and 38, respectively) on swimming distance and velocity was analyzed using EthoVision XT-11.5. All treatments were run together, but for ease of viewing, the graphs are separated according to the compound being tested. Thus, the controls in **B**, **D,** and **F** are similar, and the controls in **C**, **E,** and **G** are similar. Swimming distance (mm) and mean velocity of burst swimming (mm/s) was examined by testing each animal individually. N=4 experiments with 9-13 animals per experiment for each treatment. * Indicates treatment groups which are significantly different from the vehicle control group where: ** $p < 0.01$, *** $p < 0.001$ (One-Way ANOVA, followed by Dunnett's multiple comparisons test). Columns indicate mean values, while error bars represent standard error of the mean (SEM).

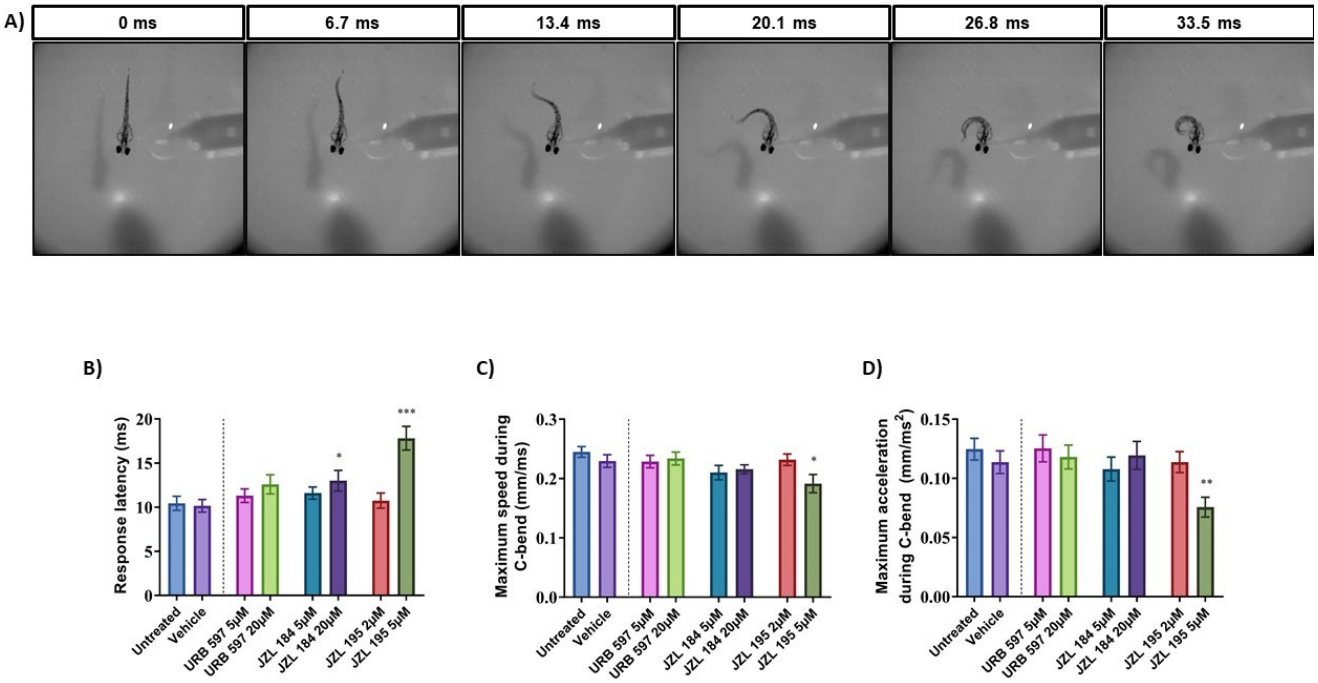
A)
0 ms
6.7 ms
13.4 ms
20.1 ms
26.8 ms
33.5 ms
B)
Response latency (ms)
20
15
10
5
0
***
*
Untreated
Vehicle
URB 597 5μM
URB 597 20μM
JZL 184 5μM
JZL 184 20μM
JZL 195 2μM
JZL 195 5μM
C)
Maximum speed during C-bend (mm/ms)
0.3
0.2
0.1
0.0
*
Untreated
Vehicle
URB 597 5μM
URB 597 20μM
JZL 184 5μM
JZL 184 20μM
JZL 195 2μM
JZL 195 5μM
D)
Maximum acceleration during C-bend (mm/ms^2)
0.15
0.10
0.05
0.00
**
Untreated
Vehicle
URB 597 5μM
URB 597 20μM
JZL 184 5μM
JZL 184 20μM
JZL 195 2μM
JZL 195 5μM

Figure 3.3: C-start escape is partially altered by exposure to high concentrations of JZL 184, and is severely altered by high concentrations of JZL 195. Embryos at the age of 2 days post-fertilization (dpf) were partially embedded in 2% low-melting point agarose (LMPA) and acclimated for 20-minutes before using a Picospritzer II to deliver an acute pulse of 2% phenol red solution to the head as a mechanical stimulus. (**A**) Representative images depicting the C-shaped tail flip performed by an immobilized vehicle control embryo after being stimulated. The time scale (ms) of the C-start is shown from its onset to its peak. (**B to D**) Bar graphs depict the results for untreated animals (n=20), the vehicle control (n=20) and treatments with 5 and 20 μM URB 597 (n=15 and 19), 5 and 20 μM JZL 184 (n=18 and 16), or 2 and 5 μM JZL 195 (n=14 and 15). The following metrics were assessed: (**A**) response latency (ms) to initiate C-start escape after being stimulated, (**B**) maximum speed achieved by the tail during the C-start escape (mm/s), and (**C**) maximum acceleration achieved by the tail during the C-start escape (mm/s^2). N=5 experiments with 3-5 animals per experiment. * Indicates treatment groups which are significantly different from the vehicle control group where: * $p<0.05$, ** $p<0.01$, *** $p<0.001$ (One-Way ANOVA, followed by Dunnett's multiple comparisons test). Columns indicate mean values, while error bars represent standard error of the mean (SEM).

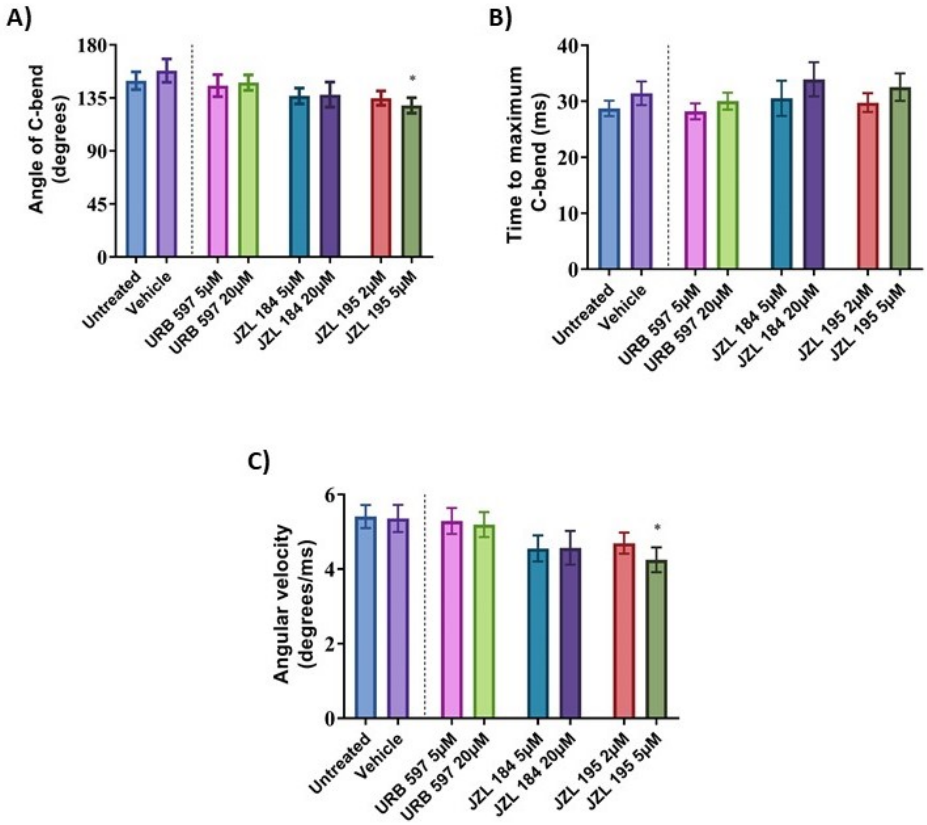
A)
Angle of C-bend (degrees)
180
135
90
45
0
*
Untreated
Vehicle
URB 597 5μM
URB 597 20μM
JZL 184 5μM
JZL 184 20μM
JZL 195 2μM
JZL 195 5μM
B)
Time to maximum C-bend (ms)
40
30
20
10
0
Untreated
Vehicle
URB 597 5μM
URB 597 20μM
JZL 184 5μM
JZL 184 20μM
JZL 195 2μM
JZL 195 5μM
C)
Angular velocity (degrees/ms)
6
4
2
0
*
Untreated
Vehicle
URB 597 5μM
URB 597 20μM
JZL 184 5μM
JZL 184 20μM
JZL 195 2μM
JZL 195 5μM

Figure 3.4: Dual FAAH/MAGL inhibition produces deficits to the C-bend properties of the tail. Immobilized embryos at the age of 2 days post-fertilization (dpf) were subjected to an acute mechanical stimulus and were assessed for their C-bend properties. (**B to D**) Bar graphs depict the results for untreated animals (n=20), the vehicle control (n=20) and treatments with 5 and 20 μM URB 597 (n=15 and 20), 5 and 20 μM JZL 184 (n=18 and 17), and 2 and 5 μM JZL 195 (n=15 and 15). The assessed metrics include: (**A**) angle of C-bend, which is depicted in terms of degrees, (**B**) the length of time to achieve the maximum C-bend angle (ms), and (**C**) angular velocity which represents the maximum C-bend angle over the time it takes to achieve it (degrees/ms). N=5 experiments with 3-5 animals per experiment. * Indicates treatment groups which are significantly different from the vehicle control group where: * $p<0.05$ (One-Way ANOVA, followed by Dunnett's multiple comparisons test). Columns indicate mean values, while error bars represent standard error of the mean (SEM).

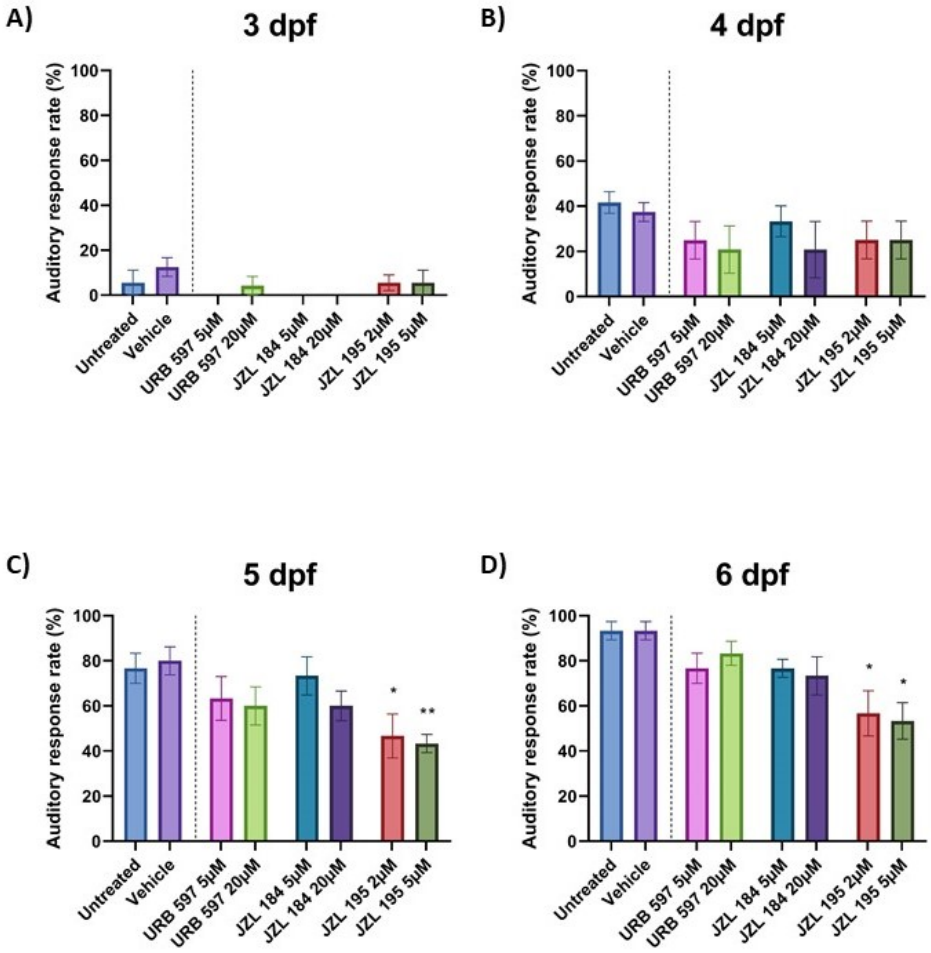
A)
3 dpf
B)
4 dpf
C)
5 dpf
D)
6 dpf
Auditory response rate (%)
0
20
40
60
80
100
Untreated
Vehicle
URB 597 5μM
URB 597 20μM
JZL 184 5μM
JZL 184 20μM
JZL 195 2μM
JZL 195 5μM
*
**

Figure 3.5: Embryonic and larval responsiveness to auditory/vibrational stimuli is altered by dual FAAH/MAGL inhibition. A 500Hz audio tone was delivered to embryos/larvae to assess their responsiveness to auditory/vibrational stimuli (A/V). Animals were tested in groups of 6 and were allowed 20-minutes of acclimation prior to receiving the stimulus. C-start escape responses were recorded and the proportion of responding larvae is shown as the response rate (%). Bar graphs depict the A/V response rates for untreated animals, the vehicle control and treatments with 5 and 20 μM URB 597, 5 and 20 μM JZL 184, and 2 and 5 μM JZL 195 in (**A**) 3 dpf embryos, (**B**) 4 dpf larvae, (**C**) 5 dpf larvae, and (**D**) 6 dpf larvae. N=4 experiments for 3 and 4 dpf, and N=5 experiments for 5 and 6 dpf with 6 animals per experiment for each treatment, thus n=24 animals for 3 and 4 dpf assessments, and n=30 animals for 5 and 6 dpf assessments. * Indicates treatment groups which are significantly different from the vehicle control group where: * $p<0.05$, ** $p<0.01$ (One-Way ANOVA, followed by Dunnett's multiple comparisons test). Columns indicate mean values, while error bars represent standard error of the mean (SEM).

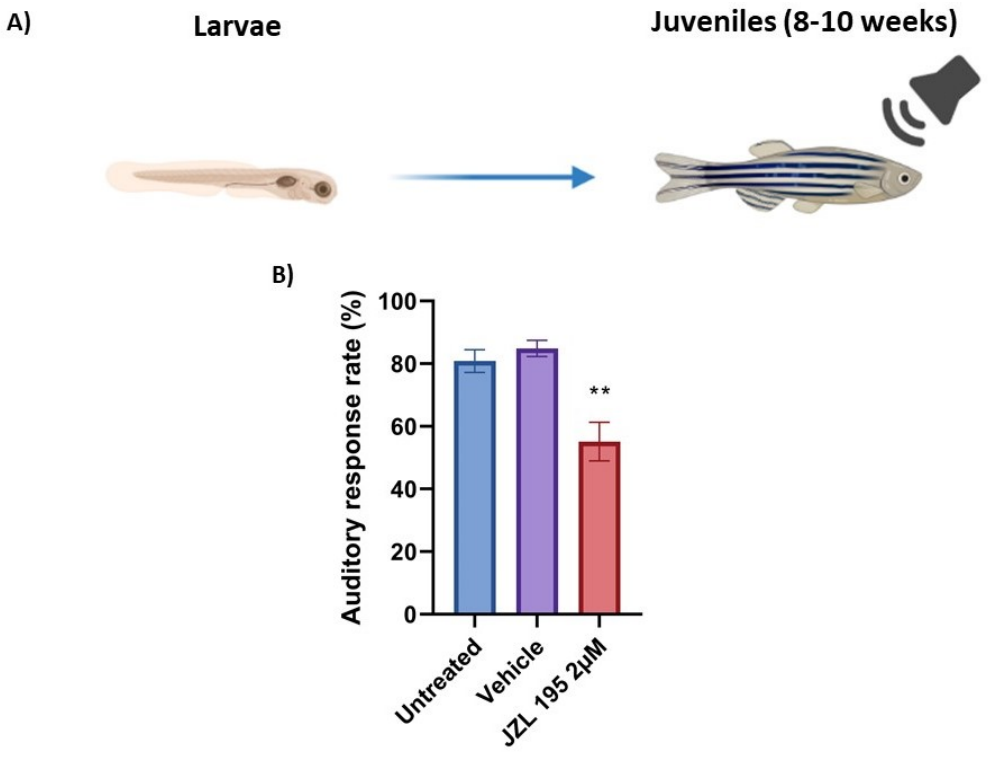
A)
Larvae
Juveniles (8-10 weeks)
B)
Auditory response rate (%)
100
80
60
40
20
0
**
Untreated
Vehicle
JZL 195 2μM

Figure 3.6: The auditory/vibrational response deficits caused by dual FAAH/MAGL inhibition are present in 8–10-week-old juvenile zebrafish. Following the ~24-hour exposure period, animals were raised to their juvenile developmental stage and were assessed individually for their responsiveness to auditory/vibrational (A/V) stimuli at 8-10 weeks of age, as depicted in the schematic (**A**). (**B**) The bar graph depicts the A/V escape response rate (%) of untreated animals (n=26), vehicle (n=26) and 2 μM JZL 195 (n=25) treated animals. N=3 experiments with 7-10 animals per experiment for each treatment. * Indicates treatment groups which are significantly different from the vehicle control group where: * $p<0.05$ (One-Way ANOVA, followed by Dunnett's multiple comparisons test). Columns indicate mean values, while error bars represent standard error of the mean (SEM). Graphics in (**A**) were created with BioRender.com.

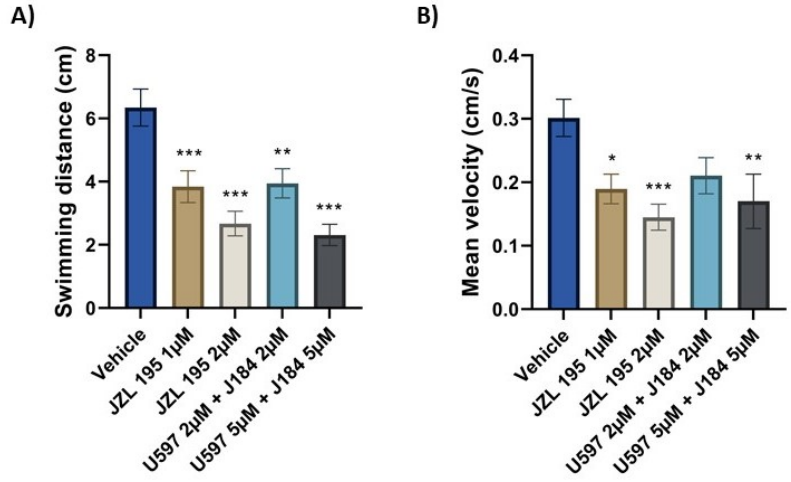
A)
Swimming distance (cm)
0
2
4
6
8
***
***
**
***
Vehicle
JZL 195 1μM
JZL 195 2μM
U597 2μM + J184 2μM
U597 5μM + J184 5μM
B)
Mean velocity (cm/s)
0.0
0.1
0.2
0.3
0.4
*
***
**
Vehicle
JZL 195 1μM
JZL 195 2μM
U597 2μM + J184 2μM
U597 5μM + J184 5μM

Figure 3.7. Treatment with both URB 597 and JZL 184 produces similar deficits to 2 dpf escape swimming locomotion as JZL 195 does. This supplementary image depicts the swimming distance (cm) and mean swimming velocity (cm/s) during escape swimming of animals treated with 5 μM URB 597 + 5 μM JZL 184. Deficits to escape swimming performance caused by combining URB 597 and JZL 195 treatments are comparable to the deficits caused by 2 μM JZL 195.

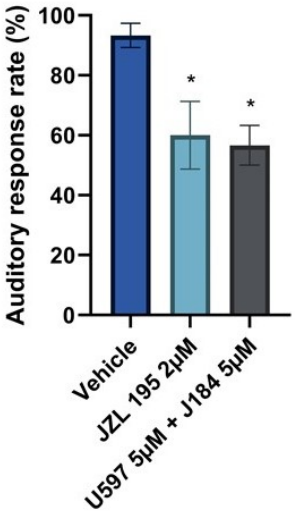
Auditory response rate (%)
100
80
60
40
20
0
*
*
Vehicle
JZL 195 2μM
U597 5μM + J184 5μM

Figure 3.8. Treatment with both URB 597 and JZL 184 produces similar deficits to 6 dpf auditory/vibrational responsiveness as JZL 195 does. This supplementary image depicts the auditory vibrational (A/V) escape response rate (%) of animals treated with 5 μM URB 597 + 5 μM JZL 184 in how this combined treatment results in A/V response deficits to 6 dpf larvae which are comparable to the deficits caused by 2 μM JZL 195.

Table 3.1: Summary of the effects of endocannabinoid catabolism inhibitors on zebrafish motor and sensorimotor activities.

Experimental assessment	Parameter	Effect of URB 597 (FAAH inhibition)	Effect of JZL 184 (MAGL inhibition)	Effect of JZL 195 (FAAH + MAGL inhibition)
Spontaneous coiling (1 dpf)	Activity (%)	↓	↓	↓
	Burst count/min	↓	↓	↓
Escape swimming (2 dpf)	Swimming distance (cm)	↔	↓	↓
	Mean velocity (cm/s)	↔	↔	↓
Embedded C-start escape response (2 dpf)	Response latency (ms)	↔	↑	↑
	Max speed (mm/ms)	↔	↔	↓
	Max acceleration (mm/ms^2)	↔	↔	↓
	Angle of C-bend (degrees)	↔	↔	↓
	Time to C-bend (ms)	↔	↔	↔
	Angular velocity (degrees/ms)	↔	↔	↓
Larval A/V escape response (3-6 dpf)	Auditory response rate (%)	↔	↔	↓
Juvenile A/V escape response (8-10 weeks old)	Auditory response rate (%)	N/A	N/A	↓

Chapter 4. Results: The endocannabinoid system's role in motor development involves cannabinoid receptors, transient receptor potential channels, and Sonic Hedgehog signaling systems

4.1 Blocking CB1R prevents swimming deficits caused by singular inhibition of MAGL and dual inhibition of FAAH/MAGL

With the 2 dpf escape swimming locomotor assay, I was interested in establishing whether co-treatment of particular drugs could offset the locomotor deficits that are experienced by 2 dpf embryos that had been exposed to inhibitors of eCB degradation enzymes. Due to FAAH and MAGL inhibition being linked to increased eCB levels, my investigation began by targeting the cannabinoid receptors that eCBs primarily bind to: CB1R and CB2R (Griebel et al., 2015; Zou and Kumar, 2018). For this series of experiments, the effects 5 μM URB 597, and the effects of 5 μM JZL 184 and 2 μM JZL 195 in combination with 10 nM AM 251 on escape swimming performance was assessed in 2 dpf larvae. The experiments in the following section were replicated 4 times (N=4).

First, I note that singular inhibition of FAAH using URB 597 did not produce significant alterations to swimming distance or to swimming velocity, relative to the vehicle control ($p=0.175$ and $p=0.218$, respectively) (Fig. 4.1A, B). Consequently, the rest of my assessments focus on the effects caused by JZL 184 and JZL 195. Here, the CB1R antagonist AM 251 was selected for co-treatment with the eCB degradation inhibitors: JZL 184, and JZL 195.

The individual treatment with the MAGL inhibitor JZL 184 caused a significant reduction to swimming distance relative to the vehicle control ($p<0.001$) (Fig. 4.1C). Compared to the swimming reductions caused by JZL 184 however, co-treatment of JZL 184 with the CB1R antagonist AM 251 rescued the deficits caused by JZL 184 ($p<0.001$), indicating that blocking CB1R prevents the hypolocomotion effects caused by MAGL inhibition. No statistically significant effect on mean swimming velocity was observed from individual and combined drug treatments (Fig. 4.1D).

Dual inhibition of FAAH/MAGL with JZL 195 caused a significant reduction of swimming distance relative to the vehicle control ($p<0.001$) (Fig. 4.1E). Co-treatment of JZL 195 with AM 251 resulted in an increase in swimming distance, relative to singular JZL 195 treatments ($p=0.020$). Similarly, JZL 195 caused a reduction to mean swimming velocity relative to the vehicle control ($p<0.001$). The combined treatment of JZL 195 with AM 251 prevented the reduction in swimming velocity caused by JZL 195 alone ($p=0.015$) (Fig. 4.1F). This finding demonstrates that blocking CB1R prevents the locomotor deficits caused by FAAH/MAGL inhibition, and overall that CB1R is involved in the motor deficits induced by perturbed eCB signaling, shown from both singular MAGL inhibition and from dual FAAH/MAGL inhibition.

It should be noted that throughout the 2 dpf experiments in this chapter (Figs. 4.1-4.4), JZL 184 and JZL 195 both caused a significant reduction to swimming distance, while only JZL 195 reduced mean velocity in a statistically significant manner. Therefore, to avoid repetition, I will not indicate the significant reductions caused by individual treatment with either of these 2 compounds throughout the remaining sections of these results and the focus will be directed

towards the effects of combined drug treatments of JZL 184 or JZL 195 with the co-treated compound.

4.2 Swimming deficits caused by FAAH/MAGL suppression are still present when blocking CB2R

After assessing the influence of CB1R by examining the effects of AM 251 co-exposure, I next examined the effects of JZL 184 or JZL 195 in conjunction with the CB2R antagonist AM 630. Here, the effects of 5 μM JZL 184 and 2 μM JZL 195 in combination with 1 μM AM 630 on escape swimming performance was assessed in 2 dpf larvae. The experiments in the following section were replicated 4 times (N=4).

With the combined treatment of JZL 184 and AM 630, there was no statistically significant effect on swimming distance relative to the individual treatment with JZL 184 ($p>0.99$), indicating that AM 630 does not offset the deficits caused by JZL 184 (Fig. 4.2A). In terms of mean swimming velocity, animals co-treated with JZL 184 + AM 630, and animals treated with only JZL 184 had similar swimming velocity in their escape responses ($p>0.99$) (Fig. 4.2B). The JZL 184 + AM 630 group did however exhibit a significant reduction in velocity relative to the vehicle control group and the AM 630 control group ($p=0.004$ and $p=0.011$, respectively).

For animals co-treated with JZL 195 and AM 630, similar results were observed in that there was no significant difference in swimming distance relative to treatment with JZL 195 alone ($p>0.99$) (Fig. 4.2C). But in observing mean swimming velocity, the reduction in velocity was not significantly different from the JZL 195 + AM 630 co-treatment group ($p>0.99$) (Fig. 4.2D).

Thus, my findings indicate that motor deficits experienced in 2 dpf embryos caused by eCS perturbation are not mediated through the activity of CB2R.

4.3 Blocking the activity of TRP channels prevents locomotor deficits caused by dual FAAH/MAGL inhibition, but not deficits caused by singular MAGL inhibition

Next, I wanted to determine if TRP channels are involved in mediating the embryonic motor deficits caused by eCS perturbation. AMG 9090 has inhibitory actions on the TRPA1, TRPV1, and TRPM8 cation channels (Klionsky et al., 2007; Miller et al., 2014). Both TRPA1 and TRPV1 are capable of interacting with cannabinoids (Morales et al., 2017; Muller et al., 2019). In this set of experiments, I examined the effects of 5 μM JZL 184 and 2 μM JZL 195 in combination with 0.01 μM AMG 9090 on escape swimming performance in 2 dpf embryos. The experiments in the following section were replicated 4 times (N=4).

In a similar manner to AM 630, co-treatment of JZL 184 with AMG 9090 did not result in significant alterations to swimming distance relative to the deficits caused by JZL 184 alone ($p>0.99$) (Fig. 4.3A). The resulting mean velocity of animals treated with JZL 184 + AMG 9090 was significantly reduced relative to the vehicle control ($p=0.039$), but was statistically similar to JZL 184 alone ($p>0.99$), and to the AMG 9090 control group ($p=0.747$) (Fig. 4.3B). These findings indicate that TRP channel inhibition does not prevent the locomotor deficits caused by JZL 184.

Interestingly, in the case of dual FAAH/MAGL inhibition with JZL 195, animals co-treated with JZL 195 and AMG 9090 experienced a recovery to escape swimming performance. For instance,

swimming distance was significantly greater in animals treated with JZL 195 + AMG 9090 compared with those treated with JZL 195 alone ($p=0.015$) (Fig. 4.3C). Additionally, mean swimming velocity was also significantly greater ($p=0.003$) (Fig. 4.3D). These results indicate that blockage of TRP channels using AMG 9090 counteracts the locomotor deficits caused by dual FAAH/MAGL inhibition, but not singular MAGL inhibition. This suggests that TRP channels may play a partial role in mediating the locomotor alterations caused by eCS perturbation.

4.4 SMO agonism rescues the attenuates the alterations to 2 dpf swimming caused by singular MAGL inhibition and partially attenuates the alterations caused by dual FAAH/MAGL inhibition

Since the SHH signaling pathway is critical in developmental neurobiological processes, and because it has known connections to eCB signaling, I also sought to determine if upregulating SHH activity offsets the locomotor deficits caused by eCS perturbation (Boa-Amponsem et al., 2019; Choudhry et al., 2014; Ericson et al., 1996; Khaliullina et al., 2015). Here, I examined the escape swimming performance of 2 dpf embryos that had been exposed to either 5 μM JZL 184 or 2 μM JZL 195 in combination with the SMO agonist purmorphamine (5 μM). The experiments in the following section were replicated 4 times (N=4).

The co-treatment of JZL 184 with purmorphamine resulted in an increase in swimming distance, relative to the reduction caused by JZL 184 alone ($p<0.007$) (Fig. 4.4A). There was no statistically significant effect of any JZL 184 treatments on mean swimming velocity ($p>0.05$) (Fig. 4.4B).

For the dual inhibitor JZL 195, purmorphamine co-treatment resulted in a statistically significant increase in swimming distance relative to the distance swam by embryos exposed to JZL 195 alone ($p=0.011$) (Fig. 4.4C). Co-treatment with purmorphamine did not increase mean swimming velocity in a statistically significant manner relative to JZL 195 alone ($p=0.928$), and the swimming velocity of animals exposed to JZL 195 + purmorphamine also was not statistically different from the purmorphamine control group ($p=0.130$) (Fig. 4.4D). However, mean swimming velocity of the JZL 195 + purmorphamine treatment group was different from the vehicle control in a statistically significant manner ($p=0.003$). These findings demonstrate a purmorphamine-associated recovery from the deficits to swimming distance caused by JZL 184 and JZL 195. For JZL 195, this recovery is partial in that purmorphamine is capable of restoring swimming distance, but not velocity. Despite this, the observations reported here supports the involvement of the SHH signaling pathway in mediating the developmental influence of the eCS on motor development.

4.5 Co-treatment with AM 251 or AM 630 did not result in observable recoveries to the 6 dpf A/V response deficits caused by JZL 195 treatment

After assessing the possible receptor mechanisms involved in the 2 dpf escape swimming deficits caused by perturbation of eCB signaling, I next sought to determine if inhibition of CB1R or CB2R during the ~0-24 hpf exposure period would prevent the deficits to A/V responsiveness experienced by 6 dpf larvae that were exposed to the dual FAAH and MAGL inhibitor, JZL 195. In this section, the effects of 2 μM JZL 195 in combination with either 10 nM AM 251 or 1 μM

AM 630 on auditory response rate (%) was assessed in 6 dpf larvae. The experiments in the following section were replicated 6 times (N=6).

It should be noted that JZL 195 treatment caused a statistically significant reduction in auditory response rate relative to the vehicle control ($p<0.01$). This reduction occurred in all cases for the 6 dpf co-treatment experiments (Figs. 4.5-4.7). Therefore, this significant reduction caused by the individual treatment of JZL 195 will not be mentioned again throughout the remaining sections of this chapter.

Animals treated with JZL 195 in combination with AM 251 did not result in a statistically significant effect on A/V escape response rate compared to treatment with JZL 195 alone ($p=0.65$), indicating that AM 251 is unable to prevent the A/V response deficits caused by JZL 195 (Fig. 4.5A). Next, the effect of AM 630 co-treatments was examined. Similar to AM 251, treatment with JZL 195 + AM 630 did not affect auditory response rates, relative to singular treatment with JZL 195 ($p=0.96$), which indicates that AM 630 is also unable to prevent the deficits to 6 dpf A/V responsiveness that are caused by early exposure to JZL 195 (Fig. 4.5B). Thus, in examining this behavior at 6 dpf, co-treatment of zebrafish during ~0-24 hpf with JZL 195 and either the CB1R antagonist AM 251, or the CB2R antagonist AM 630, does not produce a detectable recovery to the decreased A/V responsiveness caused by JZL 195.

4.6 Co-treatment with AMG 9090 fails to produce a detectable recovery of 6 dpf A/V response deficits caused by JZL 195 treatment

After being unable to detect observable recoveries from AM 251 and AM 630, the effects of the TRP channel inhibitor AMG 9090 on JZL 195-induced A/V response deficits was examined next. The experiments in the following section were replicated 6 times (N=6).

Animals which had been exposed to both JZL 195 and AMG 9090 together did not display any alterations to their reduced auditory response rates compared to animals treated with JZL 195 ($p>0.99$), (Fig. 4.6). This lack of statistically significant effects of AMG 9090 co-treatment on 6 dpf A/V responsiveness indicates that TRP channel inhibition with AMG 9090 does not lead to observable effects on the JZL 195-induced reductions to A/V responsiveness.

4.7 Deficits to A/V responsiveness caused by JZL 195 are not prevented by treatment with purmorphamine

Lastly, the effects of co-treatment with the SMO agonist purmorphamine on A/V responsiveness was tested. The experiments in the following section were replicated 5 times (N=5). Treatment with purmorphamine + JZL 195 did not affect the auditory response rate of 6 dpf larvae in a statistically significant manner when compared to animals treated with JZL 195 alone ($p>0.99$), (Fig. 4.7). This result indicates that the deficits to A/V responsiveness observed at 6 dpf that are caused by JZL 195 are not prevented through combined treatment with the SMO agonist purmorphamine.

When all the results in this chapter are viewed together, the data that I have presented indicates that 2 dpf swimming deficits caused by eCS perturbations partially occurs through CB1R, TRP channels, and the SHH signaling pathway. However, when examining the A/V response deficits at 6 dpf, this was not observed, as there was no detectable recovery to the A/V escape response when co-treating animals with AM 251, AM 630, AMG 9090, or purmorphamine.

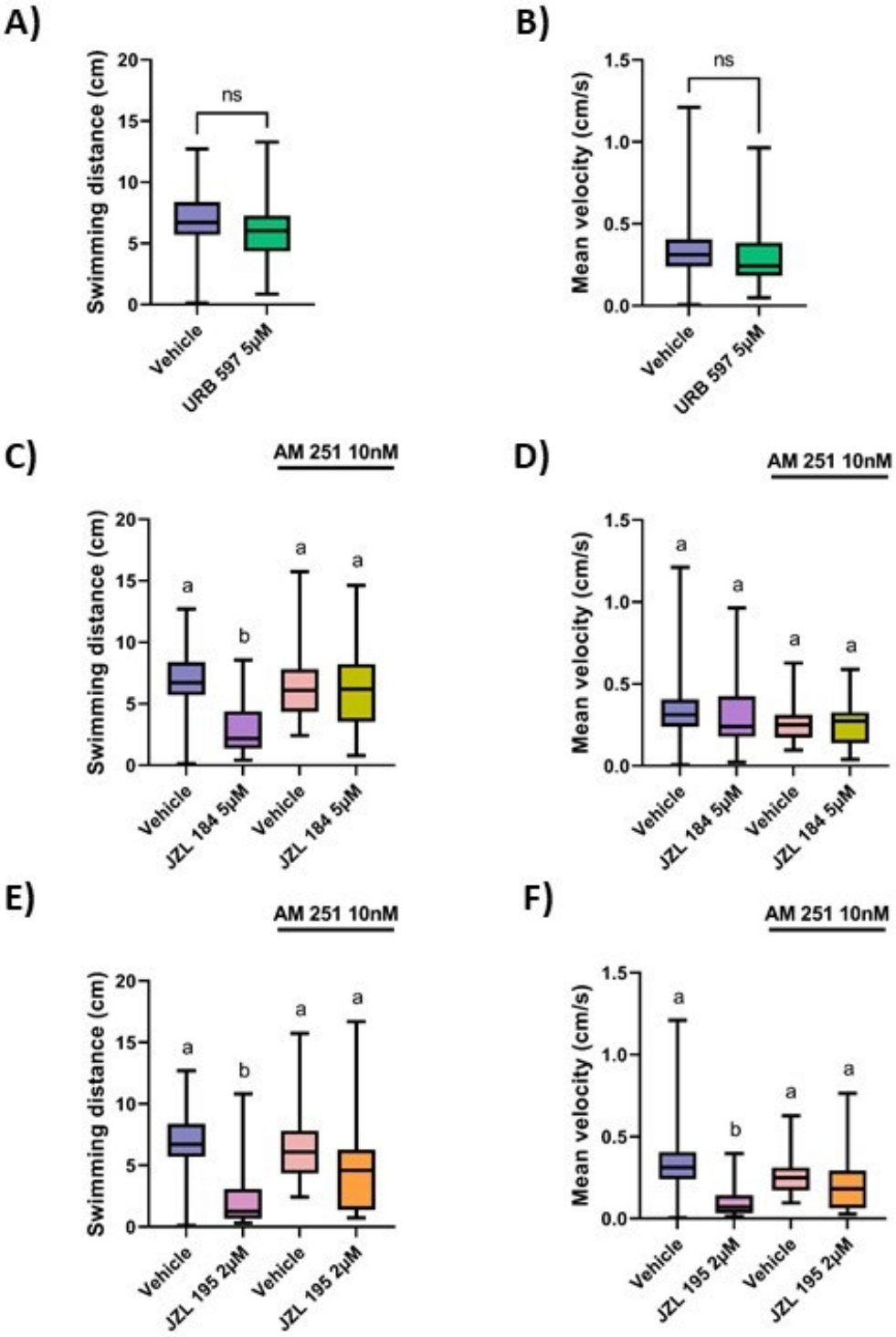
A)
Swimming distance (cm)
ns
Vehicle
URB 597 5μM
B)
Mean velocity (cm/s)
ns
Vehicle
URB 597 5μM
C)
AM 251 10nM
Swimming distance (cm)
a
b
a
a
Vehicle
JZL 184 5μM
Vehicle
JZL 184 5μM
D)
AM 251 10nM
Mean velocity (cm/s)
a
a
a
a
Vehicle
JZL 184 5μM
Vehicle
JZL 184 5μM
E)
AM 251 10nM
Swimming distance (cm)
a
b
a
a
Vehicle
JZL 195 2μM
Vehicle
JZL 195 2μM
F)
AM 251 10nM
Mean velocity (cm/s)
a
b
a
a
Vehicle
JZL 195 2μM
Vehicle
JZL 195 2μM

Figure 4.1: Escape swimming deficits caused by singular MAGL or dual FAAH/MAGL inhibition are rescued by blocking CB1R. Escape swimming in response to an acute touch stimulus was assessed in zebrafish embryos at 2 days post-fertilization (dpf). The effect of ~24-hour drug treatment on embryonic escape swimming distance (cm) and mean velocity (cm/s) was measured and mean ranks of treatment groups were compared against each other. In each respective treatment group, the horizontal line within its box plot represents the median value which is surrounded by the interquartile range, while the error bars represent the maximum and minimum values. (**A and B**) The effects of 5 μM URB 597 (n=38) on escape swimming is compared relative to the vehicle control (n=34), where ns = not statistically significant (Mann-Whitney test – where statistical significance was determined as $p<0.05$). (**C and D**) The effects of the vehicle control (n=34), 5 μM JZL 184 (n=30), 10 nM AM 251 (n=33), and JZL 184 in the presence of AM 251 (n=43) on escape swimming were compared. (**E and F**) The effects the vehicle control (n=34), 2 μM JZL 195 (n=39), 10nM AM 251 (n=33), and JZL 195 in the presence of AM 251 (n=34) on escape swimming were compared. N=4 experiments with 8-11 animals per experiment for each treatment. For panels **C-F**, columns which share the same letter(s) of the alphabet are not statistically different from one another (Kruskal-Wallis, followed by Dunn's multiple comparisons test – where statistical significance was determined as $p<0.05$).

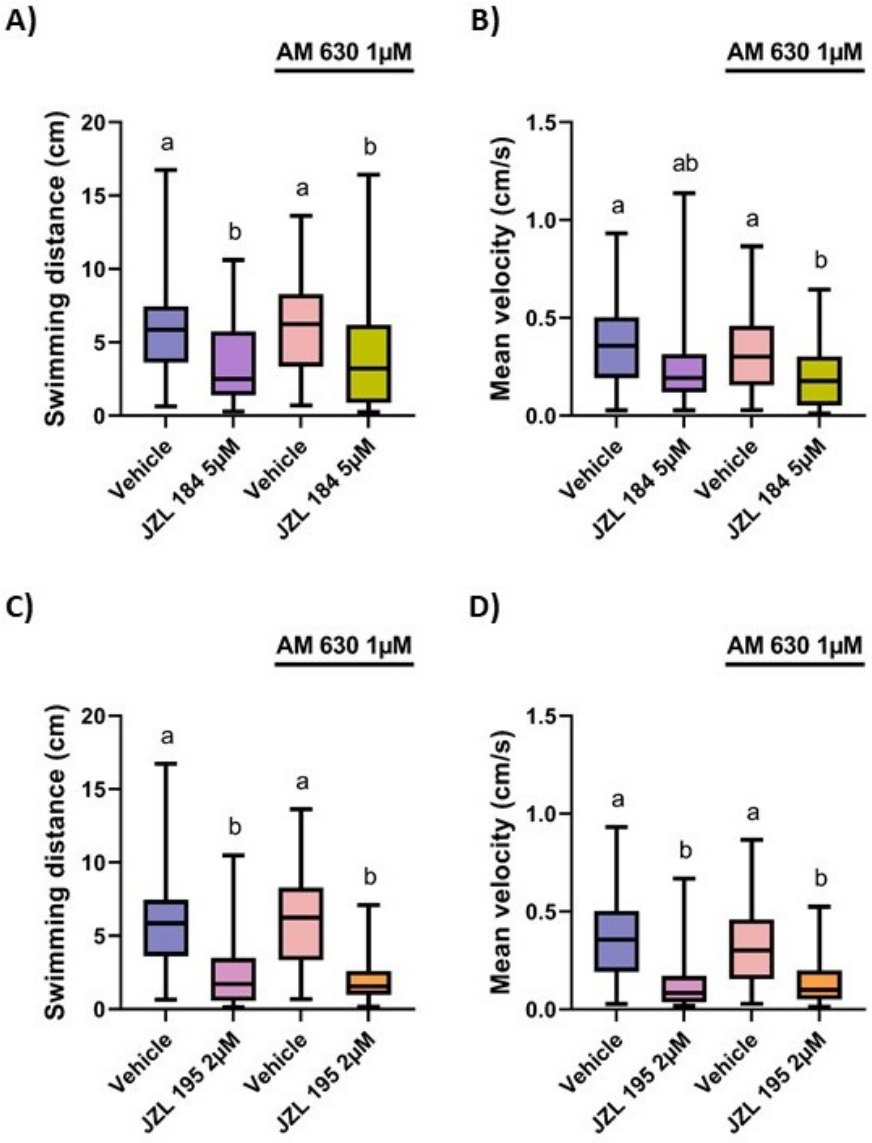
A)
AM 630 1μM
Swimming distance (cm)
20
15
10
5
0
a
b
a
b
Vehicle
JZL 184 5μM
Vehicle
JZL 184 5μM
B)
AM 630 1μM
Mean velocity (cm/s)
1.5
1.0
0.5
0.0
a
ab
a
b
Vehicle
JZL 184 5μM
Vehicle
JZL 184 5μM
C)
AM 630 1μM
Swimming distance (cm)
20
15
10
5
0
a
b
a
b
Vehicle
JZL 195 2μM
Vehicle
JZL 195 2μM
D)
AM 630 1μM
Mean velocity (cm/s)
1.5
1.0
0.5
0.0
a
b
a
b
Vehicle
JZL 195 2μM
Vehicle
JZL 195 2μM

Figure 4.2: Reductions to swimming performance caused by singular MAGL or dual FAAH/MAGL inhibition are still observed when blocking CB2R. Escape swimming in response to an acute touch stimulus was assessed in zebrafish embryos at 2 days post-fertilization (dpf). The effect of ~24-hour drug treatment on embryonic escape swimming distance (cm) and mean velocity (cm/s) was measured, and mean ranks of treatment groups were compared against each other. In each respective treatment group, the horizontal line within its box plot represents the median value which is surrounded by the interquartile range, while the error bars represent the maximum and minimum values. (**A and B**) The effects of the vehicle control (n=35), 5 μM JZL 184 (n=36), 1 μM AM 630 (n=52), and JZL 184 in the presence of AM 630 (n=36) on escape swimming were compared. (**C and D**) The effects the vehicle control (n=35), 2 μM JZL 195 (n=36), 1μM AM 630 (n=52), and JZL 195 in the presence of AM 630 (n=28) on escape swimming were compared. N=4 experiments with 7-13 animals per experiment for each treatment. Columns which share the same letter(s) of the alphabet are not statistically different from one another (Kruskal-Wallis, followed by Dunn's multiple comparisons test – where statistical significance was determined as $p<0.05$).

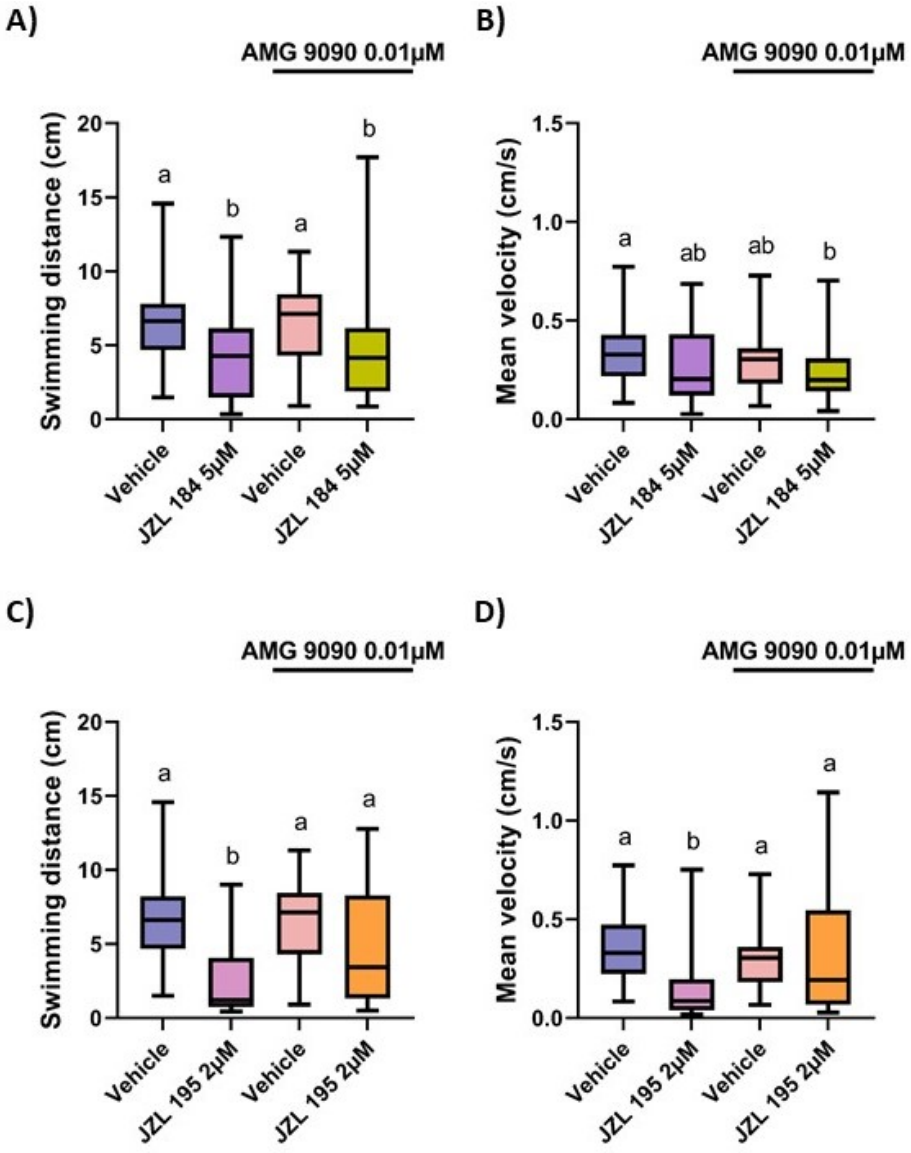
A)
AMG 9090 0.01μM
Swimming distance (cm)
20
15
10
5
0
a
b
a
b
Vehicle
JZL 184 5μM
Vehicle
JZL 184 5μM
B)
AMG 9090 0.01μM
Mean velocity (cm/s)
1.5
1.0
0.5
0.0
a
ab
ab
b
Vehicle
JZL 184 5μM
Vehicle
JZL 184 5μM
C)
AMG 9090 0.01μM
Swimming distance (cm)
20
15
10
5
0
a
b
a
a
Vehicle
JZL 195 2μM
Vehicle
JZL 195 2μM
D)
AMG 9090 0.01μM
Mean velocity (cm/s)
1.5
1.0
0.5
0.0
a
b
a
a
Vehicle
JZL 195 2μM
Vehicle
JZL 195 2μM

Figure 4.3: Blocking TRP channels with AMG 9090 prevents the escape swimming deficits caused by dual FAAH/MAGL inhibition, but not deficits caused by singular MAGL inhibition. Escape swimming in response to an acute touch stimulus was assessed in zebrafish embryos at 2 days post-fertilization (dpf). The effect of ~24-hour drug treatment on embryonic escape swimming distance (cm) and mean velocity (cm/s) was measured, and mean ranks of treatment groups were compared against each other. In each respective treatment group, the horizontal line within its box plot represents the median value which is surrounded by the interquartile range, while the error bars represent the maximum and minimum values. (**A and B**) The effects of the vehicle control (n=35), 5 μM JZL 184 (n=33), 0.01 μM AMG 9090 (n=40), and JZL 184 in the presence of AMG 9090 (n=40) on escape swimming were compared. (**C and D**) The effects the vehicle control (n=35), 2 μM JZL 195 (n=38), 0.01 μM AMG 9090 (n=40), and JZL 195 in the presence of AMG 9090 (n=39) on escape swimming were compared. N=4 experiments with 8-10 animals per experiment for each treatment. Columns which share the same letter(s) of the alphabet are not statistically different from one another (Kruskal-Wallis, followed by Dunn's multiple comparisons test – where statistical significance was determined as $p<0.05$).

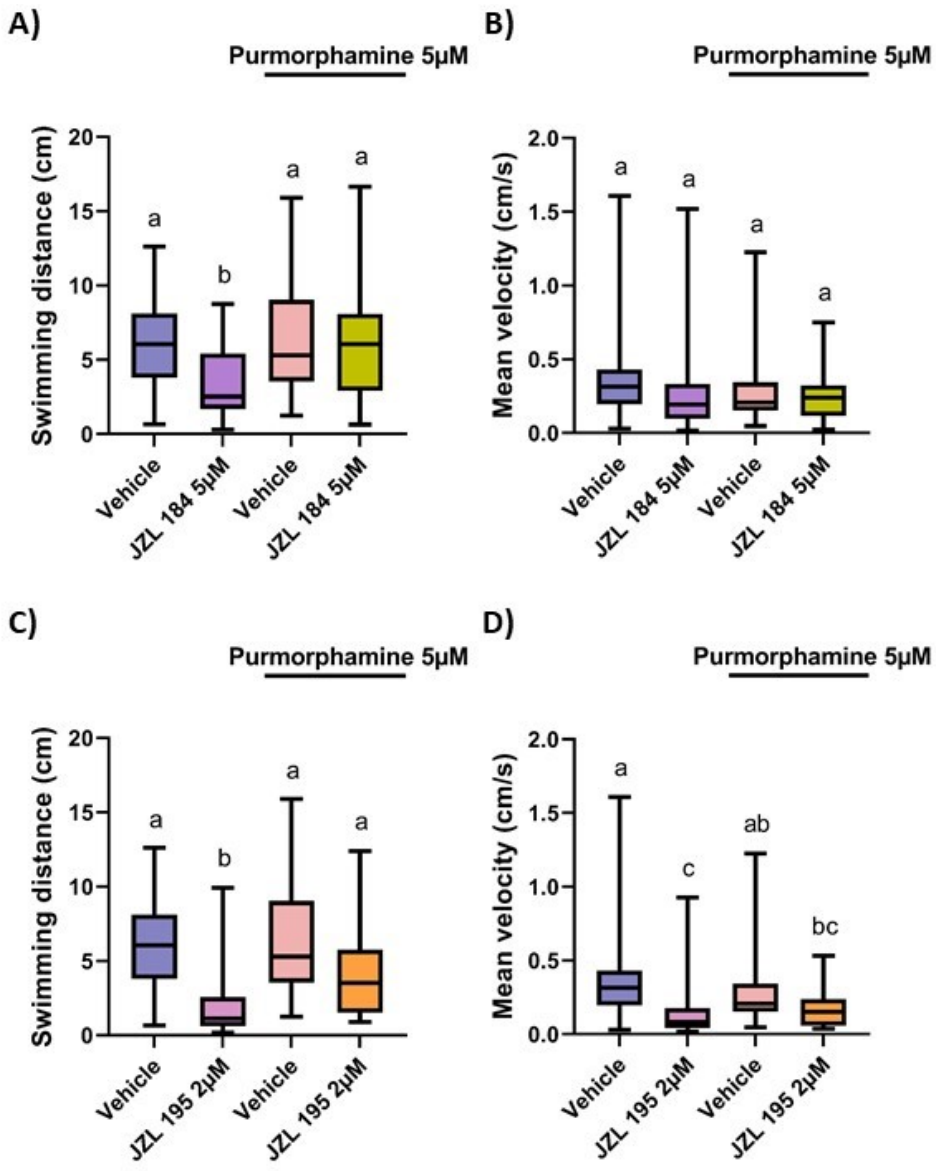
A)
Purmorphamine 5μM
Swimming distance (cm)
20
15
10
5
0
a
b
a
a
Vehicle
JZL 184 5μM
Vehicle
JZL 184 5μM
B)
Purmorphamine 5μM
Mean velocity (cm/s)
2.0
1.5
1.0
0.5
0.0
a
a
a
a
Vehicle
JZL 184 5μM
Vehicle
JZL 184 5μM
C)
Purmorphamine 5μM
Swimming distance (cm)
20
15
10
5
0
a
b
a
a
Vehicle
JZL 195 2μM
Vehicle
JZL 195 2μM
D)
Purmorphamine 5μM
Mean velocity (cm/s)
2.0
1.5
1.0
0.5
0.0
a
c
ab
bc
Vehicle
JZL 195 2μM
Vehicle
JZL 195 2μM

Figure 4.4: Activation of smoothened rescues locomotor deficits caused by MAGL inhibition and partially rescues escape swimming deficits caused by dual FAAH/MAGL inhibition. Escape swimming in response to an acute touch stimulus was assessed in zebrafish embryos at 2 days post-fertilization (dpf). The effect of ~24-hour drug treatment on embryonic escape swimming distance (cm) and mean velocity (cm/s) was measured, and mean ranks of treatment groups were compared against each other. In each respective treatment group, the horizontal line within its box plot represents the median value which is surrounded by the interquartile range, while the error bars represent the maximum and minimum values. (**A and B**) The effects of the vehicle control (n=34), 5 μM JZL 184 (n=37), 5 μM purmorphamine (n=34), and JZL 184 in the presence of purmorphamine (n=34) on escape swimming were compared. (**C and D**) The effects the vehicle control (n=34), 2 μM JZL 195 (n=38), 5 μM purmorphamine (n=34), and JZL 195 in the presence of purmorphamine (n=33) on escape swimming were compared. N=4 experiments with 8-10 animals per experiment for each treatment. Columns which share the same letter(s) of the alphabet are not statistically different from one another (Kruskal-Wallis, followed by Dunn's multiple comparisons test – where statistical significance was determined as $p<0.05$).

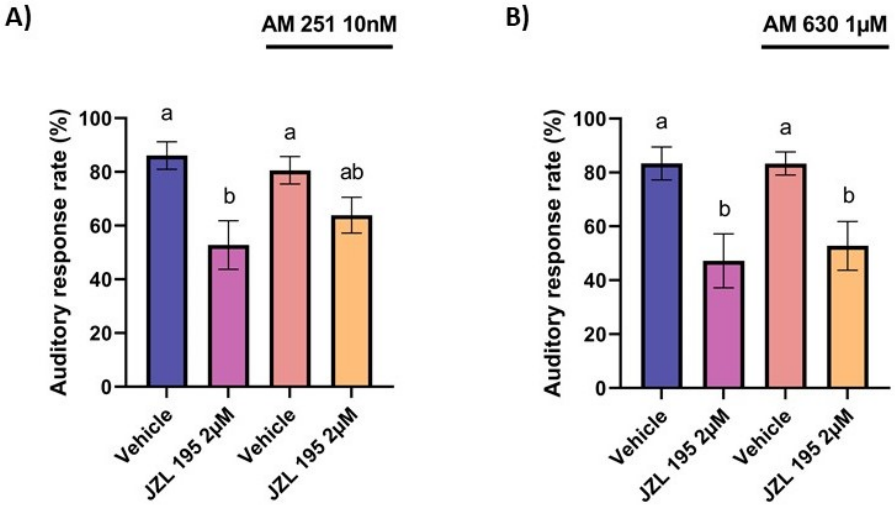
A)
AM 251 10nM
Auditory response rate (%)
100
80
60
40
20
0
a
b
a
ab
Vehicle
JZL 195 2μM
Vehicle
JZL 195 2μM
B)
AM 630 1μM
Auditory response rate (%)
100
80
60
40
20
0
a
b
a
b
Vehicle
JZL 195 2μM
Vehicle
JZL 195 2μM

Figure: 4.5: Co-treatment with cannabinoid receptor antagonists do not produce a detectable recovery in auditory/vibrational response deficits caused by JZL 195 exposure. A 500Hz audio tone was delivered to larvae at the age of 6 days post-fertilization to assess their responsiveness to auditory/vibrational stimuli. Larvae were tested in groups of 6 and allowed 20-minutes of acclimation prior to receiving the stimulus. Whether larvae responded with a short-latency C-start escape was recorded and the proportion of responding larvae is shown as the auditory response rate (%). Response rates were assessed in animals co-treated with either the **(A)** CB1R antagonist AM 251, or the **(B)** CB2R antagonist AM 630. The concentrations of co-treated compounds were 10 nM for AM 251 and 1 μM for AM 630. Exposure to either antagonist took place from ~0-24 hpf during the same period of time that animals were exposed to 2 μM JZL 195: a dual FAAH and MAGL inhibitor. N=6 with 6 animals per experiment for each treatment (n=36 animals). Columns which share the same letter(s) of the alphabet are not statistically different from one another (One-Way ANOVA, followed by Tukey's multiple comparisons test – where statistical significance was determined as $p<0.05$). Columns indicate mean values, while error bars represent standard error of the mean (SEM).

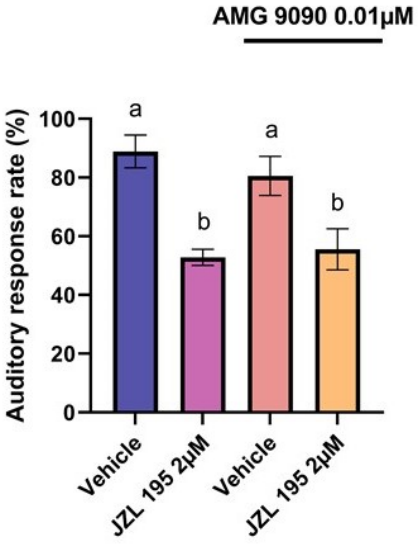
AMG 9090 0.01μM
Auditory response rate (%)
100
80
60
40
20
0
a
b
a
b
Vehicle
JZL 195 2μM
Vehicle
JZL 195 2μM

Figure 4.6: Co-treatment with the TRP channel inhibitor AMG 9090 does not produce observable recoveries in JZL 195-induced auditory/vibrational response deficits. A 500Hz audio tone was delivered to larvae at the age of 6 days post-fertilization to assess their responsiveness to auditory/vibrational stimuli. Larvae were tested in groups of 6 and allowed 20-minutes of acclimation prior to receiving the stimulus. Whether larvae responded with a short-latency C-start escape was recorded and the proportion of responding larvae is shown as the auditory response rate (%). Response rates were assessed in animals co-treated with 0.01 μM AMG 9090. Exposure to AMG 9090 took place from ~0-24 hpf during the same period of time that animals were exposed to 2 μM JZL 195: a dual FAAH and MAGL inhibitor. N=6 experiments with 6 animals per experiment for each treatment (n=36 animals). Columns which share the same letter(s) of the alphabet are not statistically different from one another (One-Way ANOVA, followed by Tukey's multiple comparisons test – where statistical significance was determined as $p<0.05$). Columns indicate mean values, while error bars represent standard error of the mean (SEM).

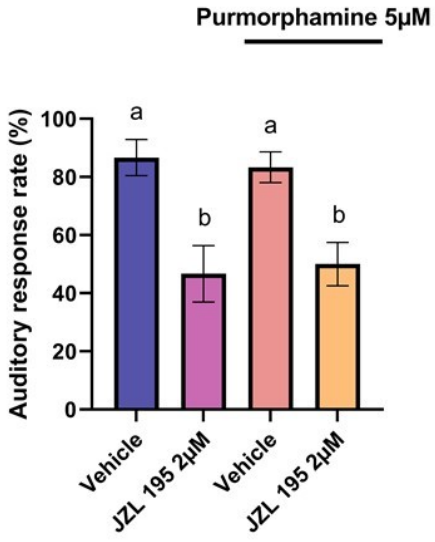
Purmorphamine 5μM
Auditory response rate (%)
100
80
60
40
20
0
a
b
a
b
Vehicle
JZL 195 2μM
Vehicle
JZL 195 2μM

Figure 4.7: Co-treatment with the Smoothened agonist purmorphamine does not result in a detectable recovery in auditory/vibrational response deficits caused by JZL 195. A 500Hz audio tone was delivered to larvae at the age of 6 days post-fertilization to assess their responsiveness to auditory/vibrational stimuli. Larvae were tested in groups of 6 and allowed 20-minutes of acclimation prior to receiving the stimulus. Whether larvae responded with a short-latency C-start escape was recorded and the proportion of responding larvae is shown as the auditory response rate (%). Response rates were assessed in animals co-treated with 5 μM purmorphamine. Exposure to purmorphamine took place from ~0-24 hpf during the same period of time that animals were exposed to 2 μM JZL 195: a dual FAAH and MAGL inhibitor. N=5 experiments with 6 animals per experiment for each treatment (n=30 animals). Columns which share the same letter(s) of the alphabet are not statistically different from one another (One-Way ANOVA, followed by Tukey's multiple comparisons test – where statistical significance was determined as $p<0.05$). Columns indicate mean values, while error bars represent standard error of the mean (SEM).

Table 4.1: Summary of the observed receptor systems in which endocannabinoid-associated sensorimotor deficits occur through. The receptor systems assessed include: CB1R, CB2R, TRP channels, and SHH signaling (SMO receptor), and their involvement in mediating the effects of JZL 184 and JZL 195 are depicted.

Experimental assessment	Parameter	Effect of JZL 184 (MAGL inhibition) occurs through:	Effect of JZL 195 (FAAH + MAGL inhibition) occurs through:
Escape swimming (2 dpf)	Swimming distance (cm)	CB1R SHH (SMO)	CB1R TRP channels SHH (SMO)
	Mean velocity (cm/s)	N/A	CB1R TRP channels
Larval A/V escape response (6 dpf)	Auditory response rate (%)	N/A	None of the selected receptor systems were capable of preventing A/V response deficits

Chapter 5. Discussion

5.1 Summary of overall findings

In this thesis, I have presented data to show that an early perturbation of the eCS by inhibiting the activity of FAAH or MAGL individually, or by inhibiting both FAAH and MAGL simultaneously during embryogenesis alters aspects of locomotor and sensorimotor function. The aim of my project was to provide a more comprehensive foundation to investigate how the eCS is involved in functional locomotor and sensorimotor development. Overall, the work explored by this thesis seeks to expand the existing body of information regarding the endocannabinoid system's role in motor development by investigating the function of specific sensorimotor activities such as escape responses that are elicited by specific stimuli. Importantly, the majority of activities assessed here are driven by specific cues and they represent the functionality of escape response circuits (Carmean and Ribera, 2010; Kohashi et al., 2012; Saint-Amant and Drapeau, 1998). With this in mind, the work presented here involves assessing complex motor and sensorimotor programs to build upon the initial foundation set up by previous studies that explored the role the eCS in neuronal development and basic locomotor function. Understanding these complex processes is crucial for continuing to expand the current body of literature revolving around the connection between the eCS and vertebrate neurobiology.

My results on the effects of the dual inhibitor JZL 195 shows that activity of both FAAH and MAGL is important for normal sensorimotor activities, as demonstrated from reduced contractile activity at 1 dpf, altered escape responses at 2 dpf, and deficits to A/V responsiveness which first appear at 5 dpf, and are still present during adolescence (summarized in Table 3.1). Singular

inhibition of FAAH had little overall effect on sensorimotor function, whereas inhibition of MAGL alone resulted in small but significant effects on the development of locomotor behaviors. Importantly, these results show that the activity of both FAAH and MAGL together is essential for normal sensorimotor development, which suggests a synergistic dynamic between these two catabolic enzymes. Additionally, in terms of early vertebrate motor development, my thesis provides some of the first evidence implicating the interplay between eCB signaling with TRP channels and the SHH pathway (summarized in Table 4.1). In particular, I observed escape swimming behaviors in 2 dpf embryos and the responsiveness to A/V stimuli in 6 dpf larvae which were altered by eCS perturbations. By focusing on these experiments, I aimed to further evaluate the mechanisms behind these locomotor and sensorimotor alterations and to establish whether non-canonical eCB signaling mechanisms play a role in mediating eCS-related sensorimotor deficits in developing zebrafish.

With regard to canonical eCB signaling, my findings suggest that hypolocomotion caused by inhibiting MAGL and by dual FAAH/MAGL inhibition occurs through a CB1R mechanism, as opposed to a CB2R mechanism. Furthermore, in terms of non-canonical eCB signaling, I found that locomotor deficits caused by dual FAAH/MAGL inhibition are attenuated through blocking TRPA1/TRPV1/TRPM8, indicating their involvement here as well. Additionally, SHH signaling is also shown to be involved, as SMO activation rescued the swimming impairments caused by inhibition of MAGL and dual inhibition of FAAH and MAGL. Importantly, these results provide a brief overview that suggests that the endocannabinoid system interacts with multiple receptor and signaling mechanisms during embryogenesis and highlights the importance of non-canonical eCB signaling mechanisms in motor development. Interestingly, when investigating the

alterations to A/V escape responses of 6 dpf fish induced by early JZL 195 treatment, there was no functional recovery when targeting the receptor systems examined in this study.

5.2 Inhibition of FAAH and MAGL perturbs eCB signaling

Targeting eCB catabolic enzymes is a very useful approach for studying the role of eCB signaling and this has been reported in literature that uses rodent models (Zou and Kumar, 2018). In mice, blocking FAAH using SSR411298 caused an increase in hippocampal AEA in a dose-dependent manner, without affecting the levels of 2-AG (Griebel et al., 2018). Additionally, similar findings are seen from administering URB 597 to rats, where blocking FAAH activity causes a significant rise in the FAAH substrates: AEA, palmitoylethanolamide (PEA), and oleoylethanolamide (OEA) (Danandeh et al., 2018). Inhibiting MAGL activity in mice with SAR127303 substantially increases hippocampal levels of 2-AG without altering the levels of AEA (Griebel et al., 2015). Meanwhile, blocking MAGL with JZL 184 in mice resulted in an 8-fold increase in the levels of 2-AG in the brain, without any significant alterations to AEA levels (Long et al., 2009a). Lastly, dual inhibition of FAAH/MAGL using JZL 195 elevated the levels of both 2-AG and AEA in the brain of mice in a dose-dependent manner (Long et al., 2009b).

My results suggest that in terms of eCB catabolic enzymes, the activity of MAGL has a more significant role than FAAH in sensorimotor development, which has implications for the abundances of AEA and 2-AG. During early development, the levels of AEA are relatively low compared to 2-AG (Fride, 2008). Furthermore, in zebrafish embryos, 2-AG is maintained at levels over 10-fold higher than AEA, indicating that 2-AG is vastly more abundant and likely has

a greater influence on receptor systems during embryogenesis (Martella et al., 2016). Although the activity of FAAH and MAGL appear to have a degree of synergy, the greater potential for 2-AG-related receptor interactions supports the implications of my results, where MAGL inhibition was capable of significantly altering aspects of 2 dpf escape swimming and the C-start escape response, which was in contrast to FAAH inhibition, as inhibiting FAAH did not alter the measured parameters of these responses.

5.3 Critical cell types involved in zebrafish sensorimotor functions

In zebrafish, primary motor neurons originate at ~9 hpf during gastrulation (Westerfield et al., 1986). These developing motor axons then extend outwards from the spinal cord to innervate muscle cells. It is likely that the locomotor deficits observed at 1 and 2 dpf are partially due to motor neuron defects caused by FAAH/MAGL inhibition, which was demonstrated previously in zebrafish embryos (Sufian et al., 2021). In particular, Sufian and colleagues revealed that primary and secondary motor neuron branching was decreased due to FAAH/MAGL inhibition. Given that the eCS is involved in axonal pathfinding, and considering the decreased motor neuron branching, this perturbation has likely led to fewer synaptic contacts being established, potentially leading to an overall reduction in neurotransmission within the neuromuscular system (Berghuis et al., 2007; Watson et al., 2008). As motor neurons establish neuromuscular connections, this coincides with the formation of functional networks for locomotor activities in zebrafish (Drapeau et al., 2002). For instance, embryonic white muscle fibers play a significant role in early locomotion, as white fibers are predominantly recruited during rapid and reflexive movements, which make up the zebrafish's motor repertoire during the 1-3 dpf period of development (Buckingham and Ali, 2004; Buss and Drapeau, 2002). Meanwhile, as larval

development progresses, the more tonic role of embryonic red muscle fibers further emerges, as rhythmic beat-and-glide swimming first develops between 3 and 4 dpf (Ahmed and Ali, 2016; Drapeau et al., 2002). Thus, functional motor neurons are critical for facilitating these diverse neuromuscular programs, and when it comes to muscular development, the innervation and morphology of white muscle is likely impacted by eCS perturbation more heavily than red muscles, especially when considering the larger role of white fibers in escape movements. Besides motor neurons and muscle fibers, the transient Rohon-Beard neurons, which typically begin undergoing apoptosis after ~34 hpf are also known to play an important role in controlling embryonic movement in zebrafish (Slatter et al., 2005). Rohon-Beard neurons, along with cerebrospinal fluid-contacting neurons are thought to control and mediate motor neuron activation in early sensorimotor processes (Henderson et al., 2019). However, it is unclear if the eCS is involved in the development and function of these cells.

Another critical cell type developing within the first 24 hours of zebrafish embryogenesis is the M-cell and its homologs MiD2cm and MiD3cm found within the hindbrain (Kimmel et al., 1990). These large neurons which begin developing at 8 hpf are essential for initiating sensorimotor escape responses, and are crucial for controlling locomotor functions and for relaying incoming mechanosensory and auditory information (Bang et al., 2002). As M-cells develop, they form complex escape circuits which involve synaptic contacts with motor neurons to orchestrate rapid escape movements (Kimmel et al., 1990). In order to coordinate escape responses, when an M-cell is stimulated by mechanical or acoustic stimuli, it transmits excitatory glutamatergic signals to the contralateral motor neurons, resulting in muscular contractions that propel the animal away from the source of the stimulus (Brownstone and Chopek, 2018).

Conversely, ipsilateral motor neurons are inhibited, leading to the inhibition of ipsilateral muscle fibers, which enables an agonist-antagonist muscular relationship to facilitate rapid escapes. Previous work shows that axonal growth and fasciculation of M-cells and hindbrain reticulospinal neurons is altered by knocking down expression of the CB1R in zebrafish (Watson et al., 2008). Furthermore, embryonic exposure to THC reduces the diameter of M-cell axons, likely suggesting that the electrophysiological properties of the M-cells have been also altered (Amin et al., 2020). These findings highlight the importance of the eCS in M-cell development. Thus, the increased response latencies observed here may be indicative of defects in the synaptic contacts of M-cells, leading to altered M-cell-mediated communication. Because this reflex response occurs on the order of milliseconds, alterations to M-cell morphology or synaptic communications may impose deficits to escape response latency. With all this in mind, the known impacts of FAAH/MAGL inhibition on motor neurons in conjunction with the potential for effects on cell populations such as Rohon-Beard neurons and M-cells must also be investigated.

5.4 Development and functionality of the A/V escape response

Within the first 7 days of zebrafish embryonic/larval development, the inner ear undergoes a large increase in the population and density of hair cells, rendering them more sensitive to auditory stimuli (Lu and DeSmidt, 2013). Additionally, M-cells also become receptive to auditory information around ~3 dpf, when synaptic connections between the M-cells and the otoliths become established (Bang et al., 2002). These developments are associated with increased receptiveness to auditory inputs, therefore, I sought to establish in general, how this aspect of sensory development is functionally affected by FAAH/MAGL inhibition. I observed

larval A/V response deficits in animals treated with the dual FAAH/MAGL inhibitor JZL 195, demonstrating that eCS activity is pertinent for the development of functional auditory-escape circuits. Because there was no significant effect from singular inhibition of FAAH or MAGL, my findings suggest a possible synergy between the activity of both FAAH and MAGL in the early development of auditory escape. Notably, significant effects of FAAH/MAGL inhibition on A/V responsiveness were observed at 5 and 6 dpf, but not at 3 and 4 dpf. M-cell synaptic contacts are still undergoing early development between 3 and 4 dpf when inner ear hair cells are still at an immature stage, therefore the sensitivity to A/V inputs is likely low. Perhaps the escape response circuit becomes more susceptible to alterations as development proceeds and the synaptic connections become more advanced by 5 and 6 dpf. However, the exact reason for the effects being experienced at 5 and 6 dpf and not at 3 and 4 dpf is unclear at this time.

Despite being adolescent animals, juvenile zebrafish exhibit most of their adult characteristics, with the exception of male/female sexual differentiation (Parichy et al., 2009). Juveniles at ~8 weeks of age possess functionally mature lateral line and inner ear hair cells, indicating that auditory receptiveness of juvenile zebrafish likely reflects that of fully developed adults (Olt et al., 2014). Interestingly, despite the functional maturation of these cells, juveniles experienced the same response deficits as larval animals after treatment with JZL 195, indicating that there was no recovery from the effects of eCS perturbation on A/V responses. In mammals, CB1Rs are shown to be expressed in the cochlea (Zheng et al., 2007), while CB2Rs are expressed in inner ear hair cells, and to a smaller extent, in outer ear hair cells (Martín-Saldaña et al., 2016). Since a likely consequence of JZL 195 treatment would be the abnormal activation of cannabinoid receptors located within the inner and outer ear, it is possible that this leads to hair cell

dysfunction. Furthermore, given the prevalent expression of TRPA1 and TRPV4 channels in the hair cells of the zebrafish lateral line and inner ear organs, and the known agonistic actions of eCBs with TRPA1, TRPV1, and TRPV4 (Germanà et al., 2018), eCS perturbation may impact auditory development through TRP channel interactions (Amato et al., 2012; Corey et al., 2004; Watanabe et al., 2003). Over-activation of eCB signaling likely exhibits premature and extensive activation of these receptor systems, consequently impinging upon auditory function during early life as well as during later developmental stages.

5.5 Canonical cannabinoid receptor mechanisms involved in mediating locomotor development

In terms of the canonical cannabinoid receptors CB1R and CB2R, their genetic expression is detectable at very early periods of development. For example, in rat embryos, CB1R mRNA expression is detected as early as gestational day 11, and CB2R mRNA expression is detected at gestational day 13 (Buckley et al., 1997). In zebrafish, genetic expression of CB1R and CB2R is present as early as 1 hpf, indicating that the primary eCS receptors are likely sensitive to the effects of eCBs within the time frame of my exposure paradigm (Oltrabella et al., 2017). Previous work in rodent models studying the effects of dysregulated eCB signaling found that the anxiolytic effects and locomotor alterations caused by FAAH/MAGL inhibition are prevented through blocking CB1R. In rats, the anti-anxiety effects induced by the FAAH inhibitor URB 597 can be blocked with the CB1R antagonist rimonabant (Danandeh et al., 2018; Kathuria et al., 2003). In zebrafish, the increased risk-taking and exploratory locomotor behaviors caused by the dual FAAH/MAGL inhibitor JZL 195 was partially blocked by treatment with the CB1R antagonist SR141716A (Boa-Amponsem et al., 2019). Lastly,

hypolocomotion in adult rats caused by treatment with the MAGL inhibitor JZL 184 and JZL 195 was prevented by treatment with SR141716A (Seillier et al., 2014). Furthermore, activity of CB1R is critical for the development of reticulospinal neurons involved in locomotor and sensorimotor programs (Rodríguez de Fonseca et al., 1998; Watson et al., 2008). The findings outlined here indicate the prevalent involvement of CB1R when it comes to the role of eCB signaling in sensorimotor processes. Additionally, similar to my findings, eCS-related locomotor alterations do not appear to occur through the CB2R (Sufian et al., 2021). With respect to binding affinity, AEA is known to preferentially bind to the CB1R, while 2-AG is known to have affinity towards both the CB1R and CB2R (Zou and Kumar, 2018). Given the preferential binding of the eCBs, and my results which indicate that eCS-related sensorimotor alterations are partially occurring through activation of the CB1R, this further exemplifies the prevalence of CB1R's involvement in early sensorimotor development.

5.6 Non-canonical cannabinoid receptor mechanisms involved in mediating locomotor development

In terms of zebrafish motor development, the involvement of TRP channels is not well characterized, as they are primarily recognized as mediators of ionic homeostasis and act as crucial receptor mechanisms in sensory systems (Nilius and Owsianik, 2011). In zebrafish, TRPA1 is abundant in the lateral line neuromast hair cells, serving as mechanosensory receptors (Germanà et al., 2018). In terms of locomotor activity, the presence of these channels likely plays an important role for sensing water motion, thus facilitating functional movement (Moorman, 2001). My findings provide evidence that the facilitation of functional locomotor development is associated with the interplay between TRP channels and eCB signaling. It

remains unclear how exactly TRP channels are associated with eCBs to facilitate functional motor systems. However, a recent study in the Ali Lab used whole-mount *in-situ* hybridization to demonstrate that *trpv1* expression is detectable as early as 1 dpf within the trigeminal neurons, lateral line, and Rohon-Beard neurons, therefore indicating that during embryogenesis, these receptor systems are located on key mechanosensory structures involved in motor and sensorimotor activities (McArthur et al., 2020; Son and Ali, 2022). Trigeminal neurons in particular are involved in relaying mechanical stimuli, along with chemical and temperature-related information across the spinal cord and hindbrain (Pan et al., 2012). Consequently, in terms of sensory function, because AEA and its derivatives are not only limited to CB1R interactions, and may also act as high affinity agonists of TRPA1 and TRPV1, these receptor systems are of great interest for further exploration, especially given my observations presented in this thesis (Morales et al., 2017; Muller et al., 2019). Given the affinities of eCBs for TRPA1 and TRPV1, my findings suggest that a potential consequence of FAAH/MAGL inhibition would be the precocious activation of TRPA1/TRPV1 located on structures such as trigeminal neurons, the lateral line, or Rohon-Bead neurons (Muller et al., 2019; Watanabe et al., 2003). This activation has likely led to the altered development or defective functionality of these structures, potentially resulting in the observed alterations to escape swimming.

My results indicated that TRP channel blockade was able to prevent deficits caused by dual FAAH/MAGL inhibition, but not by single MAGL inhibition. Although this potentially implicates the roles of AEA and the FAAH enzyme, my findings here demonstrate that singular FAAH inhibition does not alter this particular aspect of locomotion. Overall, my results suggest a more dominant influence from 2-AG signaling, but AEA's potential role here is still elusive and

must be studied further. In terms of preventing the effects of dual inhibition by JZL 195, this result might be explained through the greater extent of cannabinoid receptor activation due to the elevation of both AEA and 2-AG signaling, which potentially relates to a greater extent of eCS-TRP channel interactions. For instance, in the mouse brain, CB1Rs colocalize with TRPV1 (Cristino et al., 2006). Furthermore, this colocalization is detected in the cerebellum, implicating a relation to motor function/coordination. Additionally, CB2Rs and TRPV1 have been shown to colocalize in human dorsal root ganglia, further highlighting the interplay between these receptor systems and the eCS ligands (Anand et al., 2008). With this in mind, centrally and peripherally located TRPV1 channels may undergo crosstalk with activated CB1Rs/CB2Rs as a consequence of JZL 184 or JZL 195 treatment. In my experiments, AMG 9090 was used to block TRP channels in a system where eCB signaling has been increased, causing locomotor deficits. These deficits are also shown to occur in part through CB1Rs. Thus, using AMG 9090 to inhibit these TRP channels may mitigate this potential for the widespread activation of TRPV1 channels that are colocalizing with activated CB1Rs. Despite the interpretations proposed here, further embryonic studies must be done in zebrafish to ascertain how eCBs specifically interact with these particular TRP subtypes to influence motor development.

The SHH pathway has been recently shown to possess the capacity to interact with cannabinoids (Boa-Amponsem et al., 2019; Khaliullina et al., 2015). Proximity ligation experiments demonstrated that CB1R and SMO form a heteromer, illustrating the potential for eCB-SHH interactions (Fish et al., 2019). Both the CB1R and SHH signaling serve as critical components in neural development (Choudhry et al., 2014; Watson et al., 2008). For instance, the CB1R is important for the development of hindbrain reticulospinal neurons in zebrafish, which are crucial

for sensorimotor function as mentioned previously (Watson et al., 2008). Previous work also demonstrates that perturbations of the eCS in embryonic zebrafish leads to alterations in the development of reticulospinal and motor neurons, and these findings are also coupled with locomotor deficits (Ahmed et al., 2018; Amin et al., 2020; Sufian et al., 2019). Meanwhile, SHH signaling is crucial for neural tube formation and is required for motor neuron differentiation (Ericson et al., 1996). Furthermore, to study SHH signaling as it relates to functional motor activity in mice, one study used CTB-saporin, which is a type of cholera toxin that can be injected into the limbs to induce degeneration of motor neurons (Gulino et al., 2017). This study found that the functional motor recovery after the CTB-saporin-induced depletion of motor neurons was correlated with increased SHH expression in the lumbar spinal cord of mice (Gulino et al., 2017). Therefore, it is clear that while the eCS and SHH pathway play important roles in the neurobiology of locomotor function, my findings suggest that their influences likely converge when it comes to functional locomotor development. In my experiments, the SMO agonist purmorphamine was effective in preventing swimming deficits caused by JZL 184 and JZL 195. This indicates that 2-AG signaling is likely coupled with SMO activity, and that this dynamic must be appropriately regulated to facilitate normal motor development. Overall, the recent findings suggesting that SHH signaling is a mechanism of action for cannabinoids supports my observations of an eCS-SMO interaction in the motor development of zebrafish.

5.7 Canonical and non-canonical cannabinoid receptor systems involved in mediating the development of A/V escape responses

Despite the recoveries associated with AM 251, AMG 9090, and purmorphamine treatments on 2 dpf escape swimming, the same was not observed when assessing A/V responsiveness at 6 dpf.

This result was unexpected because most of the previously observed effects of JZL 195 have been identified to at least occur partially through the CB1R, as seen when examining locomotor behaviors in zebrafish and rats (Boa-Amponsem et al., 2019; Seillier et al., 2014). These findings were further supported through zebrafish embryonic studies done by a previous graduate student in the Ali Lab, which found JZL 195-induced motor neuron aberrations at 2 dpf, and hypolocomotion at 5 dpf are in part mediated through the CB1R (Sufian et al., 2021). Furthermore, the 2 dpf findings that I have reported also support this notion as well. From the 6 dpf A/V escape response assessments however, it appears that either the effects of JZL 195 bypasses the influence of the co-treated drugs, or that JZL 195 may be impacting different signaling systems than those considered in my experimental design. Although the escape responses at 2 dpf and 6 dpf are similar in overall function, serving as avoidance to aversive stimuli, it must be emphasized that these are complex responses that act and develop separately from each other. These responses rely upon distinct cell types, and thus involve different neuronal circuits that act through multiple cellular pathways.

The A/V-induced escape response at 6 dpf involves synaptic integration with the lateral line hair cells, as well as connections to inner ear hair cells of the otoliths – importantly, these inner ear hair cells are not present at 2 dpf (Bang et al., 2002; Kohashi et al., 2012). Hair cells of the lateral line and inner ear develop through developmental programs that are initiated through the regulation of notch-delta signaling (Baek et al., 2021; Ma and Raible, 2009). Additionally, modulation of Wnt signaling is also important for regulating hair cell proliferation, indicating that the involvement of these pathways is critical for auditory development (Head et al., 2013; Romero-Carvajal et al., 2015). One study has shown that activation of Wnt signaling leads to an

increase in hair cell proliferation, while inhibition of Wnt signaling with the Wnt antagonist IWR-1 results in decreased hair cell proliferation in the zebrafish lateral line organ (Jacques et al., 2014). Interestingly, this group also reported that IWR-1 treatment led to reduced functionality of startle responses, where the authors state that startle responses were delayed, but swimming appeared normal (Jacques et al., 2014).

Endocannabinoids and the Wnt signaling pathway appear to have interactions, as treatment with AEA resulted in an increase in the relative genetic expression of Wnt 5a in cholangiocarcinoma cells (DeMorrow et al., 2008). Moreover, treatment with recombinant Wnt 5a decreased the proliferation in these cancerous cells, while treatment with AEA was shown to also result in decreased proliferation in a similar manner as upregulating Wnt signaling. This indicates that eCBs may have potential interactions with the Wnt signaling pathway in terms of cellular proliferation. With regard to inner ear development as it relates to JZL 195 exposure, perhaps an increase in eCB activity has perturbed Wnt signaling, leading to defects in hair cell proliferation. As the eCS appears to have interactions with aspects of the Wnt signaling pathway, how these interactions play a role in zebrafish hair cell development still remains unclear. Although this may illustrate a possible mechanism by which auditory responsiveness is altered by JZL 195 treatment, more work in studying these signaling pathways is essential to better understand how the eCS impacts functional auditory development

In relation to investigating the involvement of different receptor mechanisms and signaling pathways, another point to consider when co-treating animals with the receptor

antagonists/agonists, is the time frame from the point of initial exposure to the time of endpoint assessment. This is important to acknowledge due to the limitations posed by using pharmacological compounds. For instance, recoveries may not be seen at 6 dpf because in terms of time, the effects of JZL 195 may outlast the effects of AM 251, AM 630, AMG 9090, and/or purmorphamine. The FAAH inhibitor URB 597 and the MAGL inhibitor JZL 184 have both been described to bind irreversibly to inactivate their respective enzyme targets (Gil-Ordóñez et al., 2018; Lodola et al., 2013; Tripathi, 2020). Currently it is unclear whether JZL 195 also binds in an irreversible manner, as it appears this has not yet been conclusively examined. Still, if we are to assume that JZL 195 is similar to the singular inhibitors in terms of its capacity for inactivation of FAAH and MAGL, then it is very likely that the consequences of dual FAAH/MAGL inhibition are having effects that last beyond the time frame of the drug exposure. Furthermore, a study showed that in mice, MAGL inhibition with JZL 184 led to increased 2-AG levels in the brain which was observed 24-hours after the drug administration – this has implications towards examining the effects at different time points (Kinsey et al., 2013). Thus, eCB homeostasis at later time points such as 5 and 6 dpf may still be altered, and it may lie outside of its normal range due to the exposure of the eCS enzyme inhibitors. In terms of attempting to resolve this uncertainty using the zebrafish model, one important piece of information would be to measure and compare the enzymatic activities of FAAH and MAGL between control and JZL 195-treated animals at multiple time points ranging from 2-6 dpf, as this will provide details on how the enzyme activity fares across this developmental period. This analysis will be useful when measuring endpoints at 2 dpf and beyond, in order to more appropriately estimate how JZL 195 is affecting the activity of eCB catabolic enzymes after the exposure period has ended.

Chapter 6. Future directions and conclusions

6.1 Future directions

Broadly speaking, my experimental observations involved a focus on studying behaviors representative of early zebrafish locomotor and sensorimotor development. With consideration for sensorimotor development and the role of the eCS, there are many avenues for further investigation that can be proposed to build upon the work that I have compiled within this thesis. To expand our knowledge within the perspectives of developmental neurobiology, molecular biology, and physiology, these future directions are outlined below.

The first future direction I propose involves using a quantitative analysis technique such as liquid chromatography and mass spectrometry (LCMS) to measure the levels of eCBs within embryonic samples that had been subjected to the eCS perturbation in my exposure paradigm. LCMS would do much in the vein of expanding our understanding of the direct effects on eCBs resulting from exposure to URB 597, JZL 184 and JZL 195. Up to this point, my findings demonstrate how using these compounds to perturb the eCS during embryogenesis alters sensorimotor function, and previous findings also demonstrate that these drugs act at least in-part through the eCS – given that their effects can occur through the CB1R – and that they are specific to their enzymatic targets in zebrafish (Sufian et al., 2021). However, what we do not yet know is how exactly this exposure paradigm affects the abundance and bioavailability of the eCBs in zebrafish – this represents a limitation where we cannot know for certain the extent to which eCB levels are affected, nor can we be certain about the length of time that the system's eCB levels are outside of their normal range (Kinsey et al., 2013). Additionally, another aspect to

consider would be the accumulation and release of eCBs, as the circulating levels of available eCBs during development may also be impacted by how eCBs are released by tissues, which has implications on the overall concentration of eCBs. Therefore, performing LCMS is crucial to establish a more in-depth realization for the experimental intervention that is being performed here.

Due to the variety of alterations in the zebrafish C-start escape response that was caused by eCS perturbation, an investigation aimed towards studying M-cell morphology and functionality would greatly complement these findings. Our lab previously has performed immunohistochemistry using the 3A10 and RMO44 antibodies to visualize M-cells and reticulospinal neurons of zebrafish embryos exposed to THC (Amin et al., 2020). In the 2020 study by Amin and colleagues, phytocannabinoid exposure was used to perturb the eCS, and M-cell morphology was altered. In the case of FAAH/MAGL inhibition, we may expect similar findings due to the over activation of eCB signaling, but this must be elucidated, because assessing the structures associated with sensorimotor control is important to contextualize which parts of the escape circuits have been affected. With that in mind, examining the electrophysiological activities of the M-cells will also be a critical component to understanding how eCS perturbations impact the functional development of escape circuits. Therefore in a future endeavour, whole-cell patch clamp recordings of M-cells can be performed *in vivo* to assess miniature excitatory/inhibitory postsynaptic currents, similar to previously established methods (Drapeau et al., 1999; Roy and Ali, 2013). One could also record action potential production to more fully understand how perturbing the eCS alters intracellular communication. Gaining insight towards the synaptic activities of M-cells will lend support towards establishing

a physiological basis for further explaining the sensorimotor alterations that were observed at 2, 5, and 6 dpf.

Another point of investigation would be to examine whether Rohon-Beard neurons are affected by eCS perturbation, as the relationship between eCB signaling and Rohon-Beard neuron function is largely unknown at this time. Since these cells play a significant role in guiding motor function and mechanosensory processes during early embryonic and larval periods, their morphological and functional development must be assessed (Slatter et al., 2005). One way to visualize Rohon-Beard neurons involves using transgenic animals. In particular, the tg(isl2b:GFP) transgenic line of zebrafish has been developed and is used for observing Rohon-Beard neurons during embryonic and larval development (Katz et al., 2020; Williams and Ribera, 2020). Using a transgenic model such as this may allow for a detailed examination of the abundance and the development of Rohon-Beard neurons in embryonic zebrafish to investigate whether inhibition of FAAH/MAGL alters these mechanosensory cells. Furthermore, Katz and colleagues have developed a method to record whole-cell responses from Rohon-Beard neurons in larvae using tg(isl2b:GFP) zebrafish (Katz et al., 2020). With this in mind, early assessments of how eCB signaling relates to Rohon-Beard development and functionality can be studied with the use of more advanced methods such as electrophysiology and transgenic models. Additionally, another group has demonstrated that morpholino knockdown of the *piezo2b* gene causes alterations in the response to mechanical stimuli in 24-27 hpf zebrafish (Faucherre et al., 2013). This study showed that *piezo2b* is highly expressed in Rohon-Beard neurons, and that its expression is important for their mechanosensory function. Thus, considering the altered responses to mechanical stimuli caused by eCS perturbation, a future study performing

quantitative polymerase chain reaction (qPCR) to compare the relative gene expression of *piezo2b* in animals exposed to the different FAAH and MAGL inhibitors would help advance our knowledge of the involvement of eCB signaling on sensorimotor function. Additionally, using qPCR to study this will provide a molecular biology perspective, lending more mechanistic information towards the endocannabinoid system's neurobiological role in terms of the development of sensory cell types.

As this work focuses on using pharmacological inhibitors of the eCB catabolic enzymes FAAH and MAGL, the role of eCB signaling must also be understood from the opposite perspective: through targeting the enzymes responsible for eCB synthesis. This thesis provides information that is relevant towards upregulated activity of the eCS, however, an approach that investigates the roles of the primary eCS anabolic enzymes: NAPE-PLD and DAGL, must also be considered to ascertain the role of eCB signaling more extensively during early development. Currently, as there is a larger interest in investigating the implications of increased eCS activity, less research has been done in this scope. Thus, fewer tools have been developed to study the roles of the eCS anabolic enzymes. However, in order to learn more about the fundamental biology of the eCS, researchers must also aim to examine the suppression of eCB signaling as well.

In recent years, some advancements in this area have been made such as the development of the selective NAPE-PLD inhibitors ARN19874, and LEI-401, where LEI-401 was shown to reduce the levels of AEA in the brain of mice (Castellani et al., 2017; Mock et al., 2020). Likewise, the DAGL inhibitors DH376, DO34, and LEI105 have also been developed, where DH376 and

DO34 both decrease the levels of 2-AG in the mouse brain (Baggelaar et al., 2015; Ogasawara et al., 2016). As these represent newer pharmacological tools, Martella and colleagues have also designed a *dagla* morpholino which resulted in decreased 2-AG levels, and was used in a study geared towards investigating the roles of 2-AG signaling and DAGL activity in sensory function and motor development of larval zebrafish (Martella et al., 2016). So far, these developments have set up a toolkit to further investigate eCS anabolic enzymes in the future. Ultimately, utilizing more animal models for expanding and broadening the applications of these pharmacological and molecular tools will be essential for further examining the neurobiological, homeostatic, and developmental roles of the eCS from additional perspectives.

6.2 Conclusions

The endocannabinoid system is complex in its multifaceted involvement in homeostasis and development, and while emerging work aims to understand its importance within the context of cannabis, further exploring the endogenous machinery is equally important. By studying the eCS as it pertains to neurobiological development in zebrafish, my first objective in this thesis aimed to broaden our understanding of the role of the eCS in motor systems by addressing how eCB signaling is involved in the development of functional sensorimotor activities. However, despite our current understanding of the endocannabinoid system's role in neurobiological development, the multitude of receptor and signaling mechanisms through which eCBs interact with remains enigmatic. Thus, with my second objective aiming to address this knowledge gap, I have studied the effects of eCS perturbations in order to outline the involvement of canonical and non-canonical cannabinoid receptor mechanisms in the early locomotor development of embryonic zebrafish. To my knowledge, the findings presented here represents one of the first reports of

TRP channel and SHH involvement in eCB-related motor development. While more information regarding these signaling systems is essential for effectively mapping out the different eCS interactions, the current work establishes a foundation upon which we may begin to unravel the intricacies of eCB signaling during early development. In conclusion, from examining the early life stages in zebrafish, the findings of my thesis support the existing bodies of evidence demonstrating that the eCS plays an important role in locomotor development, and expands on this by exploring sensorimotor development by providing varied assessments of sensorimotor function in developing animals to establish a stronger foundation in cannabinoid biology.

Literature Cited:

Achenbach, J. C., Leggiadro, C., Sperker, S. A., Woodland, C. and Ellis, L. D. (2020). Comparison of the Zebrafish Embryo Toxicity Assay and the General and Behavioral Embryo Toxicity Assay as New Approach Methods for Chemical Screening. *Toxics* **8**,.

Ahmed, K. T. and Ali, D. W. (2016). Nicotinic acetylcholine receptors (nAChRs) at zebrafish red and white muscle show different properties during development: nAChRs at the Zebrafish NMJ. *Devel Neurobio* **76**, 916–936.

Ahmed, K. T., Amin, M. R., Shah, P. and Ali, D. W. (2018). Motor neuron development in zebrafish is altered by brief (5-hr) exposures to THC (Δ9-tetrahydrocannabinol) or CBD (cannabidiol) during gastrulation. *Sci Rep* **8**, 10518.

Akhtar, M. T., Ali, S., Rashidi, H., van der Kooy, F., Verpoorte, R. and Richardson, M. K. (2013). Developmental Effects of Cannabinoids on Zebrafish Larvae. *Zebrafish* **10**, 283–293.

Amato, V., Viña, E., Calavia, M. g., Guerrera, M. c., LaurÀ, R., Navarro, M., De Carlos, F., Cobo, J., Germanà, A. and Vega, J. a. (2012). TRPV4 in the sensory organs of adult zebrafish. *Microscopy Research and Technique* **75**, 89–96.

Amin, M. R. and Ali, D. W. (2019). Pharmacology of Medical Cannabis. In *Recent Advances in Cannabinoid Physiology and Pathology* (ed. Bukiya, A. N.), pp. 151–165. Cham: Springer International Publishing.

Amin, M. R., Ahmed, K. T. and Ali, D. W. (2020). Early Exposure to THC Alters M-Cell Development in Zebrafish Embryos. *Biomedicines* **8**, 5.

Anand, U., Otto, W. R., Sanchez-Herrera, D., Facer, P., Yiangou, Y., Korchev, Y., Birch, R., Benham, C., Bountra, C., Chessell, I. P., et al. (2008). Cannabinoid receptor CB2 localisation and agonist-mediated inhibition of capsaicin responses in human sensory neurons. *Pain* **138**, 667–680.

Baek, S., Tran, N. T. T., Diaz, D. C., Tsai, Y.-Y., Acedo, J. N., Lush, M. E. and Piotrowski, T. (2021). *High-resolution single cell transcriptome analysis of zebrafish sensory hair cell regeneration*. Developmental Biology.

Baggelaar, M. P., Chameau, P. J. P., Kantae, V., Hummel, J., Hsu, K.-L., Janssen, F., van der Wel, T., Soethoudt, M., Deng, H., den Dulk, H., et al. (2015). Highly Selective, Reversible Inhibitor Identified by Comparative Chemoproteomics Modulates Diacylglycerol Lipase Activity in Neurons. *J. Am. Chem. Soc.* **137**, 8851–8857.

Bailone, R. L. (2022). The endocannabinoid system in zebrafish and its potential to study the effects of Cannabis in humans. 12.

Bang, P. I., Yelick, P. C., Malicki, J. J. and Sewell, W. F. (2002). High-throughput behavioral screening method for detecting auditory response defects in zebrafish. *J. Neurosci. Methods* **118**, 177–187.

Berghuis, P., Rajnicek, A. M., Morozov, Y. M., Ross, R. A., Mulder, J., Urban, G. M., Monory, K., Marsicano, G., Matteoli, M., Canty, A., et al. (2007). Hardwiring the Brain: Endocannabinoids Shape Neuronal Connectivity. *Science* **316**, 1212–1216.

Blankman, J. L., Simon, G. M. and Cravatt, B. F. (2007). A Comprehensive Profile of Brain Enzymes that Hydrolyze the Endocannabinoid 2-Arachidonoylglycerol. *Chem Biol* **14**, 1347–1356.

Boa-Amponsem, O., Zhang, C., Mukhopadhyay, S., Ardrey, I. and Cole, G. J. (2019). Ethanol and cannabinoids interact to alter behavior in a zebrafish fetal alcohol spectrum disorder model. *Birth Defects Research* **111**, 775–788.

Brownstone, R. M. and Chopek, J. W. (2018). Reticulospinal Systems for Tuning Motor Commands. *Front. Neural Circuits* **12**, 30.

Buckingham, S. D. and Ali, D. W. (2004). Sodium and potassium currents of larval zebrafish muscle fibres. *Journal of Experimental Biology* **207**, 841–852.

Buckley, N. E., Hansson, S., Harta, G. and Mezey, É. (1997). Expression of the CB1 and CB2 receptor messenger RNAs during embryonic development in the rat. *Neuroscience* **82**, 1131–1149.

Burgess, H. A. and Granato, M. (2007). Sensorimotor Gating in Larval Zebrafish. *J. Neurosci.* **27**, 4984–4994.

Buss, R. R. and Drapeau, P. (2002). Activation of Embryonic Red and White Muscle Fibers During Fictive Swimming in the Developing Zebrafish. *Journal of Neurophysiology* **87**, 1244–1251.

Carmean, V. and Ribera, A. B. (2010). Genetic Analysis of the Touch Response in Zebrafish (Danio rerio). *Int J Comp Psychol* **23**, 91.

Carty, D. R., Thornton, C., Gledhill, J. H. and Willett, K. L. (2018). Developmental Effects of Cannabidiol and Δ9-Tetrahydrocannabinol in Zebrafish. *Toxicological Sciences* **162**, 137–145.

Castellani, B., Diamanti, E., Pizzirani, D., Tardia, P., Maccesi, M., Realini, N., Magotti, P., Garau, G., Bakkum, T., Rivara, S., et al. (2017). Synthesis and characterization of the first inhibitor of N-acylphosphatidylethanolamine phospholipase D (NAPE-PLD). *Chem Commun (Camb)* **53**, 12814–12817.

Chávez, A. E., Chiu, C. Q. and Castillo, P. E. (2010). TRPV1 activation by endogenous anandamide triggers postsynaptic long-term depression in dentate gyrus. *Nat Neurosci* **13**, 1511–1518.

Choudhry, Z., Rikani, A. A., Choudhry, A. M., Tariq, S., Zakaria, F., Asghar, M. W., Sarfraz, M. K., Haider, K., Shafiq, A. A. and Mobassarah, N. J. (2014). Sonic hedgehog signalling pathway: a complex network. *Ann Neurosci* **21**, 28–31.

Colwill, R. M. and Creton, R. (2011a). Locomotor behaviors in zebrafish (Danio rerio) larvae. *Behavioural Processes* **86**, 222–229.

Colwill, R. M. and Creton, R. (2011b). Imaging escape and avoidance behavior in zebrafish larvae. *Rev Neurosci* **22**, 63–73.

Corey, D. P., García-Añoveros, J., Holt, J. R., Kwan, K. Y., Lin, S.-Y., Vollrath, M. A., Amalfitano, A., Cheung, E. L.-M., Derfler, B. H., Duggan, A., et al. (2004). TRPA1 is a candidate for the mechanosensitive transduction channel of vertebrate hair cells. *Nature* **432**, 723–730.

Cravatt, B. F., Giang, D. K., Mayfield, S. P., Boger, D. L., Lerner, R. A. and Gilula, N. B. (1996). Molecular characterization of an enzyme that degrades neuromodulatory fatty-acid amides. *Nature* **384**, 83–87.

Cristino, L., de Petrocellis, L., Pryce, G., Baker, D., Guglielmotti, V. and Di Marzo, V. (2006). Immunohistochemical localization of cannabinoid type 1 and vanilloid transient receptor potential vanilloid type 1 receptors in the mouse brain. *Neuroscience* **139**, 1405–1415.

Danandeh, A., Vozella, V., Lim, J., Oveisi, F., Ramirez, G. L., Mears, D., Wynn, G. and Piomelli, D. (2018). Effects of fatty acid amide hydrolase inhibitor URB597 in a rat model of trauma-induced long-term anxiety. *Psychopharmacology* **235**, 3211–3221.

de Oliveira, A., Brigante, T. and Oliveira, D. (2021). Tail Coiling Assay in Zebrafish (Danio rerio) Embryos: Stage of Development, Promising Positive Control Candidates, and Selection of an Appropriate Organic Solvent for Screening of Developmental Neurotoxicity (DNT). *Water* **13**, 119.

Devane, W. A., Hanuš, L., Breuer, A., Pertwee, R. G., Stevenson, L. A., Griffin, G., Gibson, D., Mandelbaum, A., Etinger, A. and Mechoulam, R. (1992). Isolation and Structure of a Brain Constituent That Binds to the Cannabinoid Receptor. *Science* **258**, 1946–1949.

Di Marzo, V., Fontana, A., Cadas, H., Schinelli, S., Cimino, G., Schwartz, J.-C. and Piomelli, D. (1994). Formation and inactivation of endogenous cannabinoid anandamide in central neurons. *Nature* **372**, 686–691.

Drapeau, P., Ali, D. W., Buss, R. R. and Saint-Amant, L. (1999). In vivo recording from identifiable neurons of the locomotor network in the developing zebrafish. *Journal of Neuroscience Methods* **88**, 1–13.

Drapeau, P., Saint-Amant, L., Buss, R. R., Chong, M., McDearmid, J. R. and Brustein, E. (2002). Development of the locomotor network in zebrafish. *Prog Neurobiol* **68**, 85–111.

Ellis, L. (2019). Zebrafish as a High-Throughput In Vivo Model for Testing the Bioactivity of Cannabinoids. In *Recent Advances in Cannabinoid Research* (ed. J Costain, W.) and B Laprairie, R.), p. IntechOpen.

Elphick, M. R. (2012). The evolution and comparative neurobiology of endocannabinoid signalling. *Phil. Trans. R. Soc. B* **367**, 3201–3215.

Ericson, J., Morton, S., Kawakami, A., Roelink, H. and Jessell, T. M. (1996). Two Critical Periods of Sonic Hedgehog Signaling Required for the Specification of Motor Neuron Identity. *Cell* **87**, 661–673.

Faucherre, A., Nargeot, J., Mangoni, M. E. and Jopling, C. (2013). piezo2b Regulates Vertebrate Light Touch Response. *J. Neurosci.* **33**, 17089–17094.

Fish, E. W., Murdaugh, L. B., Zhang, C., Boschen, K. E., Boa-Amponsem, O., Mendoza-Romero, H. N., Tarpley, M., Chdid, L., Mukhopadhyay, S., Cole, G. J., et al. (2019). Cannabinoids Exacerbate Alcohol Teratogenesis by a CB1-Hedgehog Interaction. *Sci Rep* **9**, 16057.

Fride, E. (2008). Multiple Roles for the Endocannabinoid System During the Earliest Stages of Life: Pre- and Postnatal Development. *J Neuroendocrinol* **20**, 75–81.

Friedman, D. and Sirven, J. I. (2017). Historical perspective on the medical use of cannabis for epilepsy: Ancient times to the 1980s. *Epilepsy & Behavior* **70**, 298–301.

Galiègue, S., Mary, S., Marchand, J., Dussossoy, D., Carriere, D., Carayon, P., Bouaboula, M., Shire, D., Fur, G. and Casellas, P. (1995). Expression of Central and Peripheral Cannabinoid Receptors in Human Immune Tissues and Leukocyte Subpopulations. *Eur J Biochem* **232**, 54–61.

Germanà, A., Muriel, J. D., Cobo, R., García-Suárez, O. and Cobo, J. (2018). Transient-Receptor Potential (TRP) and Acid-Sensing Ion Channels (ASICs) in the Sensory Organs of Adult Zebrafish. In *Recent Advances in Zebrafish Researches* (ed. Bozkurt, Y.), pp. 101–117. InTech.

Gil-Ordóñez, A., Martín-Fontecha, M., Ortega-Gutiérrez, S. and López-Rodríguez, M. L. (2018). Monoacylglycerol lipase (MAGL) as a promising therapeutic target. *Biochemical Pharmacology* **157**, 18–32.

Gobbi, G., Bambico, F. R., Mangieri, R., Bortolato, M., Campolongo, P., Solinas, M., Cassano, T., Morgese, M. G., Debonnel, G., Duranti, A., et al. (2005). Antidepressant-like activity and modulation of brain monoaminergic transmission by blockade of anandamide hydrolysis. *Proc Natl Acad Sci U S A* **102**, 18620–18625.

Griebel, G., Pichat, P., Beeské, S., Leroy, T., Redon, N., Jacquet, A., Françon, D., Bert, L., Even, L., Lopez-Grancha, M., et al. (2015). Selective blockade of the hydrolysis of the

endocannabinoid 2-arachidonoylglycerol impairs learning and memory performance while producing antinociceptive activity in rodents. *Sci Rep* **5**, 7642.

Griebel, G., Stemmelin, J., Lopez-Grancha, M., Fauchey, V., Slowinski, F., Pichat, P., Dargazanli, G., Abouabdellah, A., Cohen, C. and Bergis, O. E. (2018). The selective reversible FAAH inhibitor, SSR411298, restores the development of maladaptive behaviors to acute and chronic stress in rodents. *Sci Rep* **8**, 2416.

Grunwald, D. J., Kimmel, C. B., Westerfield, M., Walker, C. and Streisinger, G. (1988). A neural degeneration mutation that spares primary neurons in the zebrafish. *Developmental Biology* **126**, 115–128.

Gulino, R., Parenti, R. and Gulisano, M. (2017). Sonic Hedgehog and TDP-43 Participate in the Spontaneous Locomotor Recovery in a Mouse Model of Spinal Motoneuron Disease. *JFMK* **2**, 11.

Head, J. R., Gacioch, L., Pennisi, M. and Meyers, J. R. (2013). Activation of canonical Wnt/β-catenin signaling stimulates proliferation in neuromasts in the zebrafish posterior lateral line: Wnt Signaling Controls Neuromast Proliferation. *Dev. Dyn.* **242**, 832–846.

Henderson, K. W., Menelaou, E. and Hale, M. E. (2019). Sensory neurons in the spinal cord of zebrafish and their local connectivity. *Current Opinion in Physiology* **8**, 136–140.

Herkenham, M., Lynn, A., Johnson, M., Melvin, L., de Costa, B. and Rice, K. (1991). Characterization and localization of cannabinoid receptors in rat brain: a quantitative in vitro autoradiographic study. *J. Neurosci.* **11**, 563–583.

Howlett, A. C. (2002). International Union of Pharmacology. XXVII. Classification of Cannabinoid Receptors. *Pharmacological Reviews* **54**, 161–202.

Ingham, P. W. and Kim, H. R. (2005). Hedgehog signalling and the specification of muscle cell identity in the Zebrafish embryo. *Experimental Cell Research* **306**, 336–342.

Jacques, B. E., Montgomery, W. H., Uribe, P. M., Yatteau, A., Asuncion, J. D., Resendiz, G., Matsui, J. I. and Dabdoub, A. (2014). The role of Wnt/β-catenin signaling in proliferation and regeneration of the developing basilar papilla and lateral line: Wnt/β-Catenin in BP and Lateral Line HCs. *Devel Neurobio* **74**, 438–456.

Julian, M. D., Martin, A. B., Cuellar, B., Rodriguez De Fonseca, F., Navarro, M., Moratalla, R. and Garcia-Segura, L. M. (2003). Neuroanatomical relationship between type 1 cannabinoid receptors and dopaminergic systems in the rat basal ganglia. *Neuroscience* **119**, 309–318.

Kanyo, R., Amin, M. R., Locskai, L. F., Bouvier, D. D., Olthuis, A. M., Allison, W. T. and Ali, D. W. (2021). Medium-throughput zebrafish optogenetic platform identifies deficits in subsequent neural activity following brief early exposure to cannabidiol and Δ9-tetrahydrocannabinol. *Sci Rep* **11**, 11515.

Kathuria, S., Gaetani, S., Fegley, D., Valiño, F., Duranti, A., Tontini, A., Mor, M., Tarzia, G., Rana, G. L., Calignano, A., et al. (2003). Modulation of anxiety through blockade of anandamide hydrolysis. *Nat Med* **9**, 76–81.

Katz, H. R., Menelaou, E. and Hale, M. E. (2020). Morphological and physiological properties of Rohon-Beard neurons along the zebrafish spinal cord. *J Comp Neurol* **529**, 1499–1515.

Khaliullina, H., Bilgin, M., Sampaio, J. L., Shevchenko, A. and Eaton, S. (2015). Endocannabinoids are conserved inhibitors of the Hedgehog pathway. *Proc Natl Acad Sci USA* **112**, 3415–3420.

Kimmel, C. B., Hatta, K. and Metcalfe, W. K. (1990). Early axonal contacts during development of an identified dendrite in the brain of the zebrafish. *Neuron* **4**, 535–545.

Kimmel, C. B., Ballard, W. W., Kimmel, S. R., Ullmann, B. and Schilling, T. F. (1995). Stages of embryonic development of the zebrafish. *Dev. Dyn.* **203**, 253–310.

Kinsey, S. G., Wise, L. E., Ramesh, D., Abdullah, R., Selley, D. E., Cravatt, B. F. and Lichtman, A. H. (2013). Repeated Low-Dose Administration of the Monoacylglycerol Lipase Inhibitor JZL184 Retains Cannabinoid Receptor Type 1–Mediated Antinociceptive and Gastroprotective Effects. *J Pharmacol Exp Ther* **345**, 492–501.

Klionsky, L., Tamir, R., Gao, B., Wang, W., Immke, D. C., Nishimura, N. and Gavva, N. R. (2007). Species-specific pharmacology of Trichloro(sulfanyl)ethyl benzamides as transient receptor potential ankyrin 1 (TRPA1) antagonists. *Mol Pain* **3**, 39.

Kohashi, T., Nakata, N. and Oda, Y. (2012). Effective Sensory Modality Activating an Escape Triggering Neuron Switches during Early Development in Zebrafish. *Journal of Neuroscience* **32**, 5810–5820.

Krug, R. G. and Clark, K. J. (2015). Elucidating cannabinoid biology in zebrafish (Danio rerio). *Gene* **570**, 168–179.

Lam, C. S., Rastegar, S. and Strähle, U. (2006). Distribution of cannabinoid receptor 1 in the CNS of zebrafish. *Neuroscience* **138**, 83–95.

Lessman, C. A. (2011). The developing zebrafish (Danio rerio): A vertebrate model for high-throughput screening of chemical libraries. *Birth Defects Research Part C: Embryo Today: Reviews* **93**, 268–280.

Liu, L. Y., Alexa, K., Cortes, M., Schatzman-Bone, S., Kim, A. J., Mukhopadhyay, B., Cinar, R., Kunos, G., North, T. E. and Goessling, W. (2016). Cannabinoid receptor signaling regulates liver development and metabolism. *Development* **143**, 609–622.

Lodola, A., Capoferri, L., Rivara, S., Tarzia, G., Piomelli, D., Mulholland, A. and Mor, M. (2013). Quantum Mechanics/Molecular Mechanics Modeling of Fatty Acid Amide Hydrolase Reactivation Distinguishes Substrate from Irreversible Covalent Inhibitors. *J. Med. Chem.* **56**, 2500–2512.

Long, J. Z., Li, W., Booker, L., Burston, J. J., Kinsey, S. G., Schlosburg, J. E., Pavón, F. J., Serrano, A. M., Selley, D. E., Parsons, L. H., et al. (2009a). Selective blockade of 2-arachidonoylglycerol hydrolysis produces cannabinoid behavioral effects. *Nat Chem Biol* **5**, 37–44.

Long, J. Z., Nomura, D. K., Vann, R. E., Walentiny, D. M., Booker, L., Jin, X., Burston, J. J., Sim-Selley, L. J., Lichtman, A. H., Wiley, J. L., et al. (2009b). Dual blockade of

FAAH and MAGL identifies behavioral processes regulated by endocannabinoid crosstalk in vivo. *Proceedings of the National Academy of Sciences* **106**, 20270–20275.

Lu, Z. and DeSmidt, A. A. (2013). Early development of hearing in zebrafish. *J. Assoc. Res. Otolaryngol.* **14**, 509–521.

Lu, H.-C. and Mackie, K. (2016). An introduction to the endogenous cannabinoid system. *Biol Psychiatry* **79**, 516–525.

Ma, E. Y. and Raible, D. W. (2009). Signaling Pathways Regulating Zebrafish Lateral Line Development. *Current Biology* **19**, R381–R386.

Maccarrone, M., Bab, I., Bíró, T., Cabral, G. A., Dey, S. K., Di Marzo, V., Konje, J. C., Kunos, G., Mechoulam, R., Pacher, P., et al. (2015). Endocannabinoid signaling at the periphery: 50 years after THC. *Trends in Pharmacological Sciences* **36**, 277–296.

Mackie, K. (2008). Cannabinoid Receptors: Where They are and What They do. *J Neuroendocrinol* **20**, 10–14.

Martella, A., Sepe, R. M., Silvestri, C., Zang, J., Fasano, G., Carnevali, O., De Girolamo, P., Neuhauss, S. C. F., Sordino, P. and Di Marzo, V. (2016). Important role of endocannabinoid signaling in the development of functional vision and locomotion in zebrafish. *FASEB j.* **30**, 4275–4288.

Martín-Saldaña, S., Trinidad, A., Ramil, E., Sánchez-López, A. J., Coronado, M. J., Martínez-Martínez, E., García, J. M., García-Berrocal, J. R. and Ramírez-Camacho, R. (2016). Spontaneous Cannabinoid Receptor 2 (CB2) Expression in the

Cochlea of Adult Albino Rat and Its Up-Regulation after Cisplatin Treatment. *PLoS One* **11**, e0161954.

Mathre, M. L. (2010). *Cannabis in Medical Practice: A Legal, Historical and Pharmacological Overview of the Therapeutic Use of Marijuana*.

Matsuda, L. A. and Young, A. C. (1990). Structure of a cannabinoid receptor and functional expression of the cloned eDNA. **346**, 4.

McArthur, K. L., Chow, D. M. and Fetcho, J. R. (2020). Zebrafish as a Model for Revealing the Neuronal Basis of Behavior. In *The Zebrafish in Biomedical Research*, pp. 593–617. Elsevier.

Mechoulam, R., Ben-Shabat, S., Hanus, L., Ligumsky, M., Kaminski, N. E., Schatz, A. R., Gopher, A., Almog, S., Martin, B. R., Compton, D. R., et al. (1995). Identification of an endogenous 2-monoglyceride, present in canine gut, that binds to cannabinoid receptors. *Biochemical Pharmacology* **50**, 83–90.

Migliarini, B. and Carnevali, O. (2008). Anandamide modulates growth and lipid metabolism in the zebrafish Danio rerio. *Molecular and Cellular Endocrinology* **286**, S12–S16.

Miller, S., Rao, S., Wang, W., Liu, H., Wang, J. and Gavva, N. R. (2014). Antibodies to the Extracellular Pore Loop of TRPM8 Act as Antagonists of Channel Activation. *PLoS One* **9**, e107151.

Mock, E. D., Mustafa, M., Gunduz-Cinar, O., Cinar, R., Petrie, G. N., Kantae, V., Di, X., Ogasawara, D., Varga, Z. V., Paloczi, J., et al. (2020). Discovery of a NAPE-PLD

inhibitor that modulates emotional behavior in mice. *Nature Chemical Biology* **16**, 667–675.

Moorman, S. J. (2001). Development of Sensory Systems in Zebrafish (Donio rerio). *ILAR Journal* **42**, 292–298.

Morales, P., Hurst, D. P. and Reggio, P. H. (2017). Molecular Targets of the Phytocannabinoids: A Complex Picture. In *Phytocannabinoids* (ed. Kinghorn, A. D.), Falk, H.), Gibbons, S.), and Kobayashi, J.), pp. 103–131. Cham: Springer International Publishing.

Muller, T., Demizieux, L., Troy-Fioramonti, S., Gresti, J., Pais de Barros, J.-P., Berger, H., Vergès, B. and Degrace, P. (2017). Overactivation of the endocannabinoid system alters the antilipolytic action of insulin in mouse adipose tissue. *Am J Physiol Endocrinol Metab* **313**, E26–E36.

Muller, C., Morales, P. and Reggio, P. H. (2019). Cannabinoid Ligands Targeting TRP Channels. *Front. Mol. Neurosci.* **11**, 487.

Munro, S., Thomas, K. L. and Abu-Shaar, M. (1993). Molecular characterization of a peripheral receptor for cannabinoids. *Nature* **365**, 61–65.

Nilius, B. and Owsianik, G. (2011). The transient receptor potential family of ion channels. *Genome Biol* **12**, 218.

Ogasawara, D., Deng, H., Viader, A., Baggelaar, M. P., Breman, A., den Dulk, H., van den Nieuwendijk, A. M. C. H., Soethoudt, M., van der Wel, T., Zhou, J., et al. (2016).

Rapid and profound rewiring of brain lipid signaling networks by acute diacylglycerol lipase inhibition. *Proc. Natl. Acad. Sci. U.S.A.* **113**, 26–33.

Ohno-Shosaku, T., Maejima, T. and Kano, M. (2001). Endogenous Cannabinoids Mediate Retrograde Signals from Depolarized Postsynaptic Neurons to Presynaptic Terminals. *Neuron* **29**, 729–738.

Olt, J., Johnson, S. L. and Marcotti, W. (2014). In vivo and in vitro biophysical properties of hair cells from the lateral line and inner ear of developing and adult zebrafish. *J Physiol* **592**, 2041–2058.

Oltrabella, F., Melgoza, A., Nguyen, B. and Guo, S. (2017). Role of the endocannabinoid system in vertebrates: Emphasis on the zebrafish model. *Develop. Growth Differ.* **59**, 194–210.

Onaivi, E. S., Ishiguro, H., Gu, S. and Liu, Q.-R. (2012). CNS effects of CB2 cannabinoid receptors: beyond neuro-immuno-cannabinoid activity. *J Psychopharmacol* **26**, 92–103.

Pan, Y. A., Choy, M., Prober, D. A. and Schier, A. F. (2012). Robo2 determines subtype-specific axonal projections of trigeminal sensory neurons. *Development* **139**, 591–600.

Pandelides, Z., Thornton, C., Faruque, A. S., Whitehead, A. P., Willett, K. L. and Ashpole, N. M. (2020). Developmental exposure to cannabidiol (CBD) alters longevity and health span of zebrafish (Danio rerio). *GeroScience* **42**, 785–800.

Pandey, R., Mousawy, K., Nagarkatti, M. and Nagarkatti, P. (2009). Endocannabinoids and immune regulation. *Pharmacological Research* **60**, 85–92.

Parichy, D. M., Elizondo, M. R., Mills, M. G., Gordon, T. N. and Engeszer, R. E. (2009). Normal Table of Post-Embryonic Zebrafish Development: Staging by Externally Visible Anatomy of the Living Fish. *Dev Dyn* **238**, 2975–3015.

Pietrobono, S., Gagliardi, S. and Stecca, B. (2019). Non-canonical Hedgehog Signaling Pathway in Cancer: Activation of GLI Transcription Factors Beyond Smoothened. *Front. Genet.* **10**, 556.

Rodriguez-Martin, I., Herrero-Turrion, M. J., Marron Fdez de Velasco, E., Gonzalez-Sarmiento, R. and Rodriguez, R. E. (2007). Characterization of two duplicate zebrafish Cb2-like cannabinoid receptors. *Gene* **389**, 36–44.

Rodríguez de Fonseca, F., Del Arco, I., Martín-Calderón, J. L., Gorriti, M. A. and Navarro, M. (1998). Role of the Endogenous Cannabinoid System in the Regulation of Motor Activity. *Neurobiology of Disease* **5**, 483–501.

Rohde, L. A. and Heisenberg, C. (2007). Zebrafish Gastrulation: Cell Movements, Signals, and Mechanisms. In *International Review of Cytology*, pp. 159–192. Elsevier.

Romero-Carvajal, A., Navajas Acedo, J., Jiang, L., Kozlovskaja-Gumbrienė, A., Alexander, R., Li, H. and Piotrowski, T. (2015). Regeneration of Sensory Hair Cells Requires Localized Interactions between the Notch and Wnt Pathways. *Developmental Cell* **34**, 267–282.

Roy, B. and Ali, D. W. (2013). Patch Clamp Recordings from Embryonic Zebrafish Mauthner Cells. *JoVE* 50551.

Russo, E. B. (2014). *Handbook of Cannabis*. Oxford University Press.

Ryan, K. E. and Chiang, C. (2012). Hedgehog Secretion and Signal Transduction in Vertebrates. *J Biol Chem* **287**, 17905–17913.

Saint-Amant, L. (2006). Development of Motor Networks in Zebrafish Embryos. *Zebrafish* **3**, 173–190.

Saint-Amant, L. and Drapeau, P. (1998). Time course of the development of motor behaviors in the zebrafish embryo. *J Neurobiol* **37**, 622–632.

Seillier, A., Aguilar, D. D. and Giuffrida, A. (2014). The dual FAAH/MAGL inhibitor JZL195 has enhanced effects on endocannabinoid transmission and motor behavior in rats as compared to those of the MAGL inhibitor JZL184. *Pharmacol Biochem Behav* **0**, 153–159.

Shan, S. D., Boutin, S., Ferdous, J. and Ali, D. W. (2015). Ethanol exposure during gastrulation alters neuronal morphology and behavior in zebrafish. *Neurotoxicology and Teratology* **48**, 18–27.

Slatter, C. A. B., Kanji, H., Coutts, C. A. and Ali, D. W. (2005). Expression of PKC in the developing zebrafish,Danio rerio. *J. Neurobiol.* **62**, 425–438.

Son, H.-W. (2021). Characterizing endocannabinoid system development in zebrafish and investigating cannabidiol-mediated downregulation of the Sonic Hedgehog Pathway.

Son, H.-W. and Ali, D. W. (2022). Endocannabinoid Receptor Expression in Early Zebrafish Development. *Developmental Neuroscience* 25.

Stella, N. and Piomelli, D. (2001). Receptor-dependent formation of endogenous cannabinoids in cortical neurons. *European Journal of Pharmacology* **425**, 189–196.

Stempel, A. V., Stumpf, A., Zhang, H.-Y., Özdoğan, T., Pannasch, U., Theis, A.-K., Otte, D.-M., Wojtalla, A., Rácz, I., Ponomarenko, A., et al. (2016). Cannabinoid Type 2 Receptors Mediate a Cell Type-Specific Plasticity in the Hippocampus. *Neuron* **90**, 795–809.

Sufian, M. S. (2020). Elucidating the roles of endocannabinoid signalling pathway in motor neuron and locomotor development in zebrafish early life.

Sufian, M. S., Amin, M. R., Kanyo, R., Allison, W. T. and Ali, D. W. (2019). CB1 and CB2 receptors play differential roles in early zebrafish locomotor development. *J Exp Biol* **222**, jeb206680.

Sufian, M. S., Amin, M. R. and Ali, D. W. (2021). Early suppression of the endocannabinoid degrading enzymes FAAH and MAGL alters locomotor development in zebrafish. *Journal of Experimental Biology* jeb.242635.

Sugiura, T., Kondo, S., Sukagawa, A., Nakane, S., Shinoda, A., Itoh, K., Yamashita, A. and Waku, K. (1995). 2-Arachidonoylgylcerol: A Possible Endogenous Cannabinoid Receptor Ligand in Brain. *Biochemical and Biophysical Research Communications* **215**, 89–97.

Sztal, T. E., Ruparelia, A. A., Williams, C. and Bryson-Richardson, R. J. (2016). Using Touch-evoked Response and Locomotion Assays to Assess Muscle Performance and Function in Zebrafish. *JoVE* 54431.

Tanimura, A., Yamazaki, M., Hashimotodani, Y., Uchigashima, M., Kawata, S., Abe, M., Kita, Y., Hashimoto, K., Shimizu, T., Watanabe, M., et al. (2010). The Endocannabinoid 2-Arachidonoylglycerol Produced by Diacylglycerol Lipase α Mediates Retrograde Suppression of Synaptic Transmission. *Neuron* **65**, 320–327.

Thisse, C. and Thisse, B. (2008). High-resolution in situ hybridization to whole-mount zebrafish embryos. *Nat Protoc* **3**, 59–69.

Tripathi, R. K. P. (2020). A perspective review on fatty acid amide hydrolase (FAAH) inhibitors as potential therapeutic agents. *European Journal of Medicinal Chemistry* **188**, 111953.

Watanabe, H., Vriens, J., Prenen, J., Droogmans, G., Voets, T. and Nilius, B. (2003). Anandamide and arachidonic acid use epoxyeicosatrienoic acids to activate TRPV4 channels. *Nature* **424**, 434–438.

Watson, S., Chambers, D., Hobbs, C., Doherty, P. and Graham, A. (2008). The endocannabinoid receptor, CB1, is required for normal axonal growth and fasciculation. *Molecular and Cellular Neuroscience* **38**, 89–97.

Westerfield, M., McMurray, J. and Eisen, J. (1986). Identified motoneurons and their innervation of axial muscles in the zebrafish. *J Neurosci* **6**, 2267–2277.

Williams, K. and Ribera, A. B. (2020). Long-lived zebrafish Rohon-Beard cells. *Developmental Biology* **464**, 45–52.

Wilson, L. B., Truong, L., Simonich, M. T. and Tanguay, R. L. (2020). Systematic Assessment of Exposure Variations on Observed Bioactivity in Zebrafish Chemical Screening. *Toxics* **8**, 87.

Zhang, F., Qin, W., Zhang, J.-P. and Hu, C.-Q. (2015). Antibiotic Toxicity and Absorption in Zebrafish Using Liquid Chromatography-Tandem Mass Spectrometry. *PLoS ONE* **10**, e0124805.

Zheng, Y., Baek, J.-H., Smith, P. F. and Darlington, C. L. (2007). Cannabinoid receptor down-regulation in the ventral cochlear nucleus in a salicylate model of tinnitus. *Hearing Research* **228**, 105–111.

Zindler, F., Beedgen, F., Brandt, D., Steiner, M., Stengel, D., Baumann, L. and Braunbeck, T. (2019). Analysis of tail coiling activity of zebrafish (Danio rerio) embryos allows for the differentiation of neurotoxicants with different modes of action. *Ecotoxicology and Environmental Safety* **186**, 109754.

Zou, S. and Kumar, U. (2018). Cannabinoid Receptors and the Endocannabinoid System: Signaling and Function in the Central Nervous System. *IJMS* **19**, 833.

Zygmunt, P. M., Petersson, J., Andersson, D. A., Chuang, H., Sørgård, M., Di Marzo, V., Julius, D. and Högestätt, E. D. (1999). Vanilloid receptors on sensory nerves mediate the vasodilator action of anandamide. *Nature* **400**, 452–457.